

ABSTRACT

Title of Thesis: THE INFLUENCE OF EXPOSURE CONDITIONS ON
DELAYED ETTRINGITE FORMATION IN MORTAR
SPECIMENS.

Degree Candidate: Jorgomai Ceesay

Degree and year: Master of Science, 2004

Thesis Directed by: Professor Amde M. Amde
Department of Civil and Environmental Engineering.

The objectives of this research were to experimentally study the influence of exposure conditions on delayed ettringite formation (DEF) in mortar specimens, and to explore the complex processes of expansive cracking associated with DEF. Different exposure conditions were investigated while other parameters such as water-to-cement ratio, fine and coarse aggregates, cement and curing conditions were kept constant in order to study the influence of storage conditions on mortar damages associated with DEF.

Mortar bars and cubes were prepared using Portland cement ASTM Type III, Frederick sand and ordinary tap water. The specimens were steam-cured and then subjected to the Duggan heat cycle to introduce microcracks. Control batches of mortar mixes with no additional potassium (K_2O) content and sets with additional potassium increasing the overall potassium level to 1.5% K_2O by weight of cement were prepared.

Increasing the potassium level has a deleterious effect on the specimen expansion and causes deterioration in compressive strength. Length change measurements according to ASTM C490 and weight changes of the mortar bars were constantly monitored during the study. The pH value, Potassium ion [K^+], Sodium ion [Na^+] and Calcium ion [Ca^{2+}] concentrations of the storage solutions were also monitored to analyze the amount of alkali being leached into the water. Scanning electron microscope (SEM) equipped with high-energy dispersive analysis X-ray was used to identify materials present in the cavities, transition zones and cracks to determine failure mechanism of the specimens. X-ray computed tomography (X-ray CT), a non-destructive method was employed to reveal the internal crack patterns. Ettringite crystals are mainly found in the cavities, in the interface between the aggregate and cement paste.

Mortar bars subsequently stored in exposure conditions 1 (water pH maintained at 12.5) and 2 (plain water) after the Duggan heat cycle, clearly showed expansion against weight change results to be positive linearly correlated over the storage period. This was again observed in the mortar specimens with the higher potassium (K_2O) content.

Results from the petrography analyses of the expanded mortar specimens revealed delayed ettringite formation (DEF) without detecting alkali-silica reaction (ASR). The results also show that deleterious expansions caused by DEF prevails in exposure conditions with high potential leaching of alkali hydroxide to the storage solution.

THE INFLUENCE OF EXPOSURE CONDITIONS ON
DELAYED ETTRINGITE FORMATION IN MORTAR SPECIMENS

By

Jorgomai Ceesay

Thesis Submitted to the Faculty of the Graduate School of the
University of Maryland, College Park in partial fulfillment
of the requirements for the degree of
Master of Science
2004

Advisory Committee:

Professor Amde M. Amde, Chair/Advisor
Professor M. Sherif Aggour
Professor Chung C. Fu

ACKNOWLEDGMENTS

I first thank my adviser, Professor Amde M. Amde for his support, suggestions and guidance throughout the entire research.

Special thanks to Dr. Richard Livingston, Senior Physical Scientist at Turner-Fairbank Highway Research Center (FHWA) in McLean, Virginia for his knowledge and advice during the course of the research.

I am very grateful to Dr. Clay Ormsby, Research Chemist at FHWA, for his technical support and assistance in the SEM sample preparation and analysis.

Thanks also to Dr. Habeeb Saleh, Senior Scientist at FHWA for his assistance in the samples x-ray computed tomography analyses.

Special thanks to Gary M. Mullings and Solomon Ben-Barka at National Ready Mixed Concrete Association Laboratory, College Park, Maryland for their assistance in sample preparations.

Thanks to LAFARGE – North America, Frederick, Maryland for their generous donation of the sand and coarse aggregate used in this research and Tom Horbaker, Field Technician, Quality Control, LAFARGE, for his help in providing technical information for the aggregates.

Finally, I thank my wife, Mariama, Mum, family and friends for their encouragement, support and understanding.

Thank You.

TABLE OF CONTENTS

ACKNOWLEDGEMENTS.....	ii
TABLE OF CONTENTS.....	iii
LIST OF TABLES.....	viii
LIST OF FIGURES.....	x
LIST OF ABBREVIATIONS.....	xv
CHAPTER 1: INTRODUCTION.....	1
1.1 Background.....	1
1.2 Literature Review.....	4
1.3 Research Approach.....	10
1.4 Problem Statement.....	12
1.5 Objectives and Scope of This Study.....	15
1.6 Structure of Thesis.....	15
CHAPTER 2: CHEMISTRY OF CEMENT AND ETTRINGITE FORMATION.....	16
2.1 Introduction.....	16
2.2 Portland Cement Composition.....	17
2.3 Portland Cement Hydration.....	18
2.3.1 Hydration of Calcium Silicate.....	20
2.3.2 Calcium Hydroxide.....	20
2.3.3 Hydration of Aluminates.....	21
2.4 Heat of Hydration.....	22
2.5 Heat Treatment of Mortar and Concrete.....	23
2.5.1 Effect of Heat Treatment on the Stability and Formation of Ettringite.....	24
2.5.2 Effect of Heat Treatment on the Strength of Mortar and Concrete.....	26
2.5.3 Effect of Heat Treatment on Cement Chemistry and Microstructure.....	27

CHAPTER 3: DELAYED ETTRINGITE FORMATION.....	31
3.1 Introduction.....	31
3.2 Damage Caused by DEF.....	32
3.3 Conditions for DEF.....	33
3.3.1 Sulfate in Cement and Cement Clinker.....	34
3.3.2 Presence of Microcracks.....	35
3.3.3 Exposure to Moisture.....	36
3.3.4 High Temperature Curing.....	37
3.4 The Morphology of Ettringite.....	38
3.5 Detecting DEF.....	39
3.6 ASR and DEF.....	40
3.7 Stability of Ettringite.....	41
3.7.1 The Chemical Stability of Ettringite.....	41
3.7.2 Effect of Temperature.....	42
3.7.3 Effect of Alkalis.....	43
3.7.4 Effect of CO ₂	44
3.8 Expansion Mechanisms due to Ettringite Formation.....	45
3.8.1 Topochemical Reaction with Directional Growth Theory.....	45
3.8.2 The Uniform Paste Expansion Theory.....	47
3.9 Rapid Test For Predicting Expansion Due to Ettringite Formation.....	49
CHAPTER 4: SAMPLE PREPARATION, MATERIALS, AND TEST METHOD.....	50
4.1 Introduction.....	50
4.2 Experimental.....	50
4.2.1 UMD/FHWA Modified Sample Preparation.....	51
4.2.2 Duggan Heat Cycle.....	51
4.3 Materials.....	52
4.3.1 Molds.....	52
4.3.2 Cement.....	52
4.3.3 Sand.....	53
4.3.4 Potassium Carbonate.....	55
4.3.5 Potassium Sulfate.....	55
4.3.6 Calcium Hydroxide (Hydrated Lime).....	55

4.4 Storage Conditions	55
4.4.1 Isothermal Water Bath, pH maintained at 12.5 (Exp. Cond. 1).....	56
4.4.2 Plain Water at room temperature (Exp. Cond. 2).....	56
4.4.3 Moist Air Chamber, R.H maintained at 97% (Exp. Cond. 3).....	56
4.4.4 Field Conditions (Exp. Cond. 4).....	56
4.5 Sample Preparation.....	57
4.5.1 Phase One.....	58
4.5.2 Phase Two.....	60
4.6 Test Procedures.....	60
4.6.1 Compressive Strength.....	60
4.6.2 Expansion Measurements.....	61
4.6.3 Weight Change Measurements.....	62
4.7 Water Analysis.....	63
4.8 Petrography Analysis for Identifying DEF.....	64
4.8.1 Scanning Electron Microscopy (SEM) and X-ray analyzer (EDAX).....	65
4.8.2 X-ray Computed Tomography (X-ray CT).....	66
CHAPTER 5: MORTAR SAMPLES (CONTROL).....	68
5.1 Introduction	68
5.2 Influence of Exposure Conditions.....	69
5.3 Mortar Samples Subjected to Duggan Heat Cycles Test Results.....	69
5.3.1 Expansion Results.....	69
5.3.2 Weight Change Results.....	73
5.3.3 Expansion against Weight Change of Specimens.....	77
5.3.4 Compressive Strength Results.....	81
5.4 Field Samples (No Duggan Heat Cycle).....	81
5.4.1 Expansion Results.....	82
5.4.2 Weight Change Results.....	85
5.4.3 Compressive Strength Results.....	87
5.5 Water Analysis Results of Storage Solution.....	88
5.5.1 Water Analysis of Exposure Condition 1.....	88
5.5.2 Water Analysis of Exposure Condition 2.....	89
5.5.2.1 Amount of Alkalis.....	89
5.5.2.3 pH Value.....	90
5.5.2.4 Calcium Concentration.....	90
5.6 Microstructure Analysis Using (SEM) and (EDAX)	92

5.6.1 Mortar Samples in Exposure Condition 1.....	92
5.6.2 Mortar Samples in Exposure Condition 2.....	94
5.6.3 Mortar Samples in Exposure Condition 3.....	96
5.6.4 Mortar Samples in Exposure Condition 4A.....	97
5.6.5 Mortar Samples in Exposure Condition 4B.....	99
5.7 X-ray Computed Tomography (X-ray CT) Analysis.....	102
5.8 Summary and Discussions of Control Mortar Samples.....	103
CHAPTER 6: MORTAR SAMPLES WITH 1.5% POTASSIUM CONTENT.....	107
6.1 Introduction.....	108
6.2 Influence of Potassium Content and Exposure Conditions.....	108
6.3 Mortar Samples Subjected to Duggan Heat Cycles Test Results.....	108
6.3.1 Expansion Results.....	108
6.3.2 Weight Change Results.....	112
6.3.3 Expansion against Weight-Change of Specimens.....	115
6.3.4 Compressive Strength Results.....	119
6.4 Field Samples (No Duggan Heat Cycle).....	119
6.4.1 Expansion Results.....	120
6.4.2 Weight-Change Results.....	122
6.4.3 Compressive Strength Results.....	125
6.5 Water Analysis Results of Storage Solution.....	125
6.5.1 Water Analysis of Exposure Condition 1.....	125
6.5.2 Water Analysis of Exposure Condition 2.....	126
6.5.2.1 Amount of Alkalis.....	126
6.5.2.2 pH Value.....	127
6.5.2.3 Calcium Concentration.....	127
6.6 Microstructure Analysis Using (SEM) and (EDAX).....	128
6.6.1 Mortar Samples in Exposure Condition 1.....	129
6.6.2 Mortar Samples in Exposure Condition 2.....	130
6.6.3 Mortar Samples in Exposure Condition 3.....	130
6.6.4 Mortar Samples in Exposure Condition 4A.....	131
6.6.5 Mortar Samples in Exposure Condition 4B.....	132
6.7 X-ray Computed Tomography (X-ray CT) Analysis.....	134
6.8 Summary and Discussion of Results	136

CHAPTER 7: SUMMARY AND CONCLUSIONS.....	138
7.1 Introduction.....	138
7.2 Summary.....	138
7.3 Conclusions.....	140
REFERENCES.....	142

LIST OF TABLES

4.1	Chemical Composition of Type III Portland Cement.....	53
4.2	Technical Specification Sheet for Frederick Sand.....	54
4.3	Total Number of Mortar Samples Prepared.....	58
4.4	Mixing Proportions for Each Batch of Mortar Specimens.....	58
4.5	Batches and Exposure Conditions.....	60
5.1	Linear and Polynomial Equations for Expansion vs. Age of Steam-Cured Mortar Samples Stored Under Different Exposure Conditions.....	73
5.2	Linear and Polynomial Equations for Weight-Change vs. Age of Steam-Cured Mortar Samples Stored Under Different Exposure Conditions.....	77
5.3	Linear and Polynomial Equations for Expansion vs. Weight Change of Steam-Cured Mortar Samples Stored Under Different Exposure Conditions.....	80
5.4	Compressive Strength of Mortar Specimens Subjected to Duggan Heat Cycle and Stored Under Different Exposure Conditions.....	81
5.5	Linear and Polynomial Equations for Length vs. Age of Mortar Samples Stored Under Field Conditions.....	84
5.6	Linear and Polynomial Equations for Weight Change vs. Age of Mortar Samples Stored Under Field Conditions.....	87
5.7	Compressive Strength of Mortar Specimens Exposed to Field Conditions.....	87
6.1	Linear and Polynomial Equations for Expansion vs. Age of Steam-Cured Mortar Samples Stored Under Different Exposure Conditions.....	111
6.2	Linear and Polynomial Equations for Weight Change vs. Age of Steam-Cured Mortar Samples Stored Under Different Exposure Conditions.....	116
6.3	Linear and Polynomial Equations for Expansion Against Weight Change of Mortar Samples Subjected to Duggan Heat cycle and Stored Under Different Exposure Conditions.....	118
6.4	Compressive Strength of Mortar Specimens Subjected to Duggan Heat Cycle and Stored Under Different Exposure Conditions.....	119

6.5	Linear and Polynomial Equations for Length vs. Age of Mortar Samples Stored Under Field Conditions.....	122
6.6	Linear and Polynomial Equations for Weight Change vs. Age of Mortar Samples Stored Under Exposed Conditions.....	124
6.7	Compressive Strength of Mortar Specimens Exposed to Field Conditions.....	125

LIST OF FIGURES

2.1	Heat Treatment Program.....	24
4.1	Mortar Specimens Exposed to Field Conditions.....	57
4.2	Identification of Specimens.....	59
4.3	Comparator Set up for Length Change Measurements.....	62
4.4	Weighing Mortar Bars.....	63
4.5	ISE and Benchtop Meter Set up for Water Analysis.....	64
5.1	Expansion of Mortar Samples Subjected to Duggan Heat Cycle and Stored Under Different Exposure Conditions.....	70
5.2	Expansion of Mortar Samples Subjected to Duggan Heat Cycle and Stored in Isothermal Water Bath, pH maintained at 12.5 (Regression Curves).....	71
5.3	Expansion of Mortar Samples Subjected to Duggan Heat Cycle and Stored in Plain Water at Room Temperature (Regression Curves).....	72
5.4	Expansion of Mortar Samples Subjected to Duggan Heat Cycle and Stored in Moist Air Chamber, R.H maintained at 97% (Regression Curves).....	72
5.5	Weight Change of Mortar Samples Subjected to Duggan Heat Cycle and Stored Under Different Exposure Conditions.....	74
5.6	Weight Change of Mortar Samples Subjected to Duggan Heat Cycle and Stored in Isothermal Water Bath, pH maintained at 12.5 (Regression Curves)....	75
5.7	Weight Change of Mortar Samples Subjected to Duggan Heat Cycle and Stored in Plain Water at Room Temperature (Regression Curves).....	76
5.8	Weight Change of Mortar Samples Subjected to Duggan Heat Cycle and Stored in Moist Air Chamber, R.H maintained at 97% (Regression Curves).....	76
5.9	Expansion Against Weight Change of Mortar Samples Subjected to Duggan Heat Cycle and Stored Under Different Exposure Conditions.....	78
5.10	Expansion Against Weight Change of Mortar Samples Subjected to Duggan Heat Cycle and Stored in Isothermal Water Bath, pH maintained at 12.5 (Regression Curves).....	79

5.11	Expansion Against Weight Change of Mortar Samples Subjected to Duggan Heat Cycle and Stored in Plain Water at Room Temperature (Regression Curves).....	79
5.12	Expansion Against Weight-Change of Mortar Samples Subjected to Duggan Heat Cycle and Stored in Moist Air Chamber, R.H maintained at 97% (Regression Curves).....	80
5.13	Length Change of Mortar Samples Exposed to Field Conditions.....	83
5.14	Length Change vs. Age of Steam-Cured Mortar Samples and Stored Under Field Condition 4A (Regression Curves).....	83
5.15	Length Change vs. Age of Mortar Samples and Stored Under Field Condition 4B (Regression Curves).....	84
5.16	Weight Change of Mortar Samples Exposed to Field Conditions.....	85
5.17	Weight Change vs. Age of Steam-Cured Mortar Samples and Stored Under Field Condition 4A (Regression Curves).....	86
5.18	Weight-Change vs. Age of Mortar Samples and Stored Under Field Condition 4B (Regression Curves).....	86
5.19	Alkalis Leaching from Mortar Samples Stored in Isothermal Water Bath, pH maintained at 12.5.....	89
5.20	Alkalis Leaching from Mortar Samples Stored in Plain Water at Room Temperature.....	90
5.21	Calcium Leached from Mortar Samples Stored in Plain Water at room Temperature.....	91
5.22	SEM and EDAX of Mortar Specimens in Exposure Condition 1 at Age of 40 days, Showing Ettringite Crystals and Patches of Calcium Hydroxide.....	93
5.23	EDAX of the Elemental Analysis of Massive Deposits that Shown in Figure 5.22.....	93
5.24	SEM and EDAX Analysis of Mortar Specimens in Exposure Condition 1 at Age of 100 days, Showing Clusters of Ettringite Needles Filling Cavities.....	94
5.25	SEM and EDAX Analysis of Mortar Specimens in Exposure Condition 2 at Age of 40 days, Showing Ettringite Balls Filling the Cavity.....	95

5.26	SEM of Mortar Specimens in Exposure Condition 2 at a Higher Magnification.....	95
5.27	SEM and EDAX Analysis of Mortar Specimens in Exposure Condition 2 at Age of 100 days, Showing Ettringite Balls Filling an Aggregate Pull-Out.....	96
5.28	SEM and EDAX Analysis of Mortar Specimens in Exposure Condition 3 at Age of 40 days, Showing Ettringite Needles and CH Crystals Filling the Cavity.....	97
5.29	SEM Micrograph of Mortar Specimens Under Field Condition 4A at Age of 40 days, Showing Ettringite Needles and CH Crystals Between Aggregate and Cement Paste.....	98
5.30	EDAX Analysis of whole area (A) and spot B (CH crystals).....	98
5.31	SEM and EDAX Analysis of Mortar Specimens Under Field Conditions 4A at Age of 100 days, Showing Ettringite Needles and CH Crystals on the Surface of An Aggregate.....	99
5.32	SEM Micrograph of Mortar Specimens Under Field Conditions 4B at Age 40 days, Showing Ettringite Needles and CH Crystals within Air Voids...	100
5.33	SEM Micrograph and EDAX Analysis of Mortar Specimens Under Field Conditions 4B at Age 100 days, Showing CH Crystals within Air Voids.....	101
5.34	SEM Micrograph of Mortar Specimens Under Field Conditions 4B at Age 100 days, Showing CH Crystals within Air Voids at a Higher Magnification.....	101
5.35	X-ray Computed Tomography Image of a Section Through a Control Mortar Cube Stored for 40 days in Exposure Condition 1.....	102
5.36	X-ray Computed Tomography Image of a Section Through a Control Mortar Cube Stored for 40 days in Exposure Condition 3.....	103
6.1	Expansion of Mortar Samples Subjected to Duggan Heat Cycle and Stored Under Different Exposure Conditions.....	109
6.2	Expansion of Mortar Samples Subjected to Duggan Heat Cycle and Stored in Isothermal Water Bath, pH maintained at 12.5 (Regression Curves).....	110
6.3	Expansion of Mortar Samples Subjected to Duggan Heat Cycle and Stored in Plain Water at Room Temperature (Regression Curves).....	110
6.4	Expansion of Mortar Samples Subjected to Duggan Heat Cycle and Stored in Moist Air Chamber, R.H maintained at 97% (Regression Curves).....	111

6.5	Weight Change of Mortar Samples Subjected to Duggan Heat Cycle and Stored Under Different Exposure Conditions.....	112
6.6	Weight Change of Mortar Samples Subjected to Duggan Heat Cycle and Stored in Isothermal Water Bath, pH maintained at 12.5 (Regression Curves).....	113
6.7	Weight Change of Mortar Samples Subjected to Duggan Heat Cycle and Stored in Plain Water at Room Temperature (Regression Curves).....	114
6.8	Weight Change of Mortar Samples Subjected to Duggan Heat Cycle and Stored in Moist Air Chamber, R.H maintained at 97% (Regression Curves)....	114
6.9	Expansion Against Weight Change of Mortar Samples Subjected to Duggan Heat Cycle and Stored Under Different Conditions.....	116
6.10	Expansion Against Weight Change of Mortar Samples Subjected to Duggan Heat Cycle and Stored in Isothermal Water Bath, pH maintained at 12.5 (Regression Curves).....	117
6.11	Expansion Against Weight Change of Mortar Samples Subjected to Duggan Heat Cycle and Stored in Plain Water at Room Temperature (Regression Curves).....	117
6.12	Expansion Against Weight Change of Mortar Samples Subjected to Duggan Heat Cycle and Stored in Moist Air Chamber, R.H maintained at 97% (Regression Curves).....	118
6.13	Length Change of Mortar Samples Exposed to Field Conditions.....	120
6.14	Length Change vs. Age of Steam-Cured Mortar Samples and Stored Under Field Condition 4A (Regression Curves).....	121
6.15	Length Change vs. Age of Steam-Cured Mortar Samples and Stored Under Field Condition 4B (Regression Curves).....	121
6.16	Weight Change of Mortar Samples Exposed to Field Conditions.....	123
6.17	Weight Change vs. Age of Steam-Cured Mortar Samples and Stored Under Field Condition 4A (Regression Curves).....	123
6.18	Weight Change vs. Age of Mortar Samples and Stored Under Field Condition 4B (Regression Curves).....	124

6.19	Alkalis Leaching from Mortar Samples Stored in Isothermal Water Bath, pH maintained at 12.5.....	126
6.20	Alkali Leaching from Mortar Samples Stored in Plain Water at Room Temperature.....	127
6.21	Calcium Leached from Mortar Samples Stored in Plain Water at Room Temperature.....	128
6.22	SEM and EDAX Analyses of Mortar Specimens in Exposure Condition 1 at Age of 40 days, Showing Ettringite Balls and CH Crystals Filling the Cavity.....	129
6.23	SEM and EDAX Analysis of Mortar Specimens in Exposure Condition 2 at Age of 40 days, Showing Ettringite Needles, Ettringite Spherical Balls and CH Clusters Filling the Air Voids and Cavities.....	130
6.24	EDAX Analysis of Mortar Specimens in Exposure Condition 3 at Age of 40 days.....	131
6.25	EDAX Analysis of Mortar Specimens Under Field Conditions (Exp. Cond. 4A) at Age of 40 days.....	132
6.26	SEM Micrograph of Mortar Specimens Under Field Conditions (Exp. Cond. 4B) at Age of 40 days.....	133
6.27	SEM Micrograph of Mortar Specimens Under Field Conditions (Exp. Cond. 4B) at Age of 40 days.....	133
6.28	X-ray Computed Tomography Image of a Section Through a Mortar Cube Made with 1.5% K ₂ O Stored for 40 days in Exposure Condition 2.....	134
6.29	X-ray Computed Tomography Image of a Section Through a Mortar Cube Made with 1.5% K ₂ O Stored for 40 days in Exposure Condition 3.....	135
6.30	X-ray Computed Tomography Image of a Section Through a Mortar Cube Made with 1.5% K ₂ O Stored for 40 days in Exposure Condition 4B.....	135

LIST OF ABBREVIATIONS AND SYMBOLS

Å	Angstrom	10^{-10} m	
AH	Aluminum Hydroxide		$\text{Al}(\text{OH})_3$
ASTM	American Society for Testing Materials		
AFm	Monosulfate	$\text{C}_3\text{A} \cdot \text{CaSO}_4 \cdot 12\text{H}_2\text{O}$	
AFt	Ettringite	$\text{C}_3\text{A} \cdot 3\text{CaSO}_4 \cdot 32\text{H}_2\text{O}$	
AAR	Alkali-Aggregate Reaction		
ASR	Alkali-Silica Reaction		
CH	Calcium Hydroxide		$\text{Ca}(\text{OH})_2$
C-S-H	Calcium Silicate Hydrate		
C_3S	Tricalcium Silicate	$3\text{CaO} \cdot \text{SiO}_2$	Alite
C_2S	Dicalcium Silicate	$2\text{CaO} \cdot \text{SiO}_2$	Belite
C_3A	Tricalcium Aluminate	$3\text{CaO} \cdot \text{Al}_2\text{O}_3$	Aluminate
C_4AF	Tetracalcium Aluminoferrite	$4\text{Ca} \cdot \text{Al}_2\text{O}_3 \cdot \text{FeO}_3$	Ferrite
DEF	Delayed Ettringite Formation		
DSC	Differential Scanning Calorimetry		
EDAX	Energy Dispersive Analysis X-ray		
ESEM	Environmental Scanning Electron Microscopy		
Exp. Cond.	Exposure Condition		
FHWA	Federal Highway Administration		
Fss	Ferrite Solid Solution		
ISA	Internal Sulfate Attack		
ISE	Ion Selective Electrode		

MDSHA	Maryland State Highway Administration
mmol/l	Millimoles per Liter 10 ⁻³ moles/l
pH	Acid Concentration Measurement
QXRD	Quantitative X-ray Diffraction
R.H	Relative Humidity
SEM	Scanning Electron Microscopy
TxDOT	Texas Department of Transportation
μm	Micrometer 10 ⁻⁶ m
UMD	University of Maryland at College Park
W/C	Water to cement ratio by weight
Wt.	Weight
X-ray CT	X-ray Computed Tomography

CHAPTER 1: INTRODUCTION

1.1 Background

The premature deterioration of mortar and concrete in the infrastructure is very significant and widely recognized in the world. Restoring and maintaining these structures is very expensive, causes delays, and hinders access. Therefore, there is an increasing demand to produce and specify more durable mortars and concretes to be used in structures in aggressive environment to satisfy the long-term economy and serviceability of the structures.

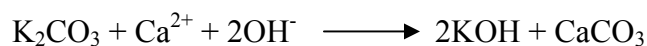
The deleterious reactions in mortar and concrete can be characterized as physical or chemical. Alkali silica reaction (ASR), sulfate attack, carbonation and delayed ettringite formation (DEF) include some of the chemical reactions in concrete, which lead to its premature deterioration. The occurrence of ASR and DEF are associated with expansion and cracks leading to deleterious effects. Based on comprehensive analysis of the literature, Day concluded that there appears to be a potential for delayed ettringite formation problems in North America with the current cement production and construction methods used especially in the Prestressed Industry (1992).

Extensive research studies have been carried out to study the influence on expansion and correlation with curing conditions, aggregate type and cement composition. According to Famy et al 2001, there is no direct correlation established between the amount of ettringite detected and expansion of the heat-cured mortars. Microcracking, late sulfate release and exposure to moisture have been identified as essential characteristics for DEF. The late sulfate release (from cement or aggregate)

would be available later to produce delayed deposition of ettringite in the pre-existing microcracks. Intermittent or continuous exposure to moisture causes swelling or crystal growth of ettringite leading to crack opening, and subsequent damage in the form of macrocracking. The Duggan test method is used to accelerate the potential expansions and generation of excessive ettringite in portland cement within a short period of time in the laboratory.

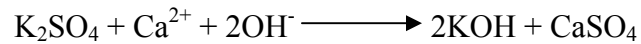
Ettringite is a complex calcium sulfoaluminate hydrate, with the chemical formula $[\text{Ca}_6 [\text{Al} (\text{OH})_6]_2 \cdot 24\text{H}_2\text{O}].(\text{SO}_4)_3 \cdot 2\text{H}_2\text{O}$ and is of practical importance in the technology of Portland cement. The curing temperature was shown to be the critical factor for expansion to occur in hardened concrete, cement paste and mortar (Skoblinskaya et al, 1975 and Famy et al, 2001).

In this experimental study two different phases of mixes are used to study the effect of increase in alkaline content on DEF. Phase I (control) has no additional potassium carbonate added to the mixing water to increase the potassium (K_2O) content, while Phase II has a total of 1.5% K_2O content by weight of cement. Throughout the entire study the same batch of cement and aggregates were used and additional potassium carbonate was added in the mix water. The carbonate salt of potassium is used because it is the ultimate form in carbonated concrete. During the curing of concrete, the carbonate precipitates out in the form of calcium carbonate as shown below:



The calcium and hydroxyl ions are products of the reaction of water and tricalcium silicate ($3\text{CaO} \cdot \text{SiO}_2$), usually abbreviated as C_3S . Thus the end result is the formation of

calcium carbonate (CaCO₃) and potassium hydroxide (KOH), which is the same as the normal form of potassium as potassium sulfate:



In most DEF studies, the heat-cured specimens are stored in water following heating cycles to accelerate expansion and without monitoring the storage conditions (Azzam, 2002 and Ramadan, 2000). Research on the effect of curing conditions and cement composition relating to expansion has been extensive, but very little work has been carried out on the influence of storage conditions after heat treatment. The monitoring of the storage conditions will also help in the understanding of DEF and predicting the amount of alkalis that are leached. Leaching is very substantial for mortars stored in water and less for those stored in 90–100% relative humidity (R.H) (Famy, 2001). In 2001, Famy et al. also estimated that more than 80% of the alkalis present in pore solution of the mortar specimens kept at 90°C in humid air (90-100% R.H) were leached out. Based on a comprehensive literature review the following storage conditions were investigated in this research study:

Isothermal water bath, pH maintained at 12.5.

Plain water and monitored the pH value.

Moist Air Chamber, R.H maintained at 97%.

Field conditions.

1.2 Literature Review

Heinz and Ludwig were the first to use the term “delayed ettringite formation” (DEF) and they used the word “delayed” to suggest that the ettringite did not form at early hydration but some time later due to restriction. Also, the terms “secondary ettringite” and “delayed ettringite formation” are often interchangeable in most research publications. In 1992, Day emphasized the term “secondary ettringite (SEF)” is preferable because, he believes, primary ettringite forms as the sulphoaluminate settles shortly after and tends to disappear when sulfate ions in the pore solution become depleted. Day, in his literature analysis, further suggested that the term DEF is not accurate because “this term implies that conditions within the microstructure might be stable for the formation of ettringite but that ettringite does not form,” which he believes is not true. Other researchers, like Fu and Beaudoin in 1996, suggested that both DEF and SEF occur in concretes and their respective occurrences were different. In this study, the term DEF is preferred over SEF because the term secondary may imply minor or less important.

The natural mineral ettringite was reported in 1847 to occur in limestone minerals in Lava at Ettringen and Mayen in the Rheinland (Dana, 1932). Ettringite was considered to be a mineral consisting of minute, colorless, hexagonal crystals. Candlot’s work published in 1890, first observed the compound now widely accepted as having a formula of $C_3A \cdot 3CaSO_4 \cdot 32H_2O$. It also occurs naturally as a mineral ettringite that consists of a number of minerals having similar structures. In normal modern cement, ettringite forms due to the reaction between gypsum and tricalcium aluminate (C_3A). In Portland cement, the source of most of the sulfate is gypsum or other forms of calcium sulfate added to the

clinker. The main purpose for this addition is to retard the quick setting of the Portland cement clinker that is due to the very high reactivity of C_3A . Calcium sulfate can occur as gypsum ($CaSO_4 \cdot 2H_2O$), hemihydrate ($CaSO_4 \cdot 1/2H_2O$) and anhydrate ($CaSO_4$). The gypsum dissolves relatively quickly in the water releasing a large amount of heat and decomposes to form hemihydrate. The addition of gypsum slows down the rapid reaction of C_3A with water through the formation of ettringite coatings around the C_3A containing grains (Scrivener and Pratt, 1984). The results obtained from most scanning electron microscopes (SEM) shows that ettringite is normally a slender, needle-like, crystal with a prismatic hexagonal cross section (Schwiete, Lucwing and Jager 1966, Midgley and Pettifer 1971, Mehta 1973, Scrivener 1984, Famy, Scrivener and et al 2001).

The action of alkalis, sodium and potassium, are believed to affect the solubilities of the reactants (e.g., tricalcium aluminate (C_3A), calcium hydroxide (CH), and gypsum) in the system and hence the concentration of the ions (e.g. hydroxide ion (OH^-), sulfate ion (SO_4^{2-}), calcium ion (Ca^{2+}), etc.). These alkalis in the Portland cement clinker are mainly from the clay components of the raw materials and from coal. Their total amount, expressed as Na_2O equivalent ($Na_2O + 0.64K_2O$), may range from 0.3 to 1.5 percent of the Portland cement clinker. Thus, alkali compounds in the clinker can be divided into three groups (Diamond, 1976): (1) Alkali sulfates, $Na_2SO_4 \cdot 2K_2SO_4$, $2CaSO_4 \cdot K_2SO_4$, and K_2SO_4 ; (2) Alkali silicate, $KC_{23}S_{12}$; (3) Alkali aluminate NC_8A_3 , and their respective solid solutions. Alkalis apparently can increase the solubility of ettringite and decrease the solubility of the CH (Wang et al 1986 and Daerr, 1977). Basically, the presence of alkali suppresses the dissolution of CH but enhances the formation of ettringite. In 1989, Duggan and Scott proposed a method, referred to as the Duggan test to predict concrete

potential for ASR formation. They subsequently concluded that expansion of specimens subjected to Duggan test is primarily a function of the amount and form of the sulfate in cement material rather than alkali-aggregate reaction (AAR).

In the production of precast concrete products, excessive heat curing at elevated temperature above 70°C is used to promote the development of strength at early ages and to allow for rapid production. Studies by Ronne and Sellevold 1994 and Taylor 1994, showed a lower strength development for concrete cured at high temperature than for concrete cured at normal room temperature. During recent years various studies have shown that Portland cement based materials exposed to temperatures higher than approximately 70°C will stop forming ettringite (AFt) and the already existing ettringite will decompose (Ronne and Sellevold, 1994, and Taylor 1994).

Various laboratory researches on the effect of heat curing have been reported in the literature and it is now generally agreed that when cured above a certain temperature the paste, mortar, or concrete may develop DEF later when exposed to moisture conditions. Most studies outlined that the calcium sulphoaluminates hydrates (AFm) in paste, mortar or concrete are very unstable thermally. In 1941, Kalousek reported that monosulphate is a metastable phase in hardened cement. Later, Heinz and Ludwig (1989) and Klemmm and Adams (1990) confirmed that the monosulphate would form at steam-curing temperatures above 70°C and then transform to ettringite at later stages. In 1988, Stadelman showed that ettringite diminishes at temperatures above 60°C. Later, in 1999, Ronne and Hammer also concluded an apparent decrease of ettringite content in cement pastes interface zone cracks with an increase in temperature from 20°C to 85°C using energy dispersive analysis x-rays (EDAX).

Some controversies concerning a critical curing temperature resulted in employing standards and guidelines. The Norwegian Standard, specifies to keep the heat of hydration generated to below a maximum temperature of 65°C (Ronne and Hammer, 1999) and the Germany Standard limits the maximum temperature of concrete during curing to 60°C for externally exposed concrete (Scrivener, Damidot and Famy, 1999). When hydration generated temperatures becomes a problem, the critical temperature will occur in the inner part of the concrete structure. The moisture content of lightweight aggregate prevents internal drying and may thus keep the moisture above the critical level (Ronne and Hammer, 1999). Consequently, if the moisture content is sufficiently high it will enhance DEF. Again, Ronne and Hammer concluded that the initial curing of concrete at high temperatures might cause volume expansion due to DEF in both normal density and lightweight concrete.

First documented in the early 1980's, laboratory research concluded that one of the factors responsible for DEF was the application of heat and excessive temperatures on the concrete during curing (Ghorah et al., 1980 and Sylla, 1988). Research studies on precast structures made of high strength concretes have been shown to be partly damaged due to loss of strength. Heinz and Taylor (1987) performed studies on, the influence of ettringite in heat-cured mortar and concrete using PZ 55 (C_3A at about 12% by wt. and SO_3 at 3.8% by wt.). They found that the damages are characterized by crack formation emerging from the edges as well as loss of bond between the cement paste and coarse aggregate. Heat treatments were carried out between the range of 20 and 100°C and then the specimens were stored in water at 20°C. Periodical measurements were taken to determine the length change and weight, as well as resonance frequency. Heinz's and

Taylor's results show that temperatures above or equal to 75°C lead to expansion linked with decreases of strength shown by the diminution of resonance frequencies and partly an over proportional increase in weight. It follows that increasing temperatures lead to increases of damage variables in the precast units. Their x-ray analysis of the heat-treated mortar specimens shows that increasing the temperature results in a decreasing amount of ettringite, seen in the basal spacing of 9.7 Å. Their results revealed that the monosulphate phase (AFm) immediately after 70°C heat treatment increases only in the presence of the sulphoaluminate. The aluminate and sulphate ions get bound within the C-S-H gel and later become available to form the AFt phase. They stored their specimens for almost 3 years and found that samples heat-cured at 80 – 100°C contained nothing but ettringite while samples heat-cured at 20°C had the AFt and AFm phases present as at the beginning of hydration. Heinz and Taylor also studied the influence of relative humidity (R.H) and found that the damage reaction became intensified with pre-storage at 60% R.H while being at relative humidity below or equal to 95% caused no expansions.

Calcium silicate hydrate, or C-S-H, in cementitious materials is a phase related to natural calcium silicate hydrates such as tobermorite and jennite. In 1951, Kalousek and Adams believed that the depletion of ettringite at high temperatures can be attributed to the substitution of sulfate ions in the structure of the C-S-H gel, resulting in the loss of sulfate for the stability of ettringite and later confirmed by Odler (1980 and Odler et al., 1987). Kalousek also shows that the amount of missing SO₃ clearly increased with the rise of temperature from 24 to 82°C (1951). He suggested that the missing SO₃ might be the source of ettringite and suspected it to be associated with the C-S-H gel structure.

Furthermore, microanalysis studies by Scrivener and Taylor, 1993; Lewis, 1996; Lewis et al., 1994; and Lewis and Scrivener, 1997 indicate that the rapid growth of the C-S-H leads to the entrapment of sulfate and aluminates species in the gel structure.

In his studies, Lawrence uses about 55 different types of Portland cement to postulate the complex relationship between expansion and curing temperatures (1995). He cured the mortar bars at various initially elevated temperatures and subsequently stored them under water at 20°C. Subsequent storage of specimens in water at 20°C under 100% relative humidity was done to minimize the leaching of alkalis from the specimens. Siliceous sands, composed largely of quartz, were employed in preparing the specimens. Lawrence revealed that at curing temperatures of 60°C or 65°C none of the mortar bars exhibited significant expansion while at 75°C only one of the 55 mortars shows expansion. He found that the critical temperature for expansion for his 55 different cements was between 65°C and 70°C. He concluded that expansion measurements on mortar bars after elevated temperature curing show a complex pattern influenced by the composition of the cement and the detailed curing conditions imposed. Furthermore, Lawrence also reported that temperature curing leads to much reduced expansions, mirroring the chemical changes involving the possibility of ettringite formation after heat curing. Ronne and Sellvold (1994) and Taylor (1994) demonstrated that ettringite would form later if sufficient amounts of moisture or humidity were available.

The implication of heat curing in railroad tie degradation in other countries such as Finland (Eriksson and Tepponen, 1985, Eriksson and Tepponen, 1987.), South Africa (Oberholster et al 1992) and Australia (Shayan and Quick, 1992, Shayan, 1996) is

controversial, as in most cases ASR was also present. Furthermore, research by Shayan in 1996 found that deleterious expansions occurred only when reactive aggregates are used with curing temperatures of 75°C. The expansion mechanism that occurs in mortars and concretes after curing at elevated temperatures is not yet understood and still there exist various uncertainties in its association with delayed ettringite formation.

1.3 Research Approach

Delayed ettringite formation (DEF) has been outlined by researchers as one of the major causes of premature deterioration of concrete structures potentially affecting the durability of concrete. In the past decade many studies on DEF have paid much attention into the potential expansion of Portland cement cured at elevated temperatures.

Extensive laboratory studies have been carried out to study the influence on expansion and its correlation with curing conditions, aggregate type and cement composition. But no correlation has been established between the amount of ettringite detected and expansion of heat-cured mortars (Famy et al, 2001).

This experimental study was conducted in two phases. Phases 1 and 2, mortar samples were mixed and stored under four different storage conditions. Each phase consisted of five (5) mortar batches. All specimens were steam-cured except one (1) set subjected to field conditions and prepared according to the UMD/FHWA modified sample preparation throughout the entire study. The Duggan heat cycle was carried out after one week of casting the specimens. It took sixteen (16) days from casting to storage of the specimens. Phase one (1), with no additional potassium carbonate (K_2CO_3) added to the batch mixes served as the control. At the end of the Duggan Cycle, the specimens

were left outside at room temperature for two (2) days to cool before storing them in various exposure conditions.

In most DEF studies, the heat-cured specimens are stored in water following heating cycles to accelerate expansion and without monitoring the storage environments. Based on extensive literature review, the following exposure conditions were used in this study: Isothermal water bath, pH maintained at 12.5 and monitor potassium and sodium concentration of storage solution; moist air chamber R.H at 97%, plain water and monitored the pH value, potassium, sodium and calcium concentration of the storage solution; and field conditions (No Duggan Heat Cycle). For detailed outlined of the exposure conditions, see Chapter 4.

Phase 2 consisted of five (5) mortar batches with potassium carbonate (K_2CO_3) by weight of cement added to the mixing water. After obtaining the result of the chemical analysis of the cement (shown in Chapter 4), the required amount of K_2CO_3 was calculated based on the potassium oxide (K_2O) content. Additional K_2CO_3 was added to accelerate the expansion rate and enhance the formation of DEF.

The objectives of Phase 1 were to study the mechanism of DEF associated with exposure conditions in a normal type III Portland cement while keeping all other parameters constant. Frederick sand and ASTM Portland Type III cement were used throughout the entire research to study DEF. The objectives of Phase 2 were to study increased potassium content and its association to DEF. Besides preparing mortar bars to study length change and weight change measurements, cubes were made to explore the influence of the different exposure conditions on compressive strength.

In this study, DEF caused by internal sulfate attack (ISA) was investigated. ISA occurs in a sulfate-free environment due to the interaction of internal sulfate (from cement or gypsum contaminated aggregate) with calcium-aluminate hydrates of the cement.

1.4 Problem Statement

Delayed ettringite formation is one form of what is termed as Internal Sulfate Attack (ISA). Sulfate attack involves a set of both chemical and physical processes. Sulfate attack is considered to be the cause of most expansions, disruption of concrete structures, and a decrease in the durability of the concrete by changing the chemical and microstructural nature of the cement paste and of the mechanical properties of the concrete, leading to their deterioration. Concrete structures such as precast units, cladding panels, railway sleepers and ties have suffered damage due to delayed ettringite formation. Delayed ettringite formation deterioration has resulted in expensive rehabilitation of concrete structures in several countries and has led to substantial litigation in the state of California (Kasdan, 2003).

Since 1965, when Kennerly first demonstrated the problems related to DEF, various case studies have been reported, mainly attributed to DEF and excluding alkali-aggregate reaction (AAR) or external sulfate attack. Kennerly revealed that ettringite was found at the cold-joints in the Roxburgh Dam, Otago, New Zealand. He further outlined that the formation of ettringite was due to the variation of the calcium hydroxide (CH) concentration at different areas of the dam. Ettringite was found at the areas of

high CH concentration because the solubility of ettringite is inversely proportional to the CH concentration in the solution.

In the 1980's, several instances of damage to concrete structures were reported as, apparently, mostly due to delayed ettringite formation. In most of the structures reported, DEF contributed a great deal to the deterioration including alkali-aggregate reaction and chloride contamination. In the English Midlands, ettringite was found in the pores, voids, and at the aggregate surfaces in the concrete bases. Also, substations in Western England and South Wales showed similar damage, with ettringite co-existing with gel from the alkali-aggregate reaction (Pettifer and Nixon, 1980). In the same year, Pettifer and Nixon detected ettringite in the concrete just four years after placement of the Pirow Street Bridge in Cape Town, South Africa. In their research studies, Volkwein and Springenschmid (1981) often found needle-like ettringite crystals near the splashing zone of the concrete bridge deck. They further postulated that the rich chloride-contaminated bridge enhanced the formation of ettringite from the sulfate originating from the cement. Deterioration was also found in reinforced concrete of marine structures in Egypt. Ettringite existed in the cracks of three out of the seven reinforced concrete structures (El-Sayed 1987). Ettringite was found in the pores and cracks of precast concrete railway ties steam-cured at high temperatures (75-80°C) using high early strength cement (Heinz 1987, Tepponen 1987). In the South of Sweden, ettringite was found in the concrete of a swimming pool along with CH, calcite and gypsum, which had been leached to the surface. The damage to the concrete was due to a combination of alkali-silica reaction (ASR) and aggressive reaction of sulphates (Chandra and Bernston, 1988).

Lawrence, et al., examined fifteen prestressed and reinforced concrete structures cast between 1963 and 1969 and found expansive cracking problems after fifteen years. They confirmed alkali-silica reaction and found ettringite around the aggregate grains (1990). In Strathclyde, Scotland, Maclead detected ettringite in the form of white spheres within the air-entrained voids of the concrete deck (1990).

A few years after installation of concrete railway ties on the East Coast of the United States, Marusin diagnosis revealed DEF crystals in the cracks (Marusin 1995). Again in the U.S., the Texas Department of Transportation (TxDOT) found premature deterioration of 56 precast/prestressed concrete box beams stored at the fabrication site, which were to be used on highway bridges. The research team postulated that DEF was the primary distress mechanism, with little association with ASR. Other cases studied by TxDOT include a parking garage in central Texas and cast-in-place concrete foundation piers for transmission of power line towers in Austin. The four-story parking garage, constructed in 1986-1987, showed substantial distress in the form of cracks with internal expansion reaction. Just after eight years of service, it was discovered that the cast-in-place concrete foundation piers exhibited premature deterioration, which was attributed to, delayed ettringite formation (Lawrence et al., 1999).

In 2000, Brewer Stadium, Appalachian State University, Boone, North Carolina, reported that 375 of 860 precast units exhibited severe cracking and delamination leading to spalling. Fibrous crystallized ettringite was identified as filling the cracks and voids in the mortar and also in the paste between coarse and fine aggregate in the concrete. Due to significant defects in the precast element attributed to DEF, reconstruction of the stadium proved to be the economical alternative (Ozol, 2000).

1.5 Objectives and Scope of This Study

1. Apply advanced material testing methods and analyze the complex process of expansive cracking associated with DEF;
2. Investigate the effects of storage conditions and their influence in DEF pertaining to weight change, expansion/contraction and damage variables;
3. Study the potential of DEF in mortar specimens as a function of the amount of alkalis leached into the storage solution by water analysis;
4. Study DEF in mortar specimens exposed to field conditions;
5. Study the influence of potassium (K_2O) content on mortar expansion; and
6. Investigate and explore the complexity of DEF at several stages.

1.6 Structure of Thesis

This thesis consists of seven chapters. The first chapter gives a brief review of the literature and background information outlining the overall research. In Chapter 2, cement chemistry and its association to ettringite formation is presented. Chapter 3 deals with a comprehensive collection of literature on delayed ettringite formation, accelerated test methods, and expansion theories. Experimental details such as sample preparation, materials used and test methods are precisely given in Chapter 4. Chapter 5 presents the results of the mortar samples (control) while chapter 6 provides an analysis of the results for the mortar samples with 1.5% potassium content. Finally, Chapter 7 provides the summary and conclusions of this study.

CHAPTER 2: CHEMISTRY OF CEMENT AND ETTRINGITE FORMATION

2.1 Introduction

Portland cement is one of the most widely used and most important materials used in the construction industry today. Cement is the key ingredient used in concrete, mortar, plaster, stucco, and grout.

Portland cement is defined, according to ASTM C150, as a hydraulic cement, one that sets or hardens when mixed with water. Particles of the cement take up water, forming a gel cementing the particles together through a process known as hydration. Cement is produced by pulverizing clinker consisting of hydraulic silicates, usually containing one or more of the forms of calcium sulfate as an interground addition (Derucher et al, 1998). The main minerals required in the production of Portland cement are lime (CaO) about 60 –65 %, silica (SiO₂) about 20 – 25%, alumina (Al₂O₃) and iron oxide (Fe₂O₃) about 7 – 12% (Atkins, 1997).

Eight types of Portland cements are recognized by the ASTM under ASTM C150; type (I, IA, II, IIA, III, IIIA, IV, V). Type I and II are normal cements used generally in most situations calling for Portland cement. Type III, or high early strength, is used when early strength is required as in precast and prestressed concrete. This cement is obtained by finer grinding and by better burning so that the dicalcium silicate (2CaO.SiO₂) is less and the tricalcium silicate is greater (3CaO.SiO₂).

Damages associated with delayed ettringite formation have been mainly with precast concrete made of high early strength cement (Lawrence 1993, Fu et al 1996).

2.2 Portland Cement Composition

In the manufacture of Portland cement, the raw materials, limestone and clay are ground up, mixed to produce the desired proportion of minerals and burned in a large kiln. The temperature of the kiln reaches about 1450°C (Taylor 1997). This drives off water and gases and then produces new chemical compositions in particles called clinker. The clinker is subsequently ground with about 5 percent gypsum (to control rate of hardening) and is then ready for use as Portland cement.

The cement compounds produced are: tricalcium silicate ($3\text{CaO}\cdot\text{SiO}_2$), dicalcium silicate ($2\text{CaO}\cdot\text{SiO}_2$), tricalcium aluminate ($3\text{CaO}\cdot\text{Al}_2\text{O}_3$) and tetracalcium aluminoferrite ($4\text{CaO}\cdot\text{Al}_2\text{O}_3\cdot\text{Fe}_2\text{O}_3$). They are the major phases in cement and usually abbreviated as C_3S , C_2S , C_3A , and C_4AF respectively. The relative amounts of these chemicals in the final product depend on the desired properties such as rate of hardening, amount of heat of hydration and resistance to sulfate attack. Hardening results from the chemical reactions between major phases and water. Hydration reactions of aluminates influence the various types of setting behavior and those of the silicates influence the strength development of mortar and concrete. Chemists normally denote these major phases in cement as: elite (C_3S), belite (C_2S), aluminate (C_3A) and ferrite (C_4AF). Several other phases, such as alkali sulfates and calcium oxide, are present in minor amounts.

Alite is tricalcium silicates ($3\text{CaO}\cdot\text{SiO}_2$ or C_3A) modified in composition and crystal structure by ionic substitutions such as Mg^{2+} , Al^{3+} and Fe^{3+} (Taylor 1997). Elite is the most important constituent and constitutes 50–70% of normal Portland cement clinker. The chemical reaction for elite (C_3S) with water is;



The product, $3\text{CaO}\cdot 2\text{SiO}_2\cdot 3\text{H}_2\text{O}$, is calcium silicate hydrate or tobermorite, which gives concrete its strength.

Belite is dicalcium silicate ($2\text{CaO}\cdot\text{SiO}_2$ or C_2S) and constitutes about 15 – 30% of normal Portland cement clinkers. It reacts with water relatively slowly and contributes little to strength during the first 28 days. It is a major phase that contributes later to the development of the strength.

Aluminate is tricalcium aluminate ($3\text{CaO}\cdot\text{Al}_2\text{O}_3$ or C_3A) and constitutes about 5-10% of most Portland cement clinkers. Its composition and sometimes structure, are significantly modified by foreign ionic substitutions such as Si^{4+} , Fe^{3+} , Na^+ and K^+ . It reacts very rapidly with water and can cause undesirably rapid setting if no set-controlling agent is added.

Ferrite is tetracalcium aluminoferrite ($4\text{CaO}\cdot\text{Al}_2\text{O}_3\cdot\text{Fe}_2\text{O}_3$ or C_4AF) and constitutes 5-15% of normal Portland cement clinkers. It is substantially modified in composition by variation in Al/Fe ratio and substitutions of foreign ions.

Alite and belite react with water to form calcium silicate hydrate (C-S-H) and calcium hydroxide (CH). Calcium silicate hydrate is commonly called C-S-H because it does not have a fixed stoichiometric composition. The aluminate phase reacts with gypsum in the presence of water and yields ettringite.

2.3 Portland Cement Hydration

The hydration of Portland cement is the chemical reaction between the cement clinker components, calcium sulfate and water and is responsible for the setting and hardening of mortar and concrete. The setting process is a consequence of changes from

a concentrated suspension of flocculated particles to a viscoelastic skeletal solid capable of supporting an applied stress (Gartner et al, 2002). The development of the solid skeleton is known as hardening and leads to the ultimate mechanical properties and durability of the mortar or concrete.

During the earliest stage of hydration, a series of rapid reactions begin which involve mainly clinker interstitial phases (i.e., aluminates and aluminoferrites, alkali sulfates, and free lime), plus calcium sulfates (gypsum, hemihydrate and/or anhydrite) that have been interground into the cement (Gartner et al. 2002). After several hours, definite shells of hydration products, mostly C-S-H, CH, ettringite needles or thin calcium monosulfate (AFm Phase) plates are sometimes present in the shells (Diamond 1987). This layer of ettringite or AFt phase is often poorly crystalline and difficult to detect by the X-ray diffraction (XRD) (Gartner, 2002 and Taylor, 1997). The AFt phase contains lots of sulfate, which comes from the rapidly soluble sources such as alkali sulphates, hemihydrate and gypsum. The continued formation of AFt and AFm phases can influence the workability but the C-S-H formation leads to the onset of normal set concrete.

Although the cement paste shrinks due to drying, hydration continues for years if water is available. The hydration products are found around the grains and prevent the access of water to the unhydrated particles, which impede the late hydration (Azzam, 2002). This causes a continuous strength increase due to porosity but at an ever-diminishing rate (Gartner, 2002).

2.3.1 Hydration of Calcium Silicate

The main product of Portland cement, $3\text{CaO}\cdot 2\text{SiO}_2\cdot 3\text{H}_2\text{O}$, is calcium silicate hydrate or tobermorite gel, C-S-H, which constitutes 50-60 % of the hydration cement paste and is the most important in determining the properties of the paste. The C-S-H quality and composition gives concrete its strength.

The C-S-H is not a well-defined compound and the C/S ratio varies between 1.5 to 2.0 (Mehta 1993). The internal structure of the C-S-H remains unsolved due to its indefinite stoichiometry. The hydrations of silicates are accelerated in the presence of sulfate ions in the solution. Various observations indicate that absorption of sulfate ions (SO_4^{2-}) by the C-S-H plays an important part in the mechanism of expansion and formation of ettringite (Older 1980, 1987, Fu et al. 1994, Scrivener 1992, 1993, Lawrence 1990, Lewis 1994, 1996, 1997 and Taylor, 1997). After storage of specimens, sulfate is released from the lighter inner C-S-H gel at a rate that is affected by the hydroxide concentration of the pore fluid, which depends on the hydroxide solution of the storage solution (Famy, 2001). Basically, the higher the hydroxide concentration, the lower the rate of sulfate release and expansion. Also, the leaching of alkalis increases the rate at which sulfate is released from the C-S-H and causes an increase in the pH level of the storage solution. Therefore, limiting alkali leaching slows down sulfate release and in turn retards the expansion process leading to the formation of DEF (Famy, 2001).

2.3.2 Calcium Hydroxide

Calcium hydroxide, $\text{Ca}(\text{OH})_2$ crystals are another major product formed during Portland cement hydration and it constitutes 20 - 25 % of the volume of solids in the

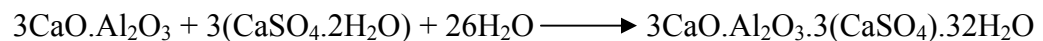
hydrated paste. Unlike C-S-H, calcium hydroxide (CH) has a definite stoichiometry and an adverse effect on the chemical durability of acidity solutions. The dissolution of CH is greatly suppressed in the presence of alkalis but this enhances the formation of ettringite. Also, the presence of CH increases expansion (Cohen and Richards, 1982, Mehta, 1973).

2.3.3 Hydration of Aluminates

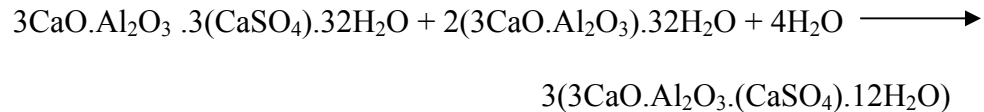
Several hydraulic calcium aluminates can occur in the CaO-Al₂O₃ system; however, tricalcium aluminate (C₃A) is the principal aluminate compound in Portland cement clinker. Calcium ferrites usually are not formed in ordinary Portland cement clinker; instead, calcium ferroaluminates that belong to the C₂A-C₂F ferrite solid solution (fss) are formed and correspond approximately to C₄AF.

The reaction of C₃A and water is very rapid and the addition of gypsum slows down the reaction. This retardation is attributed to the formation of ettringite coatings around the C₃A containing grains (Colleparidi et al, 1987, Scrivener and Pratt, 1984). Reaction of C₃A with water in the presence of sulfate may produce calcium aluminate hydrate, 3CaO.Al₂O₃.3(CaSO₄).32H₂O (ettringite) or 3(3CaO.Al₂O₃.(CaSO₄).12H₂O) (monosulfate) depending on the concentration of the aluminate and sulfate ions in the solution.

In solutions saturated with calcium and hydroxyl ions, the former crystallizes as short prismatic needles referred to as high-sulfate or ettringite and usually is termed as the AFt phase. The hydration reaction in the presence of sulfate is:



Ettringite forms immediately after mixing and acts as a skeleton, providing the principal source of early stage strength. This ettringite may be very unstable, react with more C_3A , and be converted into monosulfate. The monosulfate (AFm phase) is also called low-sulfate and crystallizes as thin hexagonal plates. The chemical reaction for monosulfate is:



2.4 Heat of Hydration

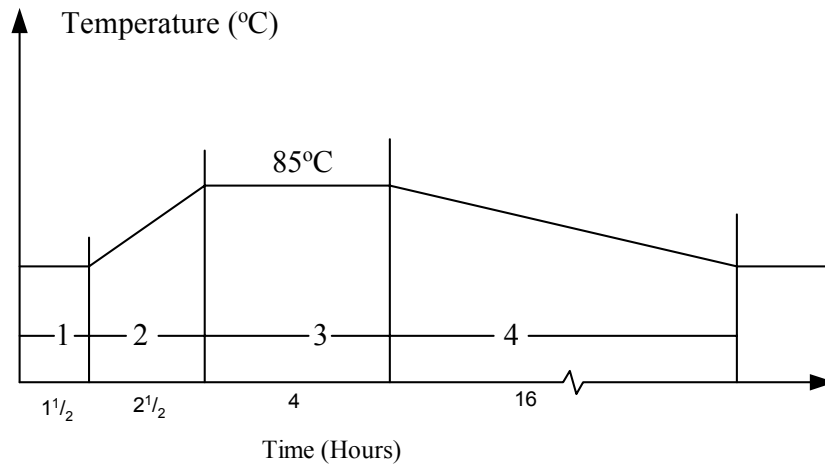
The compounds of Portland cement are none equilibrium products of high-temperature reactions and these compounds react with water to acquire stable low-energy states (Mehta, 1993). The hydration reactions involve the release of energy in the form of heat. The total amount of heat liberated and the rates of heat liberation from hydration of the individual compounds can be used as indices of their reactivity. Also, the heat of hydration characterizes the setting and hardening behavior of cements and can be used for predicting temperature rise in concrete paste.

For typical Portland cement, approximately 50 percent of the potential heat is liberated within the first 3 days and 90 percent within the first 3 months of hydration. It should be noted that, as the percentage of C_3A and C_3S increases, the heat of hydration increases. From analyses of heat of hydration of various cements by Verbeck and Foster in 1950, they computed the individual rates of heat evolution due to the four principal compounds in Portland cement. They concluded that the total heats of hydration at a

given age and under given conditions are due to the additive percentage contents of C_3S , C_2S , C_3A and C_4AF present in the cement.

2.5 Heat Treatment of Mortar and Concrete

The heat treatment method was used to accelerate the strengthening of the mortar specimens. Similar heat treatment programs have been used in the prestressed / precasted industry for the production of concrete box beams and railway sleepers to obtain high strength within short periods of time. Figure 2.1 shows the heat treatment program used. To prevent over drying and shrinkage the exposed parts of the specimens were covered with aluminum foil throughout the heat treatment program. Most DEF cases were associated with the use of high heat treatment such as this. Various researches found that the curing method plays an important role in DEF formation but is not the primary factor. In 1999, Stark and Bollmann found that ettringite also occurs in no-heat treated concrete, which is exposed only to normal climatic conditions.



- 1 – The Presetting time
- 2 – Heating
- 3 – Heat (Steam) Curing at 85°C
- 4 – Cooling, overnight

Figure 2.1 – Heat Treatment Program (Adapted from Azzam, 2002)

2.5.1 Effect of Heat Treatment on the Stability and Formation of Ettringite

Heat treatment is used in the production of precast concrete to promote the early strength development and to allow rapid production. In 1954, Powers et al revealed that the maximum curing temperature used may be in the range of 40 to 100°C (10 to 21°F), although the optimum temperature is in the range of 65 to 85°C (150 to 175°F). The heat treatment affects the stability and formation of ettringite, and absorption of sulfate ions.

Ettringite is not entirely stable; it may lose water or decompose under certain conditions. Ettringite as a crystal has 32 water molecules, which easily dehydrate upon heating in dry conditions. Parameters such as relative humidity, the pH value of storage

solutions, and the concentration of the sulfate ions in solutions affect the stability of ettringite.

In 1963, Lieber concluded that ettringite was stable in water up to 90°C. A similar study by Mehta revealed that ettringite was only stable up to 66°C if heated dry but started to decompose at 93°C (1969). Other researchers results' were controversial, when Satava and Veprek investigated the stability of ettringite in saturated steam and found that ettringite did not decompose even at 110°C (1975). In 1985, Ghorab et al studied the stability of ettringite in relation to its solubility in pure water at 30°C, 60°C and 100°C. They found that ettringite was stable up to two weeks of stirring in water at 60°C. When stirred in pure water at 100°C, after one hour the ettringite decomposes to monosulfate (AFm phase). Sylla in 1988 examined the stability of ettringite at various temperatures and his results suggested that the stability of ettringite in cementitious systems is not only related to the curing temperature but also to the maturity of the system at the time it is heat-cured. He showed that if specimens were pre-cured for several hours at room temperature, some of the ettringite persists even at 80°C heat-curing, and in the specimens that were not pre-cured, no ettringite was found after heat-curing at 80°C.

Many researchers suggested that the stability of ettringite in cementitious systems might be related not only to the curing temperature but also to the hydration of the Portland cement (Sylla, 1988, Kalousek and Adam 1951, Fu et al, 1944 and 1995). It was reported that, during heat curing, sulfate and aluminate ions may get adsorbed by the C-S-H gel. The applied high heat curing temperature destroys ettringite. Ettringite decomposition during heat curing is closely related to the adsorbing of sulfate and

aluminate ions but not to the instability nature of ettringite (Heinz and Ludwig, 1987). Fu, Xie, Gu and Beadoin, in 1994 and 1995, reported that the C-S-H gel will adsorb sulfate ions faster at high temperature and sulfate adsorbed at high temperature is desorbed more slowly than that adsorbed at normal temperature. They further concluded that the slower release of sulfate ions from an internal sulfate source might be an important condition for delayed ettringite formation in high temperature-cured cementitious systems.

In 1996, Lewis performed microanalyses on C-S-H of heat-cured cementitious systems in his investigation of delayed ettringite formations. His findings revealed that the sulfur-calcium ratio of C-S-H was high after high temperature heat curing, but decreased with the curing age. Yang et al also confirmed Lewis's results (1995 and 1996). Divet et al found that C-S-H has a high capacity of adsorbing SO_4^{2-} ions, which depends on the pH level of the pore solution of the cementitious system and on the temperature (1998). They also found that the adsorption of SO_4^{2-} ions by the C-S-H gel increases as the pH and temperature increases.

It is believed by many researchers that ettringite formation depends mainly on the exposure conditions (Lawrence, Dalziel and Hobbs, 1990 and Famy et al, 2001). The expansion and cracking of cementitious systems subjected to heat treatment above 70°C and subsequently immersed in wet or moist conditions contributed to delayed ettringite formation (Heinz, 1986, Heinz and Ludwig, 1986, Lawrence, 1990, 1995, Sylla, 1988 and Ronne, 1999).

2.5.2 Effect of Heat Treatment on the Strength of Mortar and Concrete

The influence of heat treatment on the compression and bending strengths of mortar and concrete has been researched and well documented by Chamberline, Brewer and Shideler, 1952, Klieger, 1958, Hanson, 1963, Farsky, 1971, and Ronne and Sellevold, 1994. In 1971, Farsky investigated the delayed period influences on the properties of steam-cured mortar specimens. Portland cement was used in making the mortar specimens, beams 4 x 4 x 16 cm. Investigations of various delay periods were performed, ranging from 30 minutes to 7 hours 30 minutes. Samples were then subjected to heat in a steam chamber maintained at 70°C. A set of specimens was tested in bending and compression immediately after heating. The next series were tested after twenty-four hours of hardening. Another two series were tested at the end of 28 days hardening, one of them after curing in humid atmosphere and the other after curing in water. Farsky's results revealed that curing in water has no considerable influence on the 28-day compressive strength, but results in an increase of about 10 to 15 percent in the bending strength.

The compressive strength decreases as a result of the rapid temperature rise during pretreatment of mortar and concrete specimens (Saul, 1951). The precast concrete industries use accelerated hardened of concrete (AHC) methods, which include delay period, soaking time, temperature and all other technological aspects of concrete in its condensed state. Various investigators suggest an optimum delay period of 1¹/₂ hours and they found that a shorter delay period results in a decrease in compressive strength of about 70 to 75 percent (Farsky et al, 1971).

2.5.3 Effect of Heat Treatment on Cement Chemistry and Microstructure

The utilization of heat curing in the precast industry to accelerate the hardening of the concrete in order to achieve high early strength and provide rapid production has been very successful. The high temperature used may change the composition of the hydration cement and thereby alter the microstructure of the cementitious system.

Investigation by Idorn on the effect of hydration temperature on the hydration of Portland cement revealed that, at high temperatures, smaller amounts of hydrated aluminate, ferrite or sulfoaluminate phases will be formed and the ratio of ettringite to monosulfate will be reduced (1968). A similar research by Odler et al showed that the C-S-H formed at elevated temperature has a lower water content and higher Ca/Si ratio (1987). Odler et al also revealed that the amount of foreign ions (Al^{3+} , Fe^{3+} , SO_4^{2-}) incorporated in the C-S-H phase increases with a rise in hydration temperature. They finally concluded that the decrease in compressive strength at elevated temperatures was due to the increase in porosity. In 1996, a report from Kjellsen also confirmed that the Ca/Si ratio of the outer product in heat-cured concrete was significantly higher than that in the concrete that was continuously cured at room temperature. Other researchers obtained similar results (Oztek, 1984, and Bentur and Berger, 1979).

Escalante-Garcia and Sharp postulated that the high temperature curing increases the rate of heat of hydration of all the main phases in Portland cement at early ages (1998). However, the ultimate degree of hydration was reduced by high curing temperature. In 1992, Kjellsen and Detwiler found similar results, and they concluded that the ultimate degree of hydration, evaluated by means of the non-evaporable water content, tended to increase with a rise in hydration temperature. From their research work, Verbeck and Helmuth suggested that the curing temperature at elevated

temperatures results in a non-uniform distribution of the hydration product within the microstructure of the cement paste, with a high concentration of hydration product built up around the hydrating grains which subsequently retards the hydration process (1968).

In 1996, Kjellsen studied the effect of heat curing and post-heat curing regimes on the microstructure and C-S-H composition of high performance concrete. He stored the concrete samples under different conditions and he found that the heat-cured high performance concrete showed a higher content of hollow shell pores at later ages than a continuously cured sample at room temperature. He also noticed a significant amount of CH formed in hollow shells in the concrete cured at room temperature. He postulated that this may be one of the reasons for the apparently hollow shell porosity and for the low Ca/Si ratio of the outer product in the room temperature cured concrete.

Other effects of heat curing at high temperatures may lead to the concrete paste in the vicinity of aggregates tending to be more porous and having more ettringite rods and CH crystals than the bulk paste (Mouret et al, 1999). They compared their images obtained from SEM and environmental scanning electron microscope (ESEM) and pointed out that the drying procedure in the SEM sample preparation may cause microcracking in the paste and induce gaps between paste and aggregate.

Scrivener studied the effect of heat treatment on the inner product C-S-H and revealed the “two tone” feature of the inner hydration product in the cement pastes (1992). She heat-cured specimens at 80°C and subsequently stored them in water at 20°C. She observed the “two tone” comprised of a brighter outer band, considered to be formed at 80°C, and a darker inner band, considered to be formed due to storage at 20°C. She also reported that the darker inner band increases in thickness as hydration of the

cement paste proceeds. Later, Diamond et al, presented SEM images of polished samples from room temperature cured cement paste showing the “two tone” feature. They further revealed that the “two tone” feature can occur in both heat-cured and room temperature cured concrete (1998).

CHAPTER 3: DELAYED ETTRINGITE FORMATION

3.1 Introduction

Delayed ettringite formation (DEF) has been considered as one of the potential destructive reactions affecting the durability of concrete. DEF can be defined as formation of ettringite in a paste, mortar, or concrete by a process beginning after hardening is substantially complete and in which there exists no external sulfate source. Ettringite can cause damages that may be apparent only after a period of months or years. The first reactions to occur, when Portland cement concrete is cured under ambient conditions, are associated with tricalcium aluminate (C_3A) and its reaction with sulfate ions in the pore solution to form ettringite. Ettringite that forms early is almost certainly a product of recrystallization. The later formation of ettringite after the concrete has hardened is the potential host for destruction and the cause of final deterioration of the concrete.

The potential for deterioration of Portland cement concrete due to DEF has been recognized in the precast industry since Heinz et al reported cases related to high temperature ($>75^{\circ}C$) steam-cured concrete (Heinz and Ludwig, 1987, Heinz, Ludwig and Rudiger, 1989). They argued that delayed expansion in concrete was due to the transformation of metastable monosulphate into ettringite when steam curing was subsequently followed by normal temperature moist curing at later ages. Various researchers confirmed this phenomenon (Siedel et al. 1993 and Grabowski et al. 1992).

In the presence of gypsum and lime, Portland cement hydration produces reaction products of tricalcium aluminate that include both monosulphate and tetracalcium

aluminate hydrates. These hydrated aluminates are essential components of formation of ettringite at later ages. The source of SO_3 -bearing materials in the presence of aluminate phases appears to be very critical for DEF. Sulfate attacks on concrete have been widely investigated by many researchers. Delayed ettringite formation occurrences have been reported with cements associated with high sulfate content (4 – 5% SO_3), usually high clinker sulfate (Diamond, 1996). Late discovery of DEF may be associated with changes in the cement composition, which has taken place in the last several decades. Reports of representative American cements analyses and their respective clinkers were typically less than 0.5% and the total cement sulfate contents were usually less than 2% (Lerch and Ford, 1948). Recent cements and clinker sulfate levels of 3% or more and total sulfate levels of 4 – 5% are common (Diamond 1996). Other factors reported to influence DEF include cement type, fines and composition, concrete curing and exposure conditions. All these factors contribute to the damages associated with DEF and deterioration effect on concrete structures.

3.2 Damaged Caused by DEF

In the past two decades, expansion has been associated with internal deleterious expansive reaction, known as ettringite formation in hardened concrete. Ettringite was reported as the possible damage to the concrete structure of the Roxburgh Dam, Otago, New Zealand (Kennerley, 1965). Ettringite was found in the cold-joints of the dam.

Several causes of damage to concrete structures have been reported, mostly apparently due to DEF. In the English Midlands, ettringite was found in the pores, voids and at the aggregate surfaces in the concrete bases (Pettifer and Nixon, 1980). Pettifer

and Nixon also detected ettringite in the concrete of the Pirow Street Bridge in South Africa.

In the U.S. concrete railway ties on the East Coast were diagnosed as revealing delayed ettringite crystals in the cracks (Maurusin,1995). Also, in Texas, precast concrete box beams awaiting installation on a highway bridge exhibited significant expansion cracking attributed to DEF. Other structures in Texas also identified damages due to DEF such as cast-in-place concrete foundation piers and parking garages (Lawrence et al, 1999).

Ettringite is usually found in structures such as railway ties, precast / prestress concrete, walls and stairways of parking garages, cast-in-place foundation piers, cladding panels and foundation slabs, and transmission pole footings (Mielenz, 1995, Chandra et al, 1988, Oberholster, 1992, Ozol, 2002, Schlorholtz, 1993 and 1995, and Vitousova, 1991). Expansions due to ettringite (gel-like material) are typically characterized by map cracks. SEM and X-ray analyses are commonly used to identify the chemical composition of ettringite. Exploration of the physical conditions for DEF and DEF-induced expansion would be ideal ways to examine this gel-like material. Basically, researching the different conditions for DEF would probably lead to better understanding of the complex expansive mechanism and provide appropriate test methods and suitable preventive measures.

3.3 Conditions for DEF

Various researches have been carried out to explore the complexity and conditions necessary for DEF and its associated expansion. Hypothesis and holistic

perspective that were exposed in order to satisfactorily address the necessary conditions to enhanced delayed ettringite formation were based on 3 (three) essential elements (Collepardi, 1999). The essential elements were the late sulfate release (from cement or aggregate), the pre-existing microcracks caused during manufacturing or any other initiated mechanism and intermittent or continuous exposure to environmental water or saturated air causing swelling or crystal growth of ettringite leading to crack opening, and subsequent damage in form of macrocracking. Other researchers also believe that high temperature is essential factor for DEF (Heinz and Ludwig, 1986, 1987, Heinz et al, 1989, Taylor, 1993, Ghorab et al, 1980 and Ludwig, 1991).

3.3.1 Sulfate in Cement and Cement Clinker

Modern cements such as Portland cement are manufactured in kilns that burn sulfur-rich fuels or organic residues can incorporate huge amount of sulfate (up to about 2.5%) in the clinker (Miller and Tang, 1996). Particularly in the precasted / prestressed production of concrete ties, there were significant increase in the incidence of internal sulfate attack (ISA)-related DEF in the last two decades. This may be related to the use of high-sulfur fuels and organic residues in the clinker sulfate. Different fuels are used in the manufacturing process such as gaseous or liquid hydrocarbons, as well as solid small-particle coals, depending on the cheapest available fuels. The sulfur content of these fuels can change and cause-unwitting variations of sulfate incorporated in the clinker phase of the cement.

According to Hime, some of the sulfur in the clinker phase is present as relatively slow soluble sulfate (1996). They are unavailable for the early ettringite formation but

would later be available to produce delayed ettringite formation. These sulfate enter into the solution, after hardening of the concrete and reacts with C_4AH and water to form ettringite. Delayed deposit of ettringite into these cracks expands causing the concrete to crack and deteriorate. Many researchers have attributed DEF to the sulfur in the clinker phase of the Portland cement (Hime 1996, Gress and Mielenz et al, 1995).

3.3.2 Presence of Microcracks

The pre-existing of microcracks is considered essential to damages associated with DEF. Concrete and mortar cracking can be promoted by other mechanisms that cause microcracks, which then promote the ettringite deposition into pre-existing microcracks. These mechanisms include curing at high temperatures, localized high stress in prestressed structures, freeze-thaw cycles, ASR with microcracks around aggregate particles, dynamic loads, and fatigue stresses (Fu et al, 1996, Shayan, 1995, Oberholster et al, 1992 and Tepponen and Eriksson, 1987 and Colleparidi, 1999).

Fu et al studied the significance of pre-existing cracks on nucleation of secondary ettringite in steam-cured cement paste (1994). They mechanically induced microcracks to their cement paste specimens and their respective expansions under different curing conditions. They concluded that nucleation of ettringite crystals in cement pastes will occur preferentially under conditions of supersaturation in cracked tip zones rather than on plane solid surfaces. They also postulated that high temperature steam curing followed by high temperature drying is a favorable condition for deterioration by secondary ettringite formation, and that larger, pre-existing cracks are caused by high expansion due to secondary ettringite formation.

Fu and Beaudoin investigated the influence of microcracking on delayed ettringite formation in cementitious systems (1996). Different treatments, such as high temperature curing, loading, and freezing/thawing, were applied after 24 hours to induce microcracks. They found that mortar and concrete bars that were cured at elevated temperatures (85°C for concrete, 95°C for mortar) and subsequently treated with high temperature drying showed significant expansion. All other specimens did not show any significant cracks after 250 days of storage. They revealed that the pre-existing microcracks are a precursor for delayed ettringite formation.

3.3.3 Exposure to Moisture

The intermittent or continuous exposure to water or humid air is reported to be one of the essentials for delayed ettringite formation to occur. The presence of water filling the pore system of concrete is essential for the migration of reactant ions, SO_4^{2-} , $\text{Al}(\text{OH})_4^-$ and Ca^{2+} , up to microcracks where ettringite deposition can occur. Field experience indicates that concrete ties exposed to rain and sun alternate actions are more severely damaged by Internal Sulfate Attack (ISA) than those exposed to rain but in permanent shadow conditions (Collepradi, 1999 and Thaulow et al, 1996). This different behavior could be attributed to the important role played by the degree of supersaturation in favoring the deposition of ettringite formation.

Heniz and Ludwig investigated the mechanism of secondary ettringite formation in mortars and concretes subjected to heat treatment (1987). Their results relating to the moisture conditions essential to optimize the conditions for DEF revealed that expansion could be avoided if the concrete was exposed in an environment below 59% R.H. The

concrete specimens with similar constituents subjected to similar heat treatment regimes showed severe deterioration when placed in a saturated atmosphere and stored at humidities above 60% for four months.

Microcracked concrete ties, with the same cement source and concrete composition, showed DEF in wet concrete structures while the same microcracked concrete ties, when protected from contact with water, do not show any ettringite (Mielenz et al, 1995 and Shayan, 1995). This confirms the important role played by water in the migration of reactant ions from the cement paste up to the site of microcracks, and then resulting in the deposition of ettringite crystals into the microcracks and the subsequent crack opening.

3.3.4 High Temperature Curing

The issue of high curing temperature as one of the critical elements for DEF is controversial. Some researchers believed that high curing temperatures ($> 70^{\circ}\text{C}$) are required for delayed ettringite formation (Taylor, 1997 and Lawrence, 1998). High temperature curing has been attributed to increase the expansion due to DEF (Ghorab et al, 1980 and Lawrence, 1995). In 1995, Lawrence examined expansion behavior of 55 Portland cements with a curing temperature range of 65 to 100°C . He found that a critical curing temperature for DEF is between 65 and 70°C . He also revealed that great extensions of high temperature curing periods resulted in much reduced expansions.

High temperature curing (above 70°C) may dissolve ettringite in the pore liquid of the hardened concrete (Day 1992). Also, Heinz et al suggested that, at elevated temperatures, primary ettringite is broken down to monosulfate (1987). Later, when the

concrete is exposed to moisture at normal temperatures, the monosulfate is reconverted to ettringite.

Other researchers present alternative hypotheses for the breakdown of primary ettringite at elevated temperatures. Fu and Beaudoin revealed that at temperatures above 65°C, calcium silicate hydrate (C-S-H) absorbs sulfate very quickly from gypsum, reducing the amount available for ettringite formation (1996). Later on, when the temperature of the C-S-H is returned to normal, sulfate is slowly released, through the pore solution, enhancing DEF.

According to other researchers, DEF may occur in concrete whether steam-cured or not (Collepari, 1999, Mielenz et al, 1995, Maursin, 1995, Diamond, 1996 and Hime, 1996). They believed that DEF occurs even in non-steam-cured concrete specimens at temperatures much lower than 70°C that are insufficient to cause thermal decomposition of the “normal” ettringite. This does not conform to the hypothesis that suggested that DEF is necessarily caused by thermal decomposition of ettringite at high temperatures (above 70°C).

3.4 The Morphology of Ettringite

The morphology and crystal size of ettringite varies with the different conditions under which it forms. Many SEM studies outlined that ettringite is normally formed as a slender, needle like crystals with prismatic hexagonal cross section (Schwiet et al, 1966, Midgley and Pettifer, 1971, Mehta, 1973, Mehta and Hu, 1978). Its crystal size depends on the W/C ratio, that is, the availability of sufficient space (Mehta, 1969). Cohen et al also revealed that the particle size of Al-bearing agents also affects the size of ettringite

(1985). The ettringite crystals will be smaller in the presence of calcium hydroxide (Possetti et al. 1982).

The form and shape of ettringite is relevant to studies of the mechanism of expansion. According to Lerch et al, synthetic ettringite consists of long needles, which often are sphere-like (1929). Mehta reported the presence of spherule ettringite (1976). In 1983, Mehta noted that ettringite has two types of morphology, depending upon the conditions under which it forms. In low hydroxyl ion concentration, large lath-like crystals 10-100 μm long and several μm thick are formed in solution. The other type forms in high hydroxyl ion concentration, which is the normal situation for concrete, and are small rods 1-2 μm long and 0.1-0.2 μm thick. Ogawa and Roy found that, during the heat of hydration, the ettringite is formed as very small irregular particles around the Al-bearing particles in the early stages, and then changes to long needle-like crystals (1982). Though different sizes and forms have been reported but chemical compositions of all of them remain the same.

3.5 Detecting DEF

Early ettringite formation which occurs immediately (within hours) in a plastic fresh concrete does not produce any damaging expansion and is associated with the regulation setting of Portland cement during hydration. Delayed ettringite formation (DEF) occurs at later ages and the related heterogeneous expansion in very rigid hardened concrete can produce cracking and spalling. The internal cracking is accompanied by ring cracking around the aggregates particles where ettringite is usually found.

Extensive experience of various researchers suggested that DEF should be studied using a scanning electron microscopy (SEM) equipped with an energy-dispersive X-ray analyzer and using the secondary electron mode (Hime and Marusin, 1999). Cut sections from the studied sample are coated with carbon to permit easy analysis (Marusin, 1993 and 1995). A step-stair EDAX pattern of the chemical elemental analysis of ettringite (Ca, S, Al) is characteristic of DEF. Each element is identified on the spectrum by position of its peak and the computer calculates quantitative analysis by weight of each element. The chemical composition of ettringite is 6 calcium to 3 sulfur, to 2 aluminum.

3.6 ASR and DEF

Many ASR (Alkali-Silica Reaction)-damaged structures undergo healing and filling of cracks, while DEF usually leads to widening of cracks, loss of prestress, and consequent failure of structure (Hime and Marusin, 1999). Therefore, it is very necessary to distinguish between ASR and DEF in order to be able to develop methods to mitigate or to prevent such occurrences in the future.

Many researchers have speculated that ASR was often a precursor of DEF in deteriorating concrete structures (Mielenz et al, 1995, Johansen et al, 1993 and Shayan and Quick, 1992). Shayan and Quick investigated the cause of extensive cracking in precast prestressed sleepers in Australia (1992). They found that in the badly cracked sleepers there was a simultaneous presence of large amounts of AAR (Alkali-Aggregate Reaction) gel and of ettringite crystals. They postulated that the formation of the AAR gel products weakened the cement paste and caused initial cracking, and the formation of delayed ettringite may involve the release of OH^- ions and enhance AAR.

Other researchers also reported the simultaneous presence of DEF and ASR (Oberholster et al, 1992, Johansen et al, 1993 and Marusin, 1993). It was reported that high temperature steam curing could induce immediate ASR for some reactive aggregates (Diamond and Ong, 1994). The ASR-induced cracking facilitated the formation of delayed ettringite and the combined effect is more serious for the deterioration of the concrete.

However, investigations carried out by other researchers showed that DEF can take place in cement pastes without the occurrence of ASR (Older et al, 1996, Yang et al, 1996).

3.7 Stability of Ettringite

The commonly accepted view that ettringite is more stable in sulfate solutions and lime water than in distilled water, and that monosulfate in solutions containing calcium sulfate, sodium sulfate, calcium chloride and sodium chloride may transform to ettringite is based on the work of Lerch et al (1929). Many researchers believed that these many factors affects the stability of ettringite such as chemical composition of cement or the type of aggregates, alkali, carbonation and temperature.

3.7.1 The Chemical Stability of Ettringite

Many researchers have studied the effect of cement constituents on the stability of both ettringite and monosulphate (Mehta, 1969, Jones, 1939, Hampson and Bailey, 1982 and Zhang et al, 1980). In 1969, Mehta found that monosulphate might exist along with ettringite only if the solution surrounding it has a lower concentration of sulphate than is

usually required for the existence of ettringite. The three conditions necessary for the stability of monosulphate in aqueous solution are high calcium content (CaO), low sulphate content (CaSO₄), and high temperature (Jones, 1939, Kalousek, 1941, Heinz and Ludwig, 1987).

Zhang et al. reported that the solubility product of ettringite (1.0×10^{-40}) is much lower than that of monosulphate (1.7×10^{-28}), according to the solubility product method, indicating that, under ambient temperature, ettringite is more stable in cement solution than monosulphate (1980). Therefore, monosulphate has the natural tendency to convert to ettringite. Hampson and Bailey reported the effect of pH value of the pore solution on the morphology of sulphoaluminates. At pH 11.5 to 11.8, sulphoaluminate forms as ettringite crystals and precipitates from the solution. At pH 12.5 to 12.8, the material is non-crystalline with composition similar to ettringite (1982).

3.7.2 Effect of Temperature

Many researchers have reported that calcium sulphoaluminates are thermally unstable phases (Kalousek, 1941, Heinz and Ludwig, 1989 and Daerr, 1977 and Klemm and Adams, 1990). Calcium sulphoaluminates transform from one state to the other with changes of the curing temperature, during which the sulphate-groups and water molecules are re-arranged in the structures.

Curing temperature affects the size and stability of ettringite. At curing temperature of 60°C, ettringite x-ray peaks were noted only after 15 minutes (Hekal, 1986). At curing temperature above 60°C, ettringite loses more of its water molecules as the curing temperature increases. The water molecules drop from 32 to 18 at 70.5°C

(Daerr, 1977). Abo-Elnein and Hekal reported that the loss of ettringite water molecules depends on its hydration temperature (1988). They concluded that as the hydration temperature increases, ettringite becomes stable, and water content reduction would be less.

Many researches have been carried out concerning a critical temperature resulting in the unstable ettringite-monosulphate transformation. In 1972, Mehta postulated that ettringite can be found in cement paste subjected to a 65°C drying condition and that the decomposition starts when dried at 93°C. In a moist environment at 93°C, ettringite poses no apparent decomposition but decomposes when exposed to saturated steam at 149°C. Research by Satava and Veprek also reported similar results, that ettringite can exist stably in aqueous solution up to 93°C (1975).

Kalousek postulated a transformation of sulphoaluminates; he believed that the depletion of ettringite at high temperature could be attributed to the substitution of sulphate ions in the structure of the C-S-H gel (1965). Research on cement pastes shows that the amount of the missing SO_3 clearly increases as curing temperature increases. Kalousek suggested that the missing sulfate ion (SO_3^-) might be the source of delayed ettringite formation and be associated with the C-S-H gel structure. Ghorab et al concluded that the instability of ettringite at higher curing temperatures might be associated with its higher solubility (1980 and 1985).

3.7.3 Effect of Alkalis

The presence of alkalis is believed to affect the solubilities of the reactants (e.g. C_3A , CH and CSH_2) in the $\text{C}_3\text{A} - \text{CSH}_2 - \text{CH} - \text{H}_2\text{O}$ system and hence the concentrations

of the dissolved ions (e.g., OH^- , SO_4^{2-} , Ca^{2+} , etc.). The alkalis apparently could increase the formation of ettringite and decrease the solubility of calcium hydroxide (CH) (Daerr 1977, Wang et al. 1986 and Way et al. 1989). The pH of the pore solution depends on the alkali level, the higher the level the higher the pH. Ettringite can form in alkaline solution at pH of 13.3 at normal temperatures and at alkaline concentrations as low as 0.08 M. At high temperature (60°C) or higher alkaline concentration (0.2 to 1.0 M), ettringite quickly decomposes while monosulphate appears to be more stable (Ghorab et al. 1985 and 1986).

3.7.4 Effect of CO_2

The effect of CO_2 on ettringite related systems has been widely researched. Taylor revealed that carbonation during ettringite formation results in the formation of thaumasite ($\{\text{Ca}_6\cdot[\text{Si}(\text{OH})_6]\cdot 24\text{H}_2\text{O}\}\cdot[(\text{SO}_4)_2]\cdot[(\text{CO}_3)_2]\}$), and can cause the deterioration of concrete (1997). The formation of thaumasite may occur with all sulfate salts if high relative humidity and low temperature ($< 4^\circ\text{C}$) conditions exist (Pauri and Collepari, 1989). It involves ettringite-like expansions and can cause cracking and deterioration of concrete (Hunter, 1989 and Lachaud, 1979). In 1988, Sylla found some evidence indicating that expansion can be attributed to both ettringite and thaumasite. He steam-cured his specimens at 80°C and then stored them at 5°C in the presence of CO_2 . He found a high content of thaumasite with ettringite.

Seligmann and Greening first revealed the carbonation of monosulphate to produce ettringite and hemihydrate (1964). Later Kuzel et al indicated that CO_2 acted as a catalyst to provide a favorable environment in the Portland cement for monosulphate

transformation to ettringite (1989 and 1996). Various researchers have showed that ettringite converts to monosulphate only in cases where the Portland cement contains less than 0.5% CO₂ and the instability of monosulphate in the presence of CO₂ leads to its late formation (Kuzel, 1993 and 1996, Kuzel et al, 1991 and 1993).

3.8 Expansion Mechanisms due to Ettringite Formation

The expansion mechanism due to ettringite formation is a very controversial issue. The theories of ettringite formation and its associated expansions have been classified into two particular mechanisms, the topochemical reaction with directional growth theory and the uniform paste expansion theory. For ettringite formation and expansion, both mechanisms require an alkaline environment saturated with CH. Day suggested that both expansion mechanisms are active depending on the predominant environmental conditions at particular times (1992).

3.8.1 Topochemical Reaction with Directional Growth Theory

In 1983, Cohen summarized a number of different theories and models developed to explain the formation of ettringite and its associated expansion mechanisms. He did classify them into two groups, crystal growth and the swelling theory. The crystal growth group suggested that expansion was caused by the growth of ettringite crystals on the surface of some cement particles in solution, a topochemical reaction approach. A topochemical reaction is a solid-state hydration mechanism where the product forms at the surface of the solid interface and grows in a direction perpendicular to the solid interface.

The presence of calcium hydroxide (CH) affects the properties of ettringite. Cohen also reviewed the effects of CH on the mode of ettringite formation (1983). If CH is present in solution, ettringite particles were thought to be small in size and to behave as colloidal particles, thus causing expansion. If CH is absent in solution, ettringite particles were considered to be larger in size. The magnitude of expansion does not depend on the amount of ettringite but upon the size of the crystals formed. This implies that a small number of large crystals can produce more large cracks than a large number of small crystals (Cohen, 1982 and 1983, Heinz and Ludwig, 1986, 1987, Sylla, 1988, Lawrence, 1990 and 1993, Diamond and Ong, 1994 and Maurusin, 1993).

Deng and Tang believed that expansion is the result of ettringite crystals forming on the surfaces of the Al-bearing particles in the surface (1994). They proposed that in highly alkaline pore solutions, the diffusion of aluminum hydroxide (AH) from the Al-bearing particles into the bulk of the pore solution is slow due to low concentrations of AH ions between the interface of the Al-bearing particles and the pore solution, and the bulk pore solution. The near-interface solution and the wet surfaces of the hydrating Al-bearing grains will rapidly become highly supersaturated with ettringite. The high supersaturation will lead consequently to a large nucleation rate, and thus to the formation of many crystallizing crystals around or close to the Al-bearing grains. Due to the limited space around the Al-bearing particles, the growth of these ettringite crystals will introduce high pressure on the surroundings, and a large expansion may be consequently expected. In a pore solution of low alkalinity, owing to the relatively low concentration of OH⁻ ions and low mobility of Ca²⁺ and SO₄²⁻ ions, the dissolved AH ions might diffuse into bulk solution before many nuclei of ettringite crystals can be formed. The near-

interface solution around the Al-bearing grains will not be a favored place for the nucleation of ettringite crystals. Therefore, ettringite crystals formed in pore solutions of low alkalinity will cause little or even no expansion.

Xie and Beaudoin suggested that the expansion caused by internal sulfate attack is a process in which chemical energy is converted into mechanical work to overcome the cohesion system. The expansive forces result from the crystallization pressure, which is again, a result of the interaction between the solid product of a chemical reaction and cement paste. The proposed two necessary conditions for the crystallization pressure to occur, a confined crystal growth of solid product and an “activity product” of reactants in the pore solution greater than the “solubility product” of the solid product under atmospheric pressure.

Many arguments have been surged against the crystal growth hypothesis. If the growth of ettringite is due surely to the aggregate grains on the surface, the cracks would be uniform, but ettringite crystals’ growth is usually random with associated heterogeneous cracks. Many researchers supported the hypothesis of a uniform paste expansion. They believed the ettringite-filled gaps around the aggregate in expanded mortar and concrete at the transition zone, aggregate-paste or steel paste zones was the cause of expansion (Heinz and Ludwig, 1987 and Fu et al, 1993 and 1994).

3.8.2 The Uniform Paste Theory

In this hypothesis, expansion is attributed to water-adsorption and swelling characteristic of ettringite gel which forms by a through-solution mechanism. These gel-like particles have a large specific surface area analogous to the C-S-H gel, and they

adsorb water, resulting in overall expansion (Mehta, 1983). Small ettringite crystals of colloidal size formed in a saturated CH environment possess a negative surface charge. The large surface area combined with the negative charge results in an attraction of a large amount of water. Tests on disks of pure ettringite confirmed the theory (Mehta, 1983). The disk adsorbs large quantities of water and large swelling strains occur. The X-ray diffraction pattern of the ettringite before and after shows no substantial change in the chemical composition. Many other researchers support Mehta's results (Seligman and Greening, 1964, Stefania, 1982, Sagrera, 1972 and Johansen, Thaulow and Skalny, 1993)

Sagrera mixed paste cylinders containing either calcium sulphate or sodium sulphate. He measured volume change and the quantity of ettringite in the pastes using X-ray diffraction (1972). He found that a huge amount of ettringite forms before there is any volume increase. Mather argues that the detailed formation of ettringite is of less importance than the fundamental mechanism involved in the process (1984). The ettringite attempted to form in a confined space producing very high forces of about 169,000 ft-lb (Mather, 1984).

3.9 Rapid Test For Predicting Expansion Due to Ettringite Formation

A rapid test method (Duggan Test) was used to determine the potential of expansion due to delayed ettringite formation. In 1989, Duggan and Scott first used this method to measure the potential of concrete for damage due to ASR but found that the expansion of concrete is related more to ettringite formation in the concrete matrix than the silica gel. Grabowski reported apparent expansion in the concrete samples after

severe heat-drying/re-wetting cycles used to simulate certain severe conditions relevant to the performance of railway sleepers (1992). On the basis of his investigation, Garbowski argued that the Duggan test showed that all tested concrete sleepers were potentially subject to deleterious expansion.

The Duggan test method involves taking a minimum of five concrete cylinder cores from an existing structure or laboratory prisms or cylinders. The cores (25 mm in diameter) should be parallel and smooth. The heat treatment cycles include three cycles; the first two cycles include one day in dry heat oven at 82°C, then allowing them to cool for about 1 hour and soaking for 1 day in water at 21°C. The third cycle includes 3 days in the oven at 82°C, then allowing the samples to cool down. Before immersing the cores in distilled water, measurements of the samples are taken to be used as the zero datum from which other readings are taken, then the cores are stored in water. Length measurements are recorded at intervals of 3 days over a period of 20 days. A pass/fail criterion of 0.05% at 21 days is defined. Many researchers revealed that the first 20 days expansion of the concrete subjected to the Duggan test method is caused by DEF (Abo El-Enein, 1984, Gillott, 1989 & 1990, Attiogbe, 1990 and Wells, 1990).

Criticisms of the Duggan test method have been: the collection of samples, the size of samples, lack of correlation studies between the results and field concrete, and the severe heat cycles procedures (Fu et al. 1993 and 1996). However, in this research, modifications have been made by increasing the sample size, the use of gage studs to facilitate length measurements, and the addition of potassium carbonate to accelerate expansion of the specimens.

CHAPTER 4: SAMPLE PREPARATION, MATERIALS, AND TEST METHODS

4.1 Introduction

This chapter details the procedures followed in the preparation of the mortar specimens. The materials used and corresponding specifications are outlined. The various test methods and test procedures are also detailed and explained. Water to cement ratio was 0.5 for all the batches in the entire research. For the mortar specimens, a sand to cement ratio of 2.5 was used. The specimens were subjected to the Duggan heat cycle one week after casting to accelerate DEF and its associated expansion.

4.2 Experimental

This research study was divided into two phases. The mixing and casting of the mortar specimens were done according to ASTM C109-99 and ASTM C305-99 (ASTM 2001). The specimens also were cured according to ASTM C192-00 (ASTM 2001). The Duggan test method was modified by using mortar prisms with end gage steel studs instead of concrete cores to facilitate length change measurements.

Phase 1 specimens were used as a control with no varying parameters. All specimens were steam-cured and then de-molded after 24 hours of casting except one set of specimens exposed to field conditions. Then, the specimens were stored under water at room temperature for 6 days before subjecting them to the Duggan heat cycle. After the Duggan heat cycle and allowing the specimens to cool for 2 days, the specimens were measured for length change (zero reading). Then they were stored in their respective storage conditions.

Phase 2 specimens were cured and prepared similar to Phase 1 but with additional potassium carbonate (K_2CO_3) added to the mixing water. The total potassium (K_2O) content of all the batch mixes in Phase 2 was adjusted to 1.5% (K_2O) by weight of cement to accelerate the expansion and DEF. Again, after the Duggan cycle, the specimens were stored in the different storage conditions. The specimens and the storage conditions were monitored throughout the entire research study.

4.2.1 UMD/FHWA Modified Sample Preparation

Two types of mortar specimens were prepared in this research study, 2” cubes and 1”x1”x1.25” prism bars. The 2” cubes were used for compressive strength testing and the prism bars for expansion measurements, weight-change measurements, X-ray computed tomography (X-ray CT) and scanning electron microscope (SEM). The samples were prepared in accordance with ASTM C109-99 and C305-99. The prism bars were each equipped with two steel gage studs at each end to monitor the length change of the specimens periodically, instead of drilled cores suggested by Duggan.

4.2.2 Duggan Heat Cycle

The Duggan heat cycle consists of three cycles. The first two cycles include subjecting the specimens to 1 day in a dry oven at 82°C followed by about 1¹/₂ hour cooling and 1 day soaking in water at room temperature. In the third cycle, the specimens are left in the oven for 3 days at 82°C. At the end of the third cycle, the specimens are allowed to cool for 2 days at room temperature in the laboratory. Length

change measurements were recorded at 3-5 days periodically up to 100 days and once weekly afterwards to monitor the expansion of the specimens.

The heat treatment (Duggan heat cycle) was used to reveal damage in the laboratory-prepared samples in the shortest amount of time and is intended to accelerate DEF and its associated expansion. The Duggan heat cycles were used to enhance the identification of cements with high potential for developing large amounts of ettringite.

4.3 Materials

4.3.1 Molds

Steel molds with two compartments (1"x1"x11.25") with provisions for stainless steel gage studs and an effective gage length of 10 inches was used. The length change measurement was monitored in accordance with ASTM C490-90 (ASTM 2003). Brass molds with three compartments (2" cubes) were used to prepare for the compressive strength testing.

4.3.2 Cement

Portland cement type III was used throughout the entire research. Type III cement was chosen because it has been identified as a potential cause of DEF. Its relatively high sulfate content, fineness and higher heat of hydration favors ettringite formation. The chemical analysis of the cement used in this research study is provided in Table 4.1. The chemical analysis of the cement was measured using X-ray fluorescence spectrometry by a commercial laboratory.

Table 4.1 The Chemical Composition of Type III Portland Cement

Chemical Analysis of Cement	
Analyze	Weight %
SiO ₂	19.88
Al ₂ O ₃	5.03
Fe ₂ O ₃	2.79
CaO	61.79
MgO	2.51
SO ₃	3.89
Na ₂ O	0.31
K ₂ O	0.82
TiO ₂	0.21
P ₂ O ₅	0.17
Mn ₂ O ₃	0.07
SrO	0.20
Cr ₂ O ₃	< .01
ZnO	0.02
L.I.O (950°C)	2.01
Total	99.67
Alkalis as Na ₂ O	0.85
Calculated Compounds per ASTM C150-02	
C ₃ S	51
C ₂ S	18
C ₃ A	9
C ₄ AF	8
ss(C ₄ AF + C ₂ F)	--

4.3.3 Sand

Manufactured Frederick stone sand conforming to ASTM C33-99a was used throughout the research. The Frederick sand was obtained from the Frederick Quarry, Frederick, Maryland. The Frederick sand used had moisture absorption of 1.0% and a specific gravity of 2.69. According to the Maryland State Highway Administration, the potential alkali reactivity of the sand using ASTM C1260 is 0.09% and is considered

intermediate reactive. In this research, Frederick sand was chosen because of its expansive tendencies due to DEF without the association of alkali-silica reactivity (ASR).

The technical information about the Frederick sand is given in Table 4.2.

Table 4.2 Technical Information Sheet for Frederick Sand

LAFARGE Frederick Quarry, Maryland Manufactured ASTM C33 stone sand Technical Information Sheet		
Rock Type:	Carbonate	Calcitic Limestone
Color:	Light to dark gray	
Average Gradation	Analysis	
ASTM C136	% Passing	
3/8 (in)	100	
#4	98.3	
#8	86.6	
#16	53.9	
#30	29.4	
#50	16.9	
#100	6.2	
#200	3.4	
Specific Gravity (SG)	2.69	
Absorption	1.0%	
Alkali reactivity of aggregate (ASTM C1260)	0.09% expansion	
Soundness	1.2% Loss	
Unit weight, dry rodded	109#/CF	
Los Angeles Abrasion	22.0% Loss	
Deleterious Substances - 200 Wash	3.6% Dust of Fracture	

4.3.4 Potassium Carbonate

Anhydrous granular reagent grade potassium carbonate (K_2CO_3) was used. Potassium carbonate was added to the mixing water to increase the potassium content of the mix.

4.3.5 Potassium Sulfate

Potassium sulfate (K_2SO_4), white fine crystals, was used as a means of establishing an atmosphere of 97% relative humidity (R.H) for one of the storage conditions. The solubility of potassium sulfate at 20°C is 111 grams per liter (Dean 1999).

4.3.6 Calcium Hydroxide (Hydrated Lime)

Hydrated lime, chemically known as calcium hydroxide, $Ca(OH)_2$, or caustic lime, a white powder, was used to provide a required storage condition. The hydrated lime was dissolved in water at room temperature to produce a saturated solution with a pH of 12.5.

4.4 Storage Conditions

A plastic rack was built to hold the mortar specimens in the storage containers. The storage containers were 5-gallon plastic buckets. The racks can hold as many as 12 bars and 12 cubes. Based on past research, four particular storage conditions were chosen to study their influence on DEF in mortar specimens.

4.4.1 Isothermal Water Bath, pH maintained at 12.5 (Exp. Cond. 1)

This storage condition is obtained by having a saturated solution of calcium hydroxide, $\text{Ca}(\text{OH})_2$, and water at room temperature. This makes a 12.5 pH value of the aqueous solution and the specimens are totally immersed throughout the research. The storage solution was periodically monitored for alkalis concentration using ion selective electrodes.

4.4.2 Plain Water at room temperature (Exp. Cond. 2)

Ordinary tap water at room temperature was used. The specimens were stored under water at room temperature and were periodically remove for measurements. The water was also monitored for pH value, alkalis, and calcium concentrations.

4.4.3 Moist Air Chamber, R.H maintained at 97% (Exp. Cond. 3)

A saturated solution of potassium sulfate, K_2SO_4 , was used to establish a R.H of 97%. About 2 liters of water at 25°C was mixed with 240 grams of K_2SO_4 , then poured into the plastic bucket. The specimens were arranged in a rack and placed in the bucket. The bucket was then covered airtightly with a plastic lid and was opened only during removal of specimens for measurements. All procedures per ASTM E104-85 were followed to maintain constant relative humidity using aqueous solutions.

4.4.4 Field Conditions (Exp. Cond. 4)

The specimens were prepared in the laboratory and then stored outside exposed to atmospheric conditions throughout. Figure 4.1 shows specimens under field conditions.



Figure 4.1 Mortar Specimens Exposed to Field Conditions

4.5 Sample Preparation

The mortar specimens were prepared in the laboratory per ASTM C192-00, standard practice for making and curing test specimens in the laboratory. To limit the number of varying parameters, no admixtures were used. Adding only 0.68 % potassium carbonate by weight of cement in the mixing water was utilized in phase batches, which increased the potassium level of the cement to 1.5% K_2O . All mortar batches were mixed according to ASTM C305-99. The mortar specimens were mixed in an electrically driven mixer. Mortar bars (1"x1"x11.25"), for length and weight change measurements and 2" cubes were used for compressive strength testing. The exposed parts of the specimens were covered with aluminum foil to prevent drying and shrinkage. They were then subjected to steam or cured at room temperature. The total number of mortar specimens prepared in shown in Table 4.3.

Table 4.3 Total Number of Mortar Samples Prepared

Total number of samples prepared		
	Phase I	Phase II
1"x1"x11.25" Bars	54	54
2" Cubes	76	76

4.5.1 Phase One

In this phase, five (5) sets of mortar batches were prepared. All the mix materials and proportions were kept the same. The chemical analysis of the cement indicated a 0.82% potassium content (K_2O). The cement was used, without changing the potassium content throughout Phase 1 batches, as the control. The mixing proportions of each batch are shown in Table 4.4. Specimens were then prepared by the modified sample preparation method.

Table 4.4 Mixing Proportions for Each Batch of Mortar Specimens

Mix	Phase 1					Phase 2				
	I	II	III	IV	V	I	II	III	IV	V
Water (mL)	1150	1150	1150	1546	1546	1150	1150	1150	1546	1546
Cement (g)	2300	2300	2300	3091	3091	2300	2300	2300	3091	3091
F. Agg. (g)	5750	5750	5750	7728	7728	5750	5750	5750	7728	7728
Add. P. Carbonate by weight of cement (g)	-	-	-	-	-	20	20	20	27	27

NOTE: 1mL = 0.0022 lb H₂O & 1g = 0.0022 lb mass

For batches I, II, III & IV, the exposed parts of the specimens were covered with aluminum foil. Then, the specimens while in steel molds were placed in a water bath in

an oven and the temperature raised to 85°C for 2 hours and then maintained at 85°C for 4 hours. After 4 hours, the oven was turned off and the specimens allowed to cool overnight. The specimens were then stored under water at room temperature for 6 days. After storage under water, batch IV was stored outside the laboratory under field conditions while batches I, II and III were subjected to the Duggan heat cycle. For batch V, the mortar specimens were cured inside the laboratory for 24 hours. Then the specimens were de-molded and stored under water for 6 days before being subjected to field conditions.

All specimens were marked with different codes to reflect their phase and exposure conditions respectively. The specimens were coded with the date stored, the expression P1C3.1 was used for P1 – phase one, C3 – exposure condition 3 (maintained at a RH of 97%) and 1 – the sample number as shown in Figure 4.2.

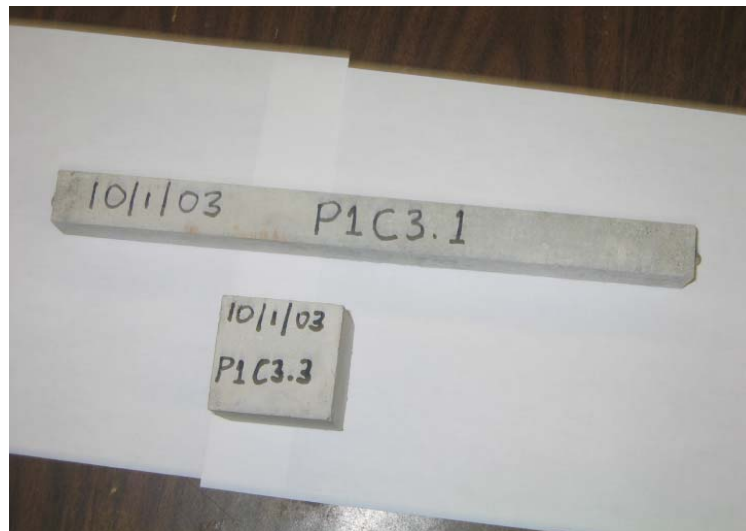


Figure 4.2 Identification of Specimens

Initial weight and length change measurements were recorded for each batch prior to storing them. Table 4.5 gives an outline of the batches and exposure conditions.

Table 4.5 Batches and Exposure Conditions

PHASE 1 / PHASE 2				
MIX I	MIX II	MIX III	MIX IV	MIX V
EXP. COD. 1	EXP. COD. 2	EXP. COD. 3	EXP. COD. 4A	EXP. COD. 4B
BARS: 10 CUBES: 12	BARS: 10 CUBES: 12	BARS: 10 CUBES: 12	BARS: 10 CUBES: 15	BARS: 10 CUBES: 15

4.5.2 Phase Two

All batches in phase 2 were prepared with a potassium content (K_2O) level of 1.5%. Additional 0.68% potassium carbonate by weight of cement was added to the mixing water to achieve the desired 1.5% K_2O . Again, all the mixing materials and proportions remained unaltered while only the potassium content of the cement was increased. The mixing proportions of each batch are shown in Table 4.4. Again, all batch mixes were identically prepared and cured similar to phase 1 and stored. Table 4.5 provides the batches and exposure conditions chart. The specimens were similarly numbered using different codes to reflect their phase and exposure conditions. Initial weight and length change measurements were recorded for each batch before storing.

4.6 Test Procedures

4.6.1 Compressive Strength

2” mortar cubes were tested to determine their compressive strength according to ASTM C109-99 “Standard Test Method for Compressive Strength of Hydraulic Cement

Mortars (Using 2-in or [50 mm] Cube Specimens.” Three (3) cubes from each exposure conditions were tested at different stages to determine the compressive strength.

4.6.2 Expansion Measurements

The mortar specimens were prepared according to ASTM C109-99 and C305-99 and length change were monitored in accordance with ASTM C490-00. Initial length change measurements were recorded immediately after the Duggan heat cycle and before storing the specimens. Five (5) mortar bars were used to measure the length change at intervals 3 – 5 days. The measurements were recorded, then the expansion of each bar calculated and the average expansion of each set calculated.

A standard length comparator equipped with a digital indicator and a reference invar bar was used to measure the length change of the specimens. The digital indication was graduated to read in 0.0001-in. units and it was accurate within 0.0001 in. in any 0.0010-in range. All length change measurements were done in a 70°C room but, prior to each measurement, the digital indicator was calibrated using the reference invar bar.

The mortar bars were all measured with the marked date part up as required by ASTM C490-00 for accurately obtaining comparator readings. Figure 4.3 shows a mortar bar carefully positioned to measured the length change with a digital comparator.



Figure 4.3 Comparator Set up for Length Change Measurements

4.6.3 Weight Change Measurements

The specimens were blotted surface dry (wiped with an absorbent paper towel until all visible films of water were removed) at the time of weight measurement. The weight changes of the specimens during exposure were calculated in percents using the equation below.

$$\text{Weight change (\%)} = [(W - W_0) / W_0] \times 100$$

Where:

W = weight of specimen at the age of measurement

W_0 = initial weight of specimen

A digital weighing scale was used for the weight change measurement. A set of 5 mortar bars was used for each exposure condition during weight change measurements. The weight change of each bar was calculated and then the average weight change for

each set was calculated. Figure 4.4 shows the digital scale used to monitor weight change of the mortar bars.



Figure 4.4 Weighing Mortar Bars

4.7 Water Analysis

Water analysis was performed for storage conditions 1 and 2 using ion selective electron (ISE) and a bench top meter. Potassium, sodium, and calcium ion selective electrodes were used to measure their respective concentrations in the storage solution at intervals of 2 weeks to a month.

About 100ml of each sample was taken periodically from each storage solution in order to perform water analysis. The sample was analyzed and the results recorded. After collecting samples for measurement, water at room temperature was added and mixed to maintain saturation in exposure condition 1. As needed, distilled water was topped up for exposure condition 2 to ensure the specimens remained totally submerged.

Prior to any analysis, the ISE was calibrated with known standardized ISE solutions, and the benchtop recorded the electrode potential in millivolts. For an accurate and precise ISE, the electrode potential should be in the range 54 to 60 mV (Thermo Orion, 2001). Figure 4.5 shows water analysis performed using an ISE and a benchtop meter.



Figure 4.5 ISE and Benchtop Meter Set Up for Water Analysis

4.8 Petrography Analysis for Identifying DEF

Visual techniques used by many researchers in the past two decades for identifying materials present in cracks and cavities of deteriorating mortar and concrete to determine the failure mechanism include scanning electron microscope (SEM) equipped with energy dispersive analyzer x-ray (EDAX), differential scanning calorimetry (DSC), quantitative X-ray diffraction (QXRD), and X-ray computed tomography (X-ray CT). The SEM and EDAX are very powerful tools to study the microstructural characteristics

of solid substances. Its high resolution and versatility make it possible to precisely examine the microstructure and identification of the material.

Many researchers have used SEM and EDAX to distinguish between DEF and ASR gel distress mechanisms (Maursin, 1994, 1995, Hime, 1996). Also, Maursin reported that SEM petrography analyses were essential in differentiating between alkali-silica and DEF morphologies and the EDAX provides the elemental analysis. In this research study, SEM equipped with EDAX, and X-ray CT were used as visual identification techniques for examining the microstructure of the mortar specimens.

4.8.1 Scanning Electron Microscopy (SEM) and X-ray analyzer (EDAX)

The specimen in a scanning electron microscope is bombarded by a beam of high-speed electrons with an accelerating voltage of 10 to 20 kV directly at the specimen. Three major types of signals are produced as a result of the interaction of the electron beam and the surface of the specimen. These signals are backscattered electrons, secondary electrons, and X-ray photons. Those signals can be used to characterize the specimen. The electron micrographs obtained by using high-energy backscattered electrons reflect differences in the atomic numbers and can distinguish among the particles based on the variation in brightness of the topography image of the specimen. The electron micrographs that are obtained by using low-energy secondary electrons are capable of showing the morphology of the microstructure in two or three dimensions. X-ray radiation produces the elemental compositions as quantitative analyses printed on a chart by wt.% of elements. Each element is identified on a spectrum by the position of its peak.

Preparation of samples for SEM analysis is very important in diagnosis of the mortar or concrete failure mechanism. Different researchers use various methods of sample preparation for SEM. In 1986 Grattan-Bellow, used polished concrete sections while Shayan 1989 used broken sections. Some used thin sections such as Shayan 1992 while others used fractured surface samples such as Shayan 1992 and Oberholster 1992. The fractured sample preparation method appears to be the best for SEM diagnosis for DEF distress mechanism in concrete and mortar specimens (Marusin, 1995 and Oberholster, 1992).

Fractured surface samples were used in this research program. From each sample two (2) specimens were collected, an interior and exterior, to qualitatively analyze the microstructure of the sample. The fractured samples, 1-1.5 cm in diameter were glued to carbon stubs with carbon paint prior to the scanning electron microscope (SEM) examination of specimens. The samples were dried in a vacuum oven at about 55°C and then coated with a thin layer of carbon. The coating was done by thermal evaporation using hummer 10.2 sputtering system with a CEA 2.2 carbon evaporation accessory. The carbon layer will minimize the charging effects. Static charges on the surface will appear as bright spots in the SEM image. Carbon was used because it does not affect results since SEM is configured to ignore carbon in its elemental analysis and has no interfering X-ray florescence.

4.8.2 X-ray Computed Tomography (X-ray CT)

The X-ray computed tomography (X-ray CT) is a nondestructive method used to study the internal and external cracking patterns of solid substances. An industrial X-ray

CT system with 420 kV photons and a 512 channel digital detector (BIR, 1998) was used to acquire images of the mortar specimens. Horizontal slices of 0.5 mm were captured for every 0.4 mm and data saved, the 20% overlap ensures that all internal structure is captured. The data was then reconstructed using back project reconstruction algorithm to generate TIF files format. The captured image consisted of 256 levels of gray intensity corresponding to different densities within the specimen.

Direct planar X-rays pass through the specimens along several different paths and directions producing sets of CT images. The intensity of the X-rays is measured after it passes through the specimens. The scan of each slice is complete after collecting the intensity measurement for a full rotation of the specimen. The specimen was then shifted vertically to generate another slice image and the entire procedure was repeated in order to generate additional slice images. The X-ray CT captured the aggregate distribution, cavities, and interior cracks of the specimen.

CHAPTER 5: MORTAR SAMPLES (CONTROL) AND DEF

5.1 Introduction

The potential for deterioration of Portland cement concrete and mortar due to DEF has been widely recognized in the precast industry. In this study, five (5) sets of mortar samples were prepared according to the modified sample preparation method. The deleterious effect due to DEF was monitored for the mortar specimens stored in four (4) different conditions. Frederick sand (manufactured sand) was used in all the batch mixes and, according to the Maryland State Highway Administration (MDSHA); the ASR result is 0.09%. The MDHSA classified the Frederick sand to be of medium reactivity. Most of the specimens were steam-cured and then stored under water. They were then subjected to the Duggan heat cycle after one week to accelerate DEF and its associated expansion.

Early measurements of the compressive strength of the mortar samples were performed after 28 days for each exposure condition. Three (3) cubes were tested from each exposure condition and the average result used. After 40 and 100 days of storage (i.e., from the end of the heat cycle), specimens were collected for scanning electron microscope (SEM) with X-ray analysis and X-ray computed tomography (X-ray CT) studies on the expanded mortar specimens. The objectives were to study the effect of using a manufactured fine aggregate and different exposure conditions on leaching of ions, weight changes, DEF, and associated expansions. Expansions, weight-change, water analysis of storage solutions, SEM with EDAX, and X-ray CT results are presented and discussed in this chapter.

5.2 Influence of Exposure Conditions

Four (4) different storage conditions were employed in this research study. After the Duggan heat cycle, the samples were stored in their respective exposure conditions and monitored for weight change, expansion, leaching of ions, SEM with EDAX and X-ray CT. Expansion and weight changes were monitored periodically. Expansion values at 21 days were compared to the threshold value of 0.05% expansion that was suggested by Duggan as pass/fail criteria. It should be noted that expansion and expansion rate are affected by specimen size (Fu, 1996). Therefore, Duggan threshold value is only considered as a suitable criterion for determining the DEF potential in Portland cement products. SEM with EDAX and X-ray CT studies were performed to reveal the presence of ettringite in different forms in the cracks and air voids. No ASR was found in any of the examined samples. Therefore, deleterious expansions of the mortar samples at different stages were associated to DEF.

5.3 Mortar Samples Subjected to Duggan Heat Cycles Test Results

The first three (3) batch mixes were all subjected to the Duggan heat cycle after one (1) week of casting. The experimental results are discussed and analyses for the different exposure conditions are presented.

5.3.1 Expansion Results

From each exposure condition, 5 mortar bars were used for each expansion measurement and the average expansion recorded. Expansion readings were collected at specific intervals. Samples measured from all three exposure conditions showed

expansion within 3 days after the end of the Duggan heat cycle. Expansion values at 21 days were compared to the threshold value of 0.05% expansion suggested by Duggan as pass/fail criteria for concrete. The expansion results for the mortar specimens (control samples) are shown in Figure 5.1.

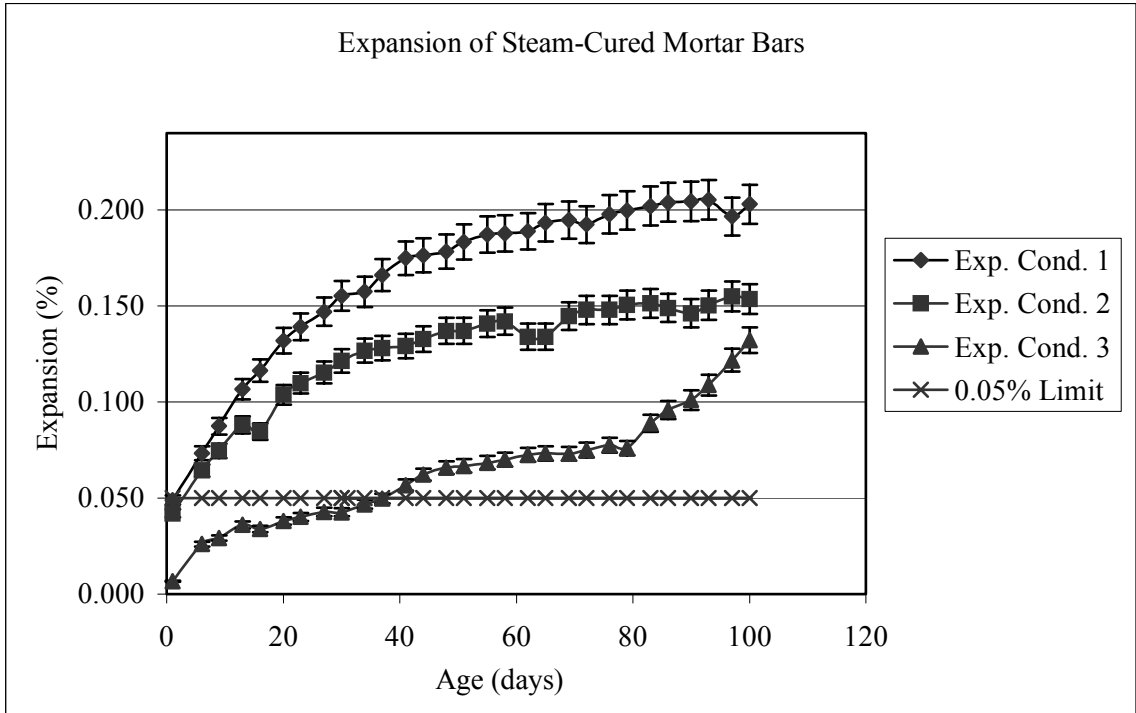


Figure 5.1 Expansion of Mortar Samples Subjected to Duggan Heat Cycle and Stored Under Different Exposure Conditions

The expansion at 21 days was about 0.132% for exposure condition 1 (pH maintained at 12.5), 0.104% for exposure condition 2 (plain water) and 0.038% for exposure condition 3 (relative humidity of 97%). Expansion values of the mortar samples stored in exposure conditions 1 and 2 exceed the Duggan threshold value of 0.05% after 21 days. These expansion results suggest that the mortar samples subjected to exposure conditions 1 and 2 have the potential for deterioration due to DEF. Mortar

samples stored in exposure condition 1 exhibited the highest expansion with an average of 0.203% at 100 days.

The polynomial and linear regression curves for each individual exposure conditions are analyzed and plotted in Figures 5.2, 5.3 and 5.4. Table 5.1 provides the results of the polynomial and linear equations used for the best fit of the experimental data. For mortar specimens in exposure conditions 1 and 2, the polynomial regression curves give the best fit for the expansion against age results. Mortar specimens stored in exposure condition 3 (R.H of 97%) show a high positive linear and polynomial correlation.

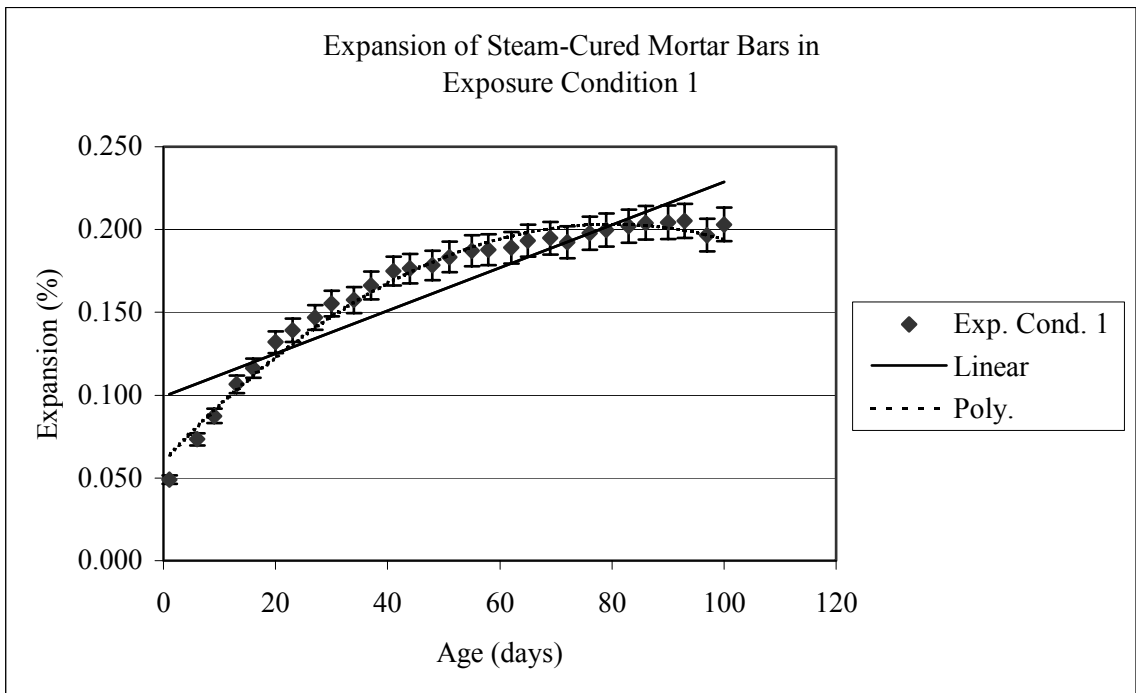


Figure 5.2 Expansion of Mortar Samples Subjected to Duggan Heat Cycle and Stored in Isothermal Water Bath, pH maintained at 12.5 (Regression Curves)

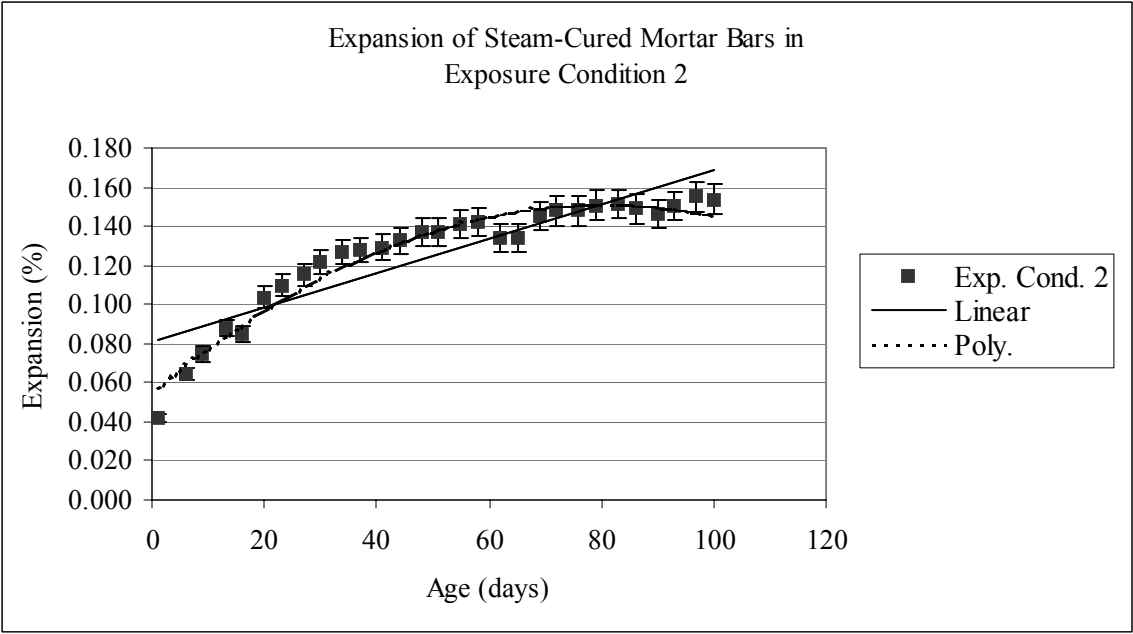


Figure 5.3 Expansion of Mortar Samples Subjected to Duggan Heat Cycle and Stored in Plain Water at Room Temperature (Regression Curves)

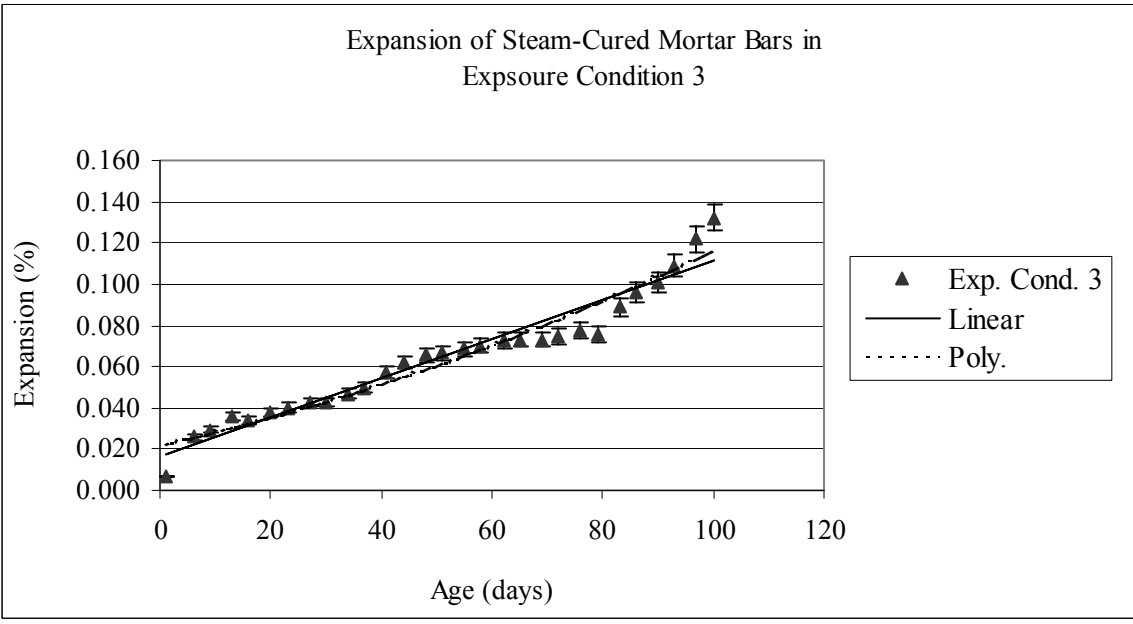


Figure 5.4 Expansion of Mortar Samples Subjected to Duggan Heat Cycle and Stored in Moist Air Chamber, R.H maintained at 97% (Regression Curves)

Table 5.1 Linear and Polynomial Equations for Expansion vs. Age of Steam-Cured Mortar Samples Stored Under Different Exposure Conditions

Phase 1 (Mortar Control Samples - Subjected to Duggan Heat Cycle)		
Exposure Condition 1 (Isothermal water, pH at 12.5)	Exposure Condition 2 (Plain water at room temp.)	Exposure Condition 3 (R.H maintained at 97%)
Linear $y=0.0013x+0.0993$ $R^2=0.8112$	Linear $y=0.0009x+0.0807$ $R^2=0.7949$	Linear $y=0.001x+0.0161$ $R^2=0.9373$
Polynomial $y=-2E-05x^2+0.0036x+0.0602$ $R^2=0.98$	Polynomial $y=-1E-05x^2+0.0024x+0.0547$ $R^2=0.9536$	Polynomial $y=3E-06x^2+0.0006x+0.022$ $R^2=0.9457$

Mortar bars stored in exposure condition 3 show visible cracks around the tip at about 104 days. The size of these cracks at the tip of the mortar bars increased as time passed. Mortar samples in the other exposure conditions did not show any visible cracks.

5.3.2 Weight Change Results

The formation of ettringite involves the uptake of water, which results in permanent weight gain of the specimen. The weight change of mortar specimens is shown in Figure 5.5 under different exposure conditions.

Just after 1 day of storage, specimens in exposure conditions 1 and 2 show very significant weight changes reaching about 10%. This might be due to the uptake of water by the mortar specimens. Mortar specimens in exposure condition 3 (R.H maintained at 97%) show weight gain of about 2%.

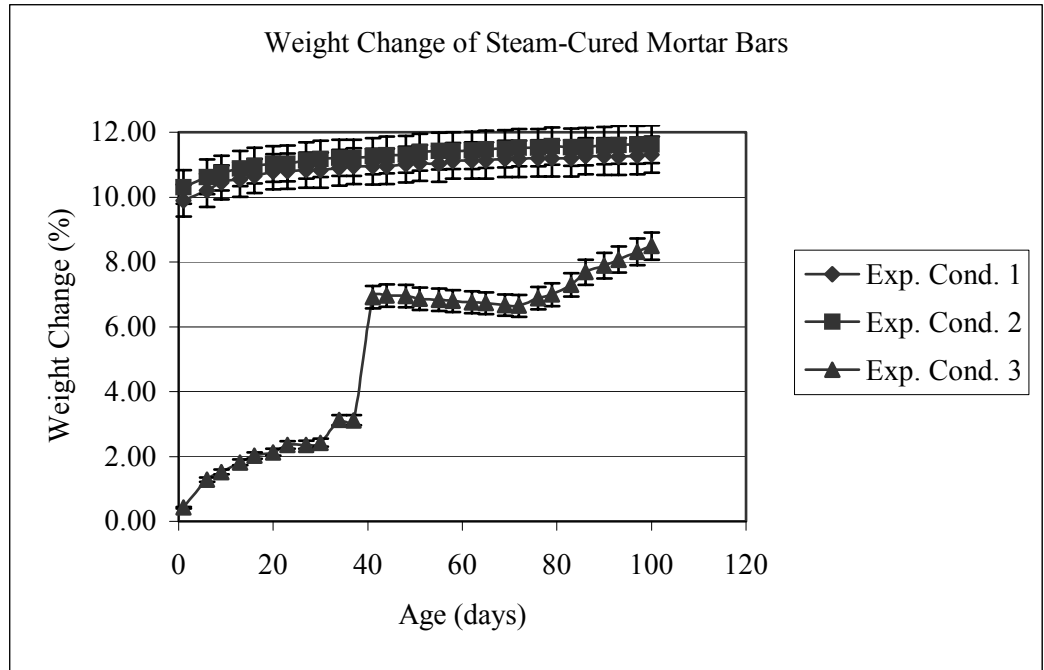


Figure 5.5 Weight-Change of Mortar Samples Subjected to Duggan Heat Cycle and Stored Under Different Exposure Conditions

Both exposure conditions 1 and 2 show similar weight change patterns. A significant jump in weight gain occurred between 37 and 41 days by mortar specimens in exposure condition 3. This might be due to the sudden weight gain of the specimens when DEF takes place. The specimens exhibited an average weight gain of 3.84% during that interval.

At 100 days, the mortar specimens still showed weight changes but the increase was not very significant. The weight changes at 100 days were 11.31% for exposure condition 1, 11.61% for exposure condition 2, and 8.31% for exposure condition 3.

Polynomial and linear regression curves were employed to obtain the best fit for the experimental data. Again, the polynomial regression curves gave the best fit for the

data. Figures 5.6, 5.7 and 5.8 show the linear and polynomial curves while Table 5.2 provides the regression equations for the data.

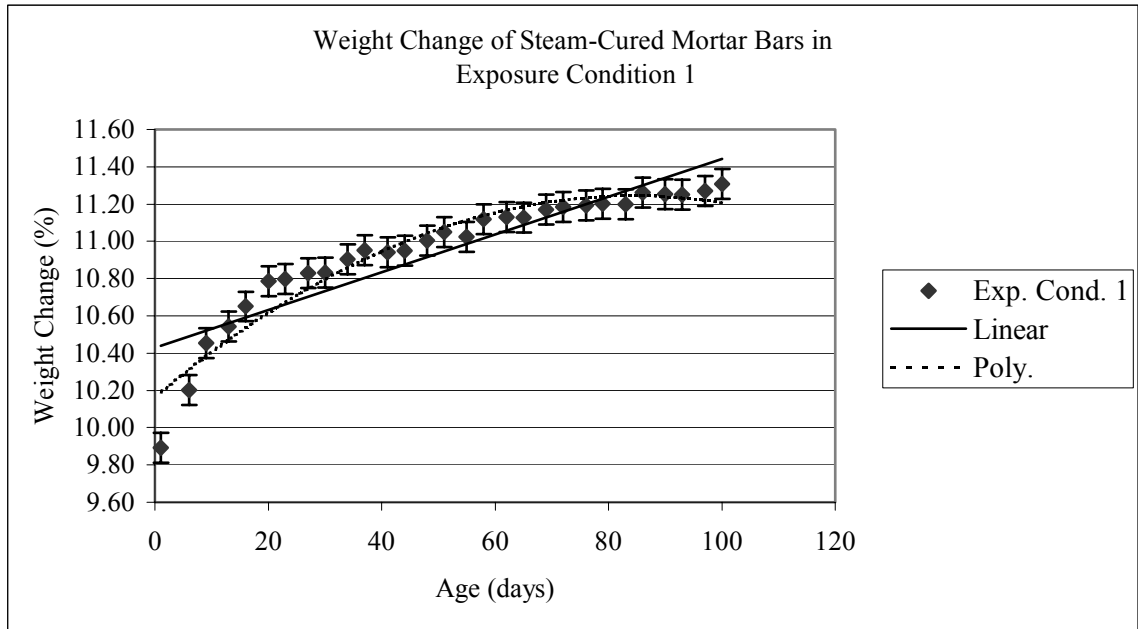


Figure 5.6 Weight Change of Mortar Samples Subjected to Duggan Heat Cycle and Stored in Isothermal Water Bath, pH maintained at 12.5 (Regression Curves)

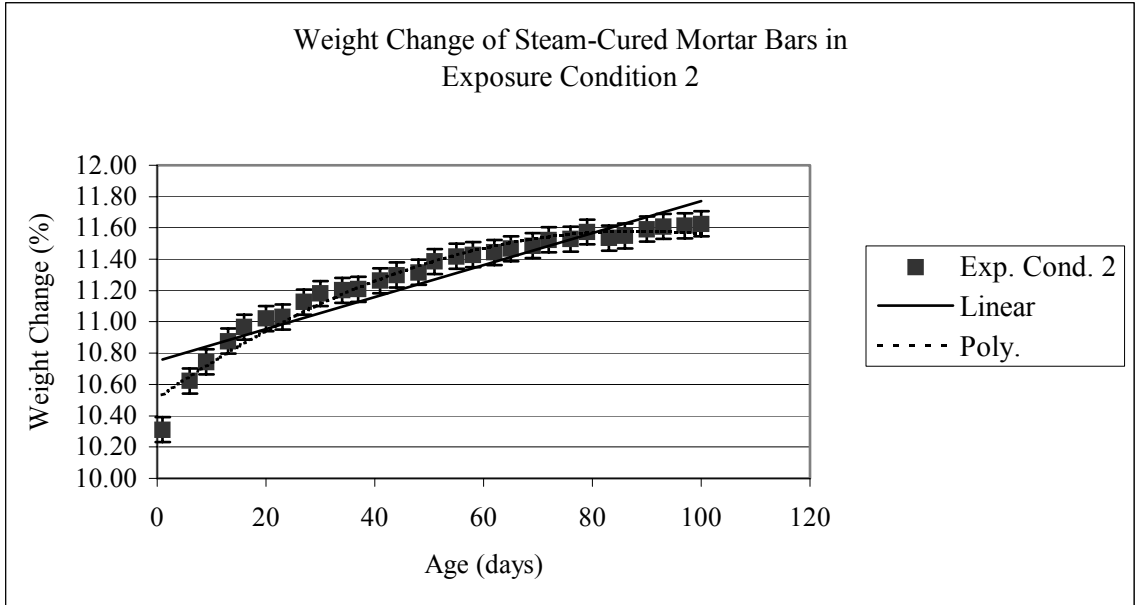


Figure 5.7 Weight Change of Mortar Samples Subjected to Duggan Heat Cycle and Stored in Plain Water at Room Temperature (Regression Curves)

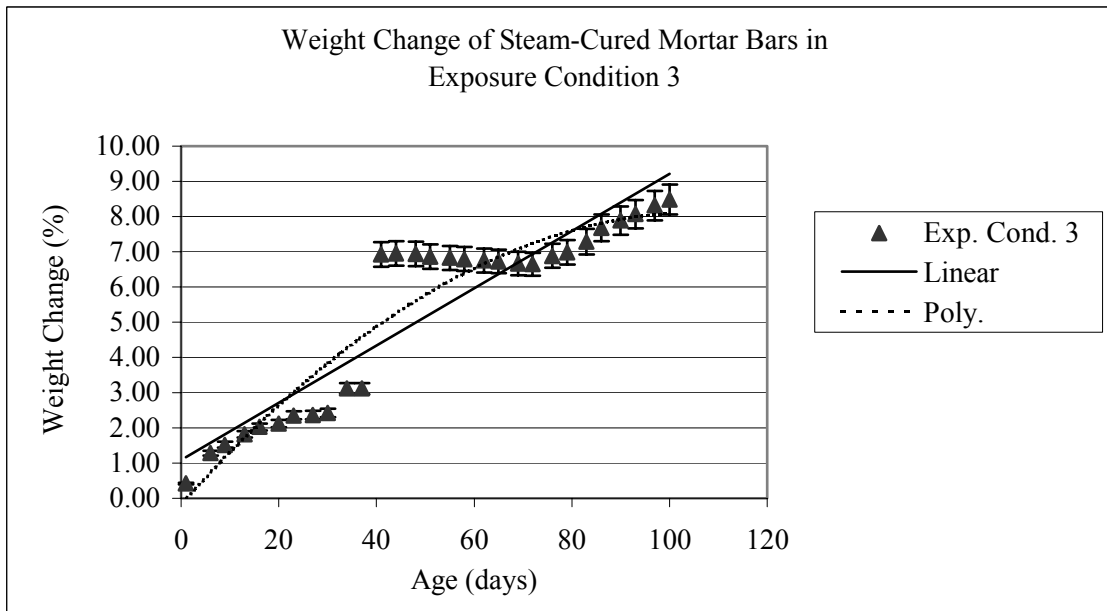


Figure 5.8 Weight Change of Mortar Samples Subjected to Duggan Heat Cycle and Stored in Moist Air Chamber, R.H maintained at 97% (Regression Curves)

Table 5.2 Linear and Polynomial Equations for Weight Change vs. Age of Steam-Cured Mortar Samples Stored Under Different Exposure Conditions

Phase 1 (Mortar Control Samples - Subjected to Duggan Heat Cycle)		
Exposure Condition 1 (Isothermal water, pH at 12.5)	Exposure Condition 2 (Plain water at room temp.)	Exposure Condition 3 (R.H maintained at 97%)
Linear $y = 0.0101x + 10.43$ $R^2 = 0.8047$	Linear $y = 0.0102x + 10.751$ $R^2 = 0.8588$	Linear $y = 0.0812x + 1.0906$ $R^2 = 0.851$
Polynomial $y = -0.0002x^2 + 0.0256x + 10.164$ $R^2 = 0.9303$	Polynomial $y = -0.0001x^2 + 0.0242x + 10.512$ $R^2 = 0.9657$	Polynomial $y = -0.0007x^2 + 0.1553x - 0.1776$ $R^2 = 0.898$

5.3.3 Expansion against Weight Change of Specimens

Expansion and weight change measurements were monitored to investigate for any correlation of expansion of mortar bars resulting in formation and growth of ettringite. Grattan-Bellew et al concluded that a linear correlation exists between mass change and expansion over the period from 17 to 59 days (1998). Figure 5.9 shows the results of expansion and weight changes of the different exposure conditions.

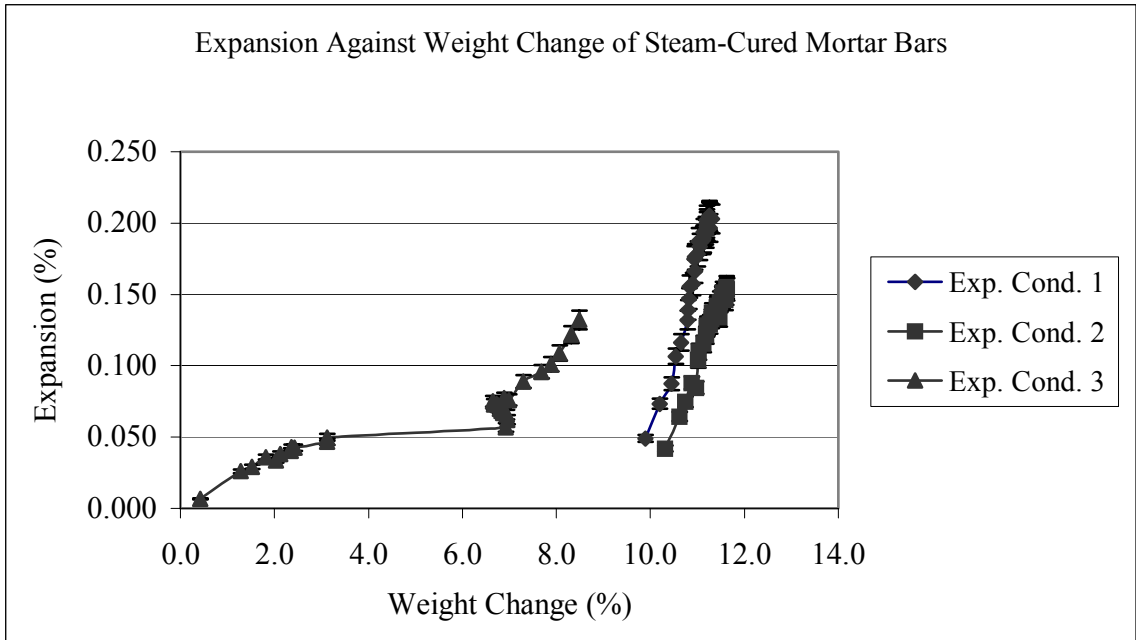


Figure 5.9 Expansion Against Weight Change of Mortar Samples Subjected to Duggan Heat Cycle and Stored Under Different Exposure Conditions

From the scatter plots of the results, polynomial and linear regression curves were applied to obtain correlation between the expansion and weight changes of the mortar specimens stored under different exposure conditions. Figures 5.10, 5.11 and 5.12 show the linear and polynomial curves of the control mortar bars results for the different exposure conditions. Table 5.3 shows the regression equations for the different exposure conditions. Analysis of the results revealed a highly positive linear and polynomial correlation exists between expansion and weight change of the mortar samples.

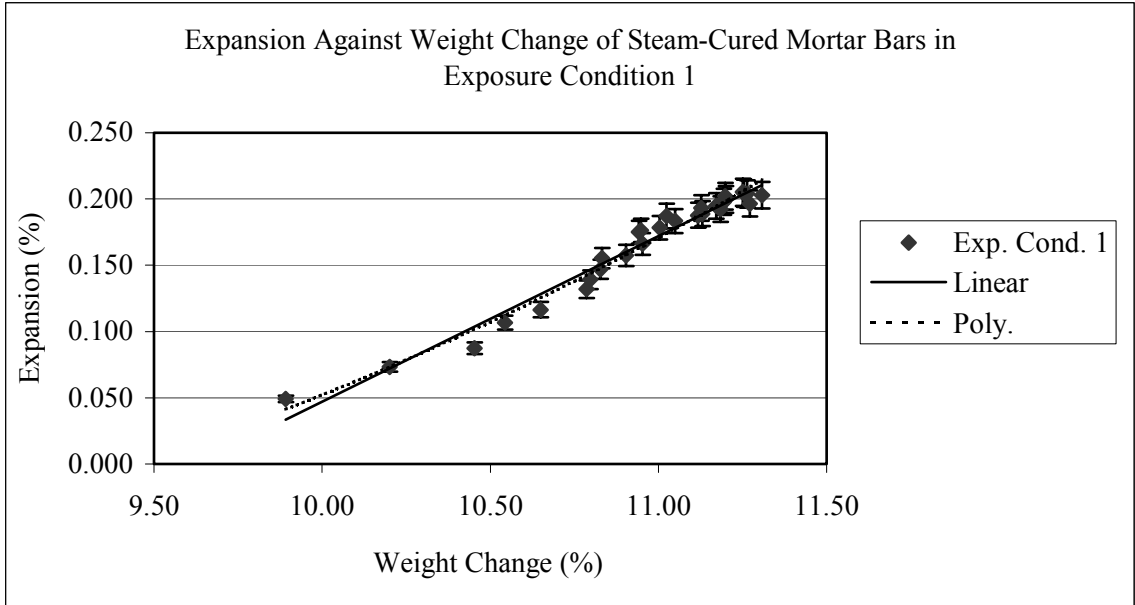


Figure 5.10 Expansion Against Weight Change of Mortar Samples Subjected to Duggan Heat Cycle and Stored in Isothermal Water Bath, pH maintained at 12.5 (Regression Curves)

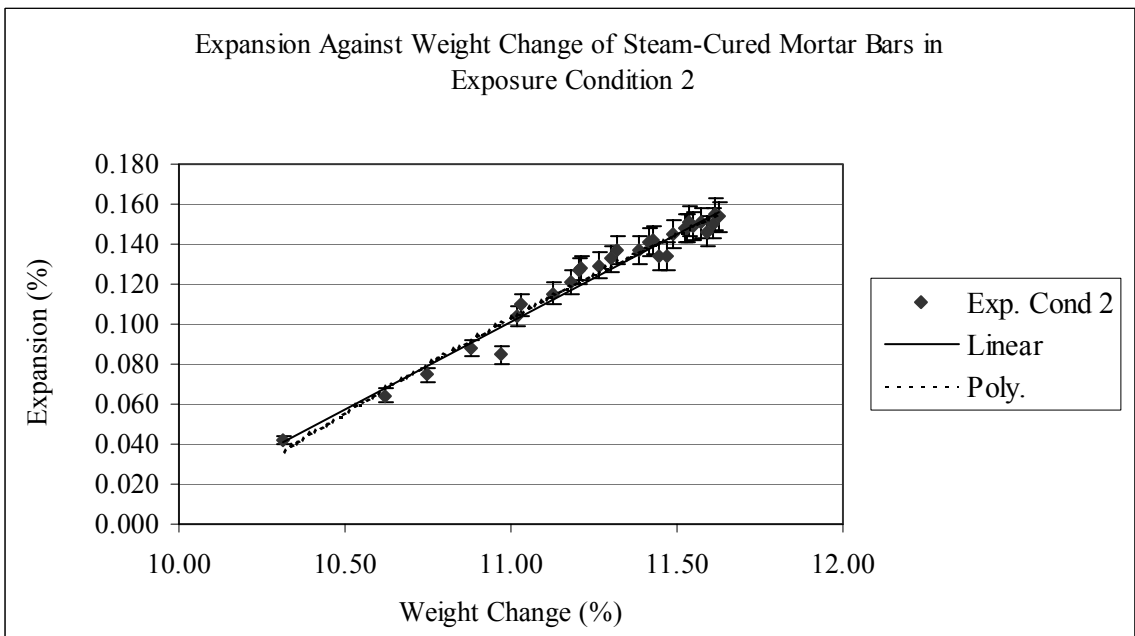


Figure 5.11 Expansion Against Weight-Change of Mortar Samples Subjected to Duggan Heat Cycle and Stored in Plain Water at Room Temperature (Regression Curves)

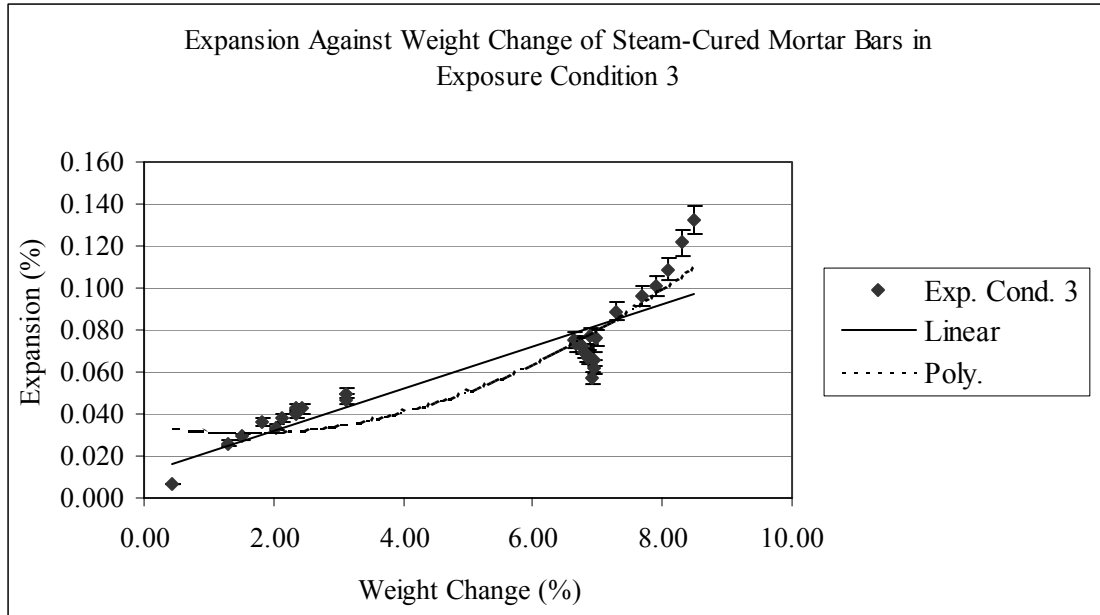


Figure 5.12 Expansion Against Weight Change of Mortar Samples Subjected to Duggan Heat Cycle and Stored in Moist Air Chamber, R.H maintained at 97% (Regression Curves)

Table 5.3 Linear and Polynomial Equations for Expansion vs. Weight Change of Steam-Cured Mortar Samples Stored Under Different Exposure Conditions

Phase 1 (Mortar Control Samples - subjected to Duggan Heat Cycle)		
Exposure Condition 1 (Isothermal water, pH at 12.5)	Exposure Condition 2 (Plain water at room temp.)	Exposure Condition 3 (R.H maintained at 97%)
Linear $y = 0.1253x - 1.2058$ $R^2 = 0.9681$	Linear $y = 0.0878x - 0.8643$ $R^2 = 0.9689$	Linear $y = 0.01x + 0.012$ $R^2 = 0.8117$
Polynomial $y = 0.0168x^2 - 0.2349x + 0.7184$ $R^2 = 0.9715$	Polynomial $y = -0.0107x^2 + 0.3241x - 2.1723$ $R^2 = 0.9712$	Polynomial $y = -0.0016x^2 - 0.0051x + 0.0353$ $R^2 = 0.8568$

5.3.4 Compressive Strength Results

The measured 28 days compressive strength results of the mortar specimens subjected to Duggan heat cycle and then stored under different exposure conditions are shown in Table 5.4. Table 5.4 also gives the calculated averages and standard deviation (Std) of the 28 days strength results. The specimens in relative humidity of 97% (Exp. Cond. 3) exhibit the highest compressive strength at this early stage.

Table 5.4 Compressive Strength of Mortar Specimens Subjected to Duggan Heat Cycle and Stored Under Different Exposure Conditions

28 Days - Comp. Strength (psi)			
Exp. Cond.	1	2	3
	5625	5813	6008
	5920	5145	6238
	5690	5468	5970
Average	5745	5475	6072
Std	155	334	145

5.4 Field Samples (No Duggan Heat Cycle)

Two batches of mortar were mixed and subjected to atmospheric conditions outside the laboratory. The first batch was steam-cured, then subsequently stored in water for 6 days and stored outside the laboratory. The second batch was cured in the laboratory at room temperature for 24 hours, and then stored under water for 6 days prior to exposure to field conditions. None of the batch mixes were subjected to the Duggan heat cycle. All other parameters such as mix proportion and cement type were unaltered.

5.4.1 Expansion Results

Figure 5.13 shows change in length of the mortar bars prepared in the laboratory and then exposed to field conditions. Different curing conditions were used for each set of mortar samples. For the initial 100 days, both mortar samples showed shrinkage. Steam-cured mortar samples (Exp. Cond. 4A) exhibited lower shrinkage values than those cured at room temperature (Exp. Cond. 4B). There was little significant difference in the shrinkage of the mortar samples, exposure condition 4A compared to exposure condition 4B.

The polynomial and linear regression curves of the field-exposed mortar samples are shown in figures 5.14 and 5.15. Table 5.5 illustrates the polynomial and linear equations for the best fit to the experimental data. None of the regression analysis performed could be regarded as a best fit to the data. Only 50% of the experimental data points fit linear or polynomial regression curves. Therefore, little or no correlation exists between shrinkage and time (duration of exposure) for the mortar samples exposed to field conditions.

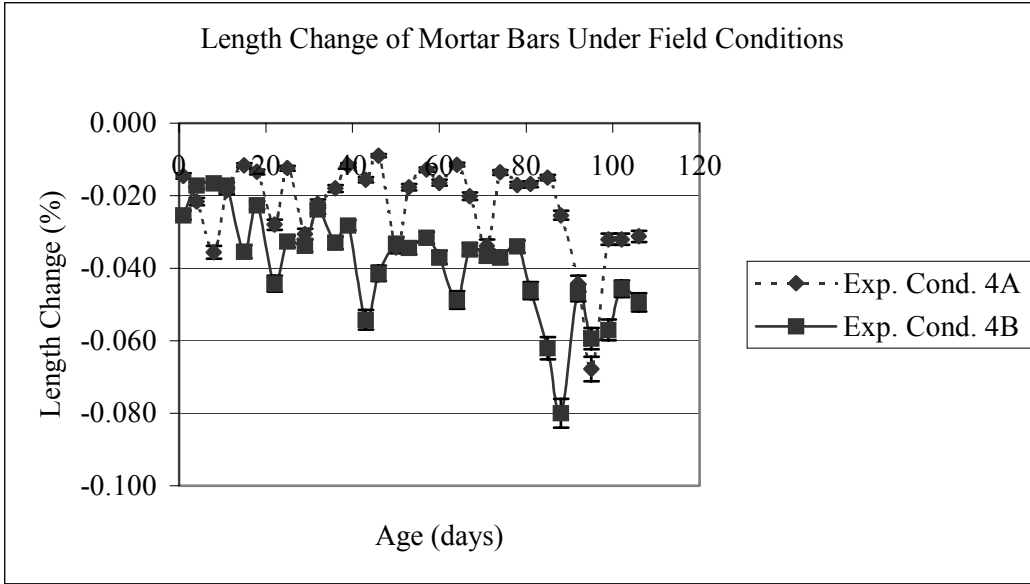


Figure 5.13 Length Change of Mortar Samples Exposed to Field Conditions

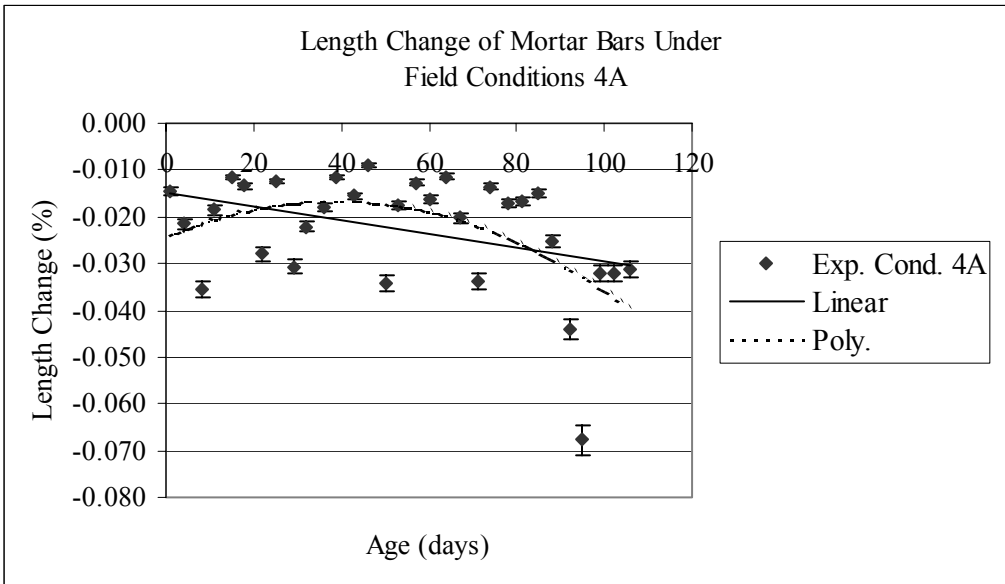


Figure 5.14 Length Change vs. Age of Steam-Cured Mortar Samples and Stored Under Field Condition 4A (Regression Curves)

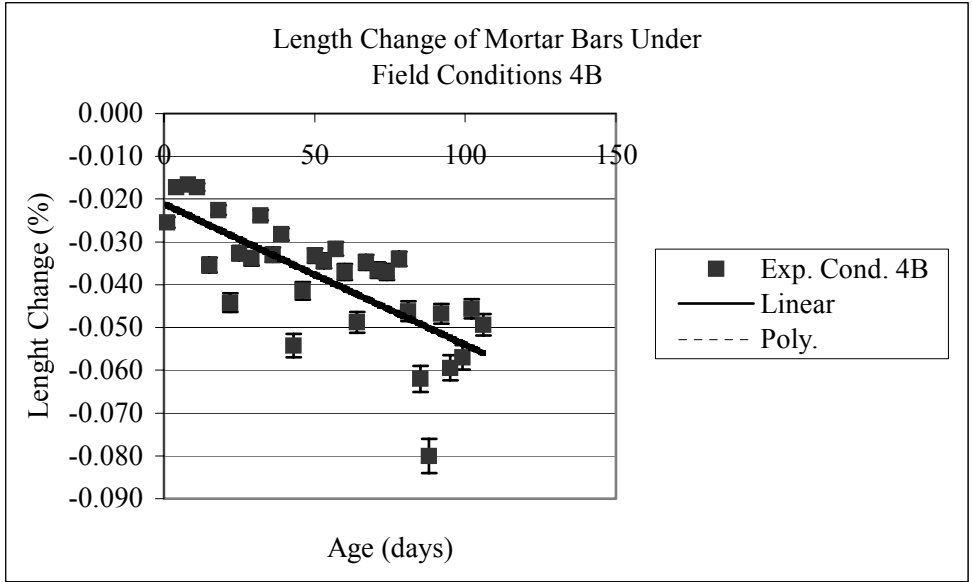


Figure 5.15 Length Change vs. Age of Mortar Samples and Stored Under Field Condition 4B (Regression Curves)

Table 5.5 Linear and Polynomial Equations for Length vs. Age of Mortar Samples Stored Under Field Conditions

Phase 1 (Mortar Control Samples - Field Conditions)	
Exposure Condition 4A	Exposure Condition 4B
Linear $y = -0.0001x - 0.0148$ $R^2 = 0.1464$	Linear $y = -0.0003x - 0.0211$ $R^2 = 0.5397$
Polynomial $y = -5E-06x^2 + 0.0004x - 0.0245$ $R^2 = 0.2865$	Polynomial $y = 3E-08x^2 - 0.0003x - 0.0211$ $R^2 = 0.5397$

5.4.2 Weight-Change Results

Weight change measurements of the mortar samples were monitored for both sets. Figure 5.16 shows the weight change results for the field-exposed mortar samples. Mortar samples in exposure condition 4B exhibits a higher weight change than those of exposure condition 4A. Both sets of mortar samples show a decrease in weight of the mortar samples for a duration of 100 days.

Figure 5.17 and 5.18 illustrate the regression curves for the best fit for the data. From the linear and polynomial equations provided in Table 5.6, there exists little or no correlation between weight change and time (duration of exposure). The fluctuation of the weight change of the mortar samples might be due to the constantly changing atmospheric conditions outside.

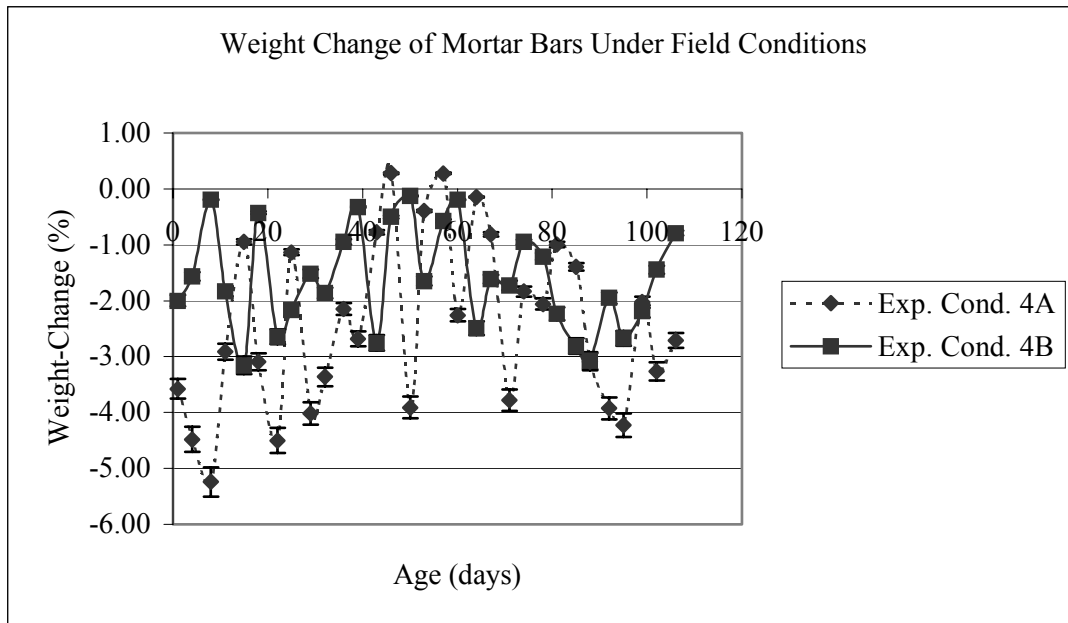


Figure 5.16 Weight Change of Mortar Samples Exposed to Field Conditions

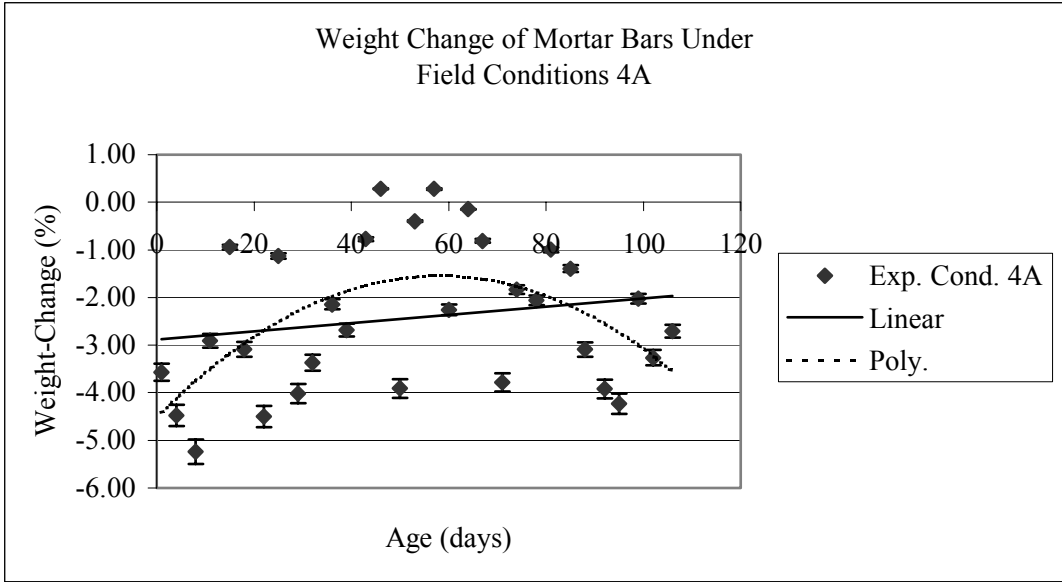


Figure 5.17 Weight Change vs. Age of Steam-Cured Mortar Samples and Stored Under Field Condition 4A (Regression Curves)

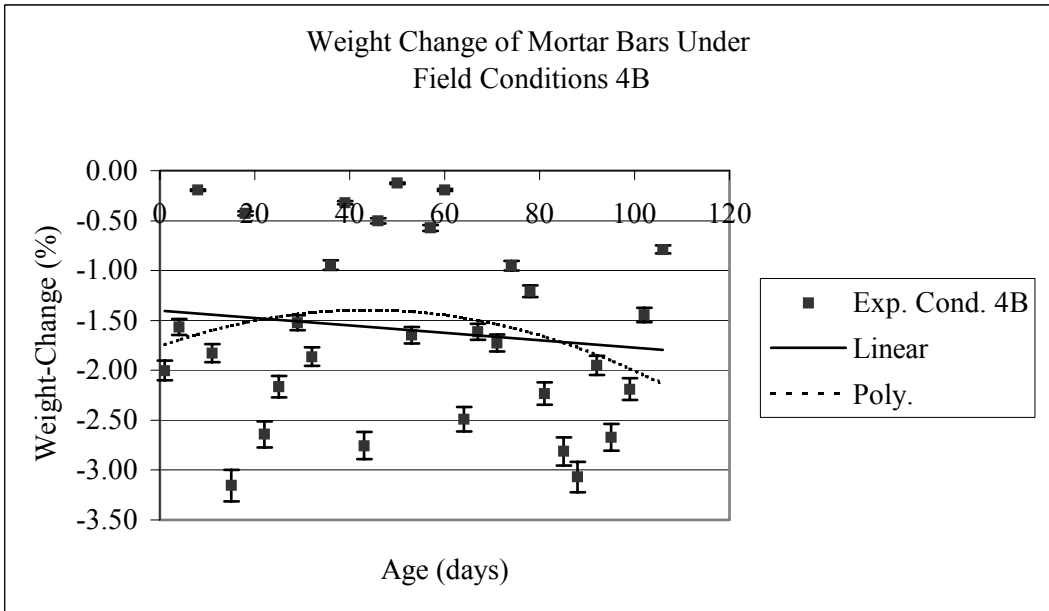


Figure 5.18 Weight Change vs. Age of Mortar Samples and Stored Under Field Condition 4B (Regression Curves)

Table 5.6 Linear and Polynomial Equations for Weight Change vs. Age of Mortar Samples Stored Under Field Conditions

Phase 1 (Mortar Control Samples - Field Conditions)	
Exposure Condition 4A	Exposure Condition 4B
Linear $y = 0.0086x - 2.8829$ $R^2 = 0.0325$	Linear $y = -0.0037x - 1.4023$ $R^2 = 0.0166$
Polynomial $y = -0.0009x^2 + 0.1022x - 4.5149$ $R^2 = 0.2952$	Polynomial $y = -0.0002x^2 + 0.0167x - 1.7584$ $R^2 = 0.0514$

5.4.4 Compressive Strength Results

The mortar specimens cured at room temperature exhibited an average compressive strength of 6996 psi at 28 days, while the steam-cured mortar specimens exhibited an average compressive strength of 6280 psi at 28 days. Table 5.8 shows the compressive strength results of the mortar specimens subjected to field conditions.

Table 5.7 Compressive Strength of Mortar Specimens Exposed to Field Conditions

28 Days - Comp. Strength (psi)		
Exp. Cond.	4A	4B
	6398	7188
	5715	6600
	6728	7200
Average	6280	6996
Std	516	343

5.5 Water Analysis Results of Storage Solution

Water analysis was performed using ion selective electrodes (ISE) and an ISE meter to obtain readings of the ions concentrations in the storage solutions. Potassium (K^+), Sodium (Na^+) and Calcium (Ca^{2+}) ion concentrations in the storage solutions were monitored periodically for depletion of alkali content. Also the pH values were monitored for exposure condition 2 to predict its effects on DEF. Analyzing the results of these selected variances may help in understanding the influence of the storage conditions after the heat treatment.

5.5.1 Water Analysis of Exposure Condition 1

Mortar samples stored in isothermal water bath, pH maintained at 12.5 (exposure condition 1) were monitored for leaching of Na^+ (sodium) and K^+ (potassium) into the storage solution. The highest concentration of alkalis leached was about 128 mmol/l recorded after 14 weeks. The measured Na^+ and K^+ concentrations in the storage solution increased with time during storage period. Figure 5.19 shows the alkalis concentration against age for the mortar samples in exposure condition 1.

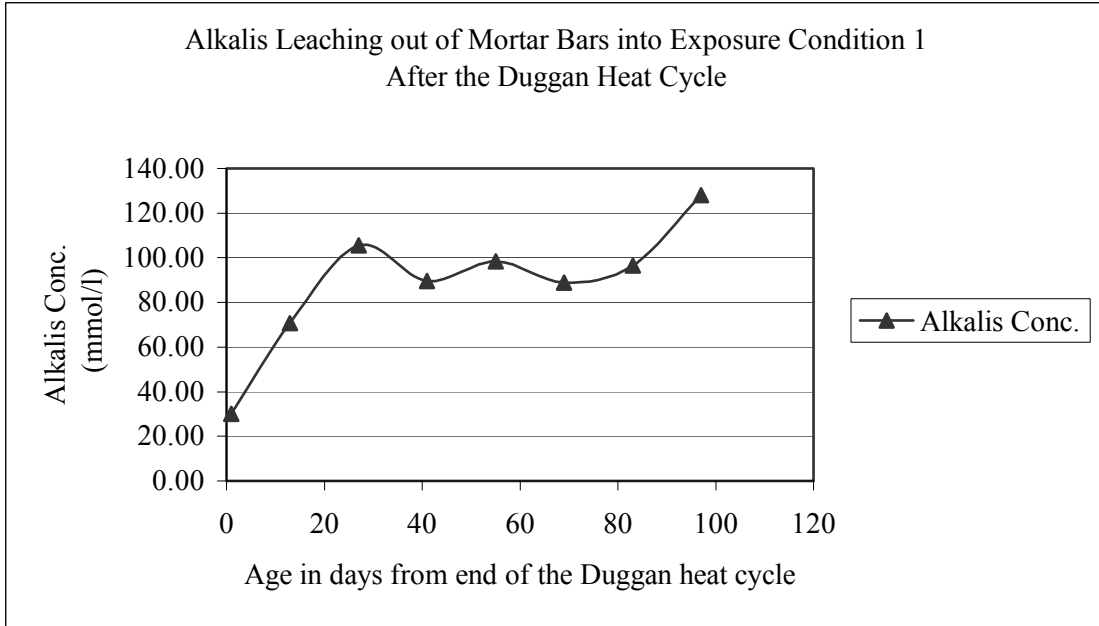


Figure 5.19 Alkalis Leaching from Mortar Samples Stored in Isothermal Water Bath, pH maintained at 12.5

5.5.2 Water Analysis of Exposure Condition 2

Mortar samples stored in exposure condition 2 (water at room temp.) are monitored for pH value, Na^+ , K^+ and Ca^{2+} ion concentrations.

5.5.2.1 Amount of Alkalis

A plateau seems to have been reached just after the fourth week from the end of the Duggan heat cycle for the mortar samples stored in exposed condition 2. At 4 weeks, the recorded alkalis concentration of the storage solution was 82 mmol/l. The alkalis concentrations decreased with time as shown in Figure 5.20.

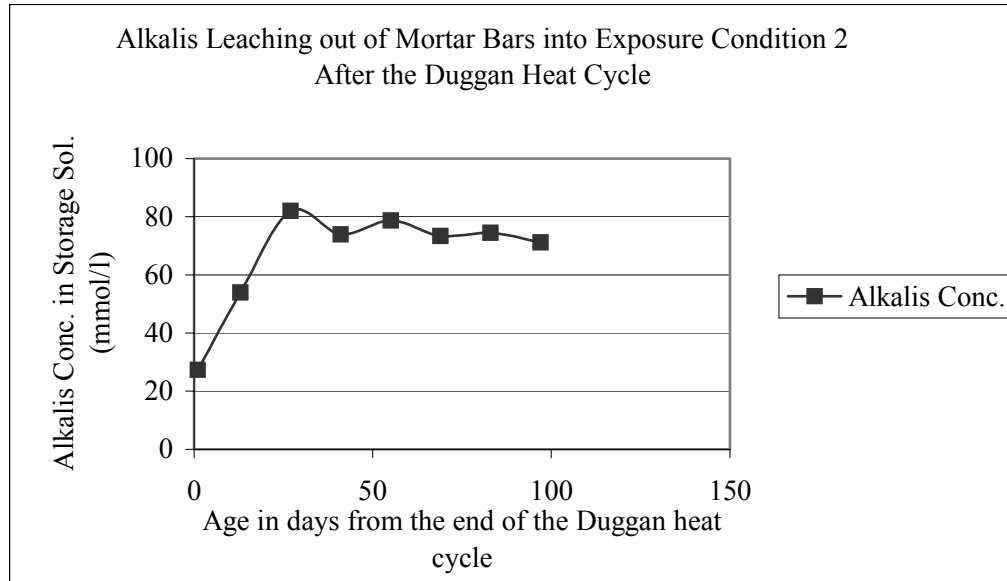


Figure 5.20 Alkalis Leaching from Mortar Samples Stored in Plain Water at Room Temperature

5.5.2.3 pH Value

The pH value of the storage solution ranged from 11.08 to 12.26 for the duration of 14 weeks. The pH value has effects on the morphology of ettringite. Hampson and Bailey concluded that at pH 11.5 to 11.8, sulphoaluminate forms as ettringite crystals and at pH 12.5 to 12.8, some non-crystalline materials might form with a composition similar to ettringite.

5.5.2.4 Calcium Concentration

Various researchers have mentioned the essential calcium to the ASR process (Chatterji et al. 1987, Diamond 1989, Struble 1987 and Kilgour 1988). They also illustrated that the presence of $\text{Ca}(\text{OH})_2$ seems to be essential for sodium and other ions to penetrate into the reacting grain. The formation of the reaction gel can take place

without deleterious expansion of concrete or mortar depending on the amount and availability of the Ca^{2+} ion. Figure 5.21 gives the calcium concentration of the storage solution for exposure condition 2.

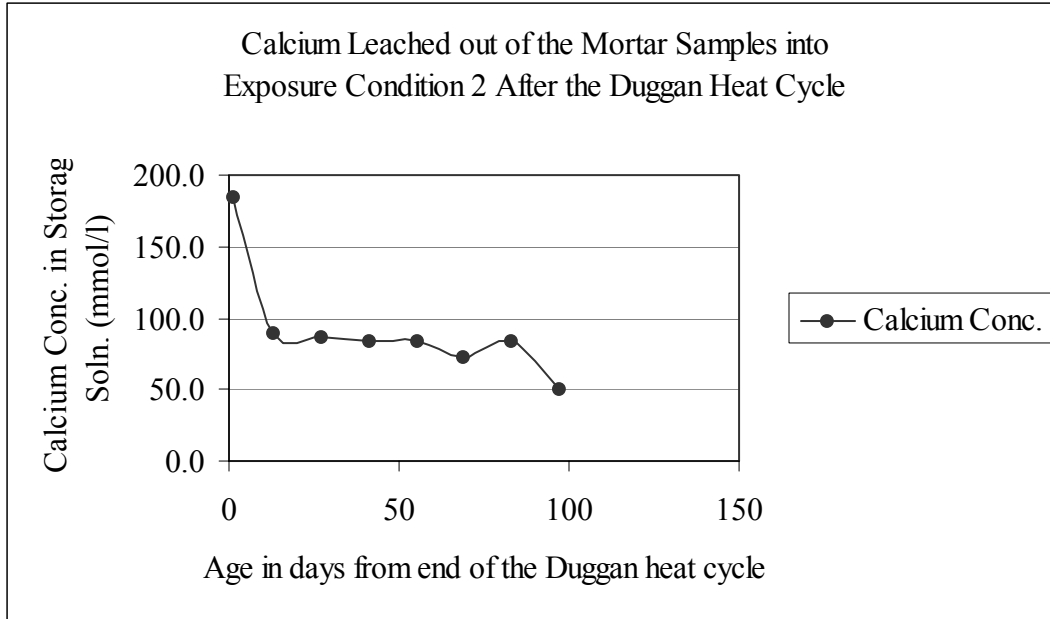


Figure 5.21 Calcium Leached from Mortar Samples Stored in Plain Water at room Temperature

The calcium concentrations of the storage solution of exposure condition 2 with time. This might be due to the highly alkaline pore solution that restricts the calcium remaining in the solution to negligible concentrations. The highest Ca^{2+} ion concentration recorded was 184 mmol/l during the storage period.

5.6 Microstructure Analysis Using SEM and EDAX

A scanning electron microscope (SEM) equipped with energy dispersive analysis X-ray (EDAX) testing was used on the samples to determine the chemical composition of the deposits within the microstructure. The samples were prepared as a fractured surface and then coated with carbon. Exposure condition influence on the ettringite shape and size was also noted during examinations.

5.6.1 Mortar Samples in Exposure Condition 1

At 40 days of storage in water, pH maintained at 12.5 (Exp. Cond. 1), SEM examination showed plenty of bubble-like needles of ettringite and patches of calcium hydroxide (CH) filling the air voids and cracks. Ettringite crystals (clusters) ($> 10\mu\text{m}$) were precipitated into the air voids and cracks within the microstructure of the mortar sample. At this early stage, well-developed and concentrated needle-like crystals completely filled voids and cracks. Figure 5.22 shows the SEM micrograph and EDAX analysis of the ettringite crystals forming at air void and cracks. Notice, also that figure 5.22 was captured at a magnification (935x), with 20,000 volts applied to filament to generate electrons. The EDAX analysis, a graph of intensity against x-ray energy, revealed ettringite having a chemical composition of Al = 5.51% wt., Si = 0.82% wt., S = 12.39% wt., and Ca = 77.57% wt as shown in figure and 5.23.

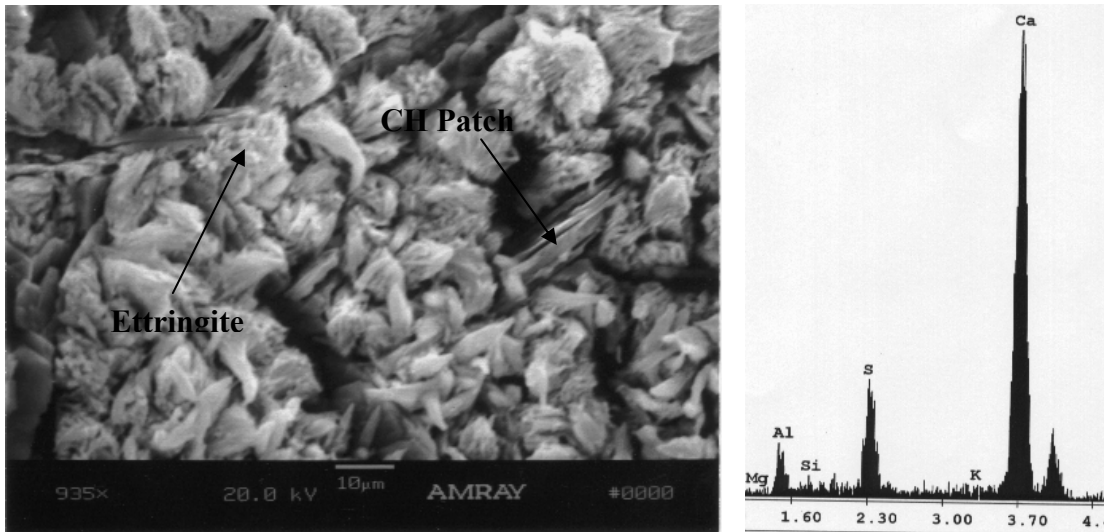


Figure 5.22 SEM and EDAX of Mortar Specimens in Exposure Condition 1 at Age of 40 days, Showing Ettringite Crystals and Patches of Calcium Hydroxide

EDAX ZAF Quantification (Standardless)
 Element Normalized
 SEC Table : Default

Element	Wt %	At %	K-Ratio	Z	A	F
MgK	0.59	0.91	0.0027	1.0255	0.4465	1.0050
AlK	5.51	7.73	0.0325	0.9951	0.5874	1.0078
SiK	0.82	1.11	0.0057	1.0238	0.6675	1.0140
S K	12.39	14.61	0.1108	1.0200	0.8503	1.0312
K K	1.08	1.04	0.0109	0.9770	0.9203	1.1275
CaK	77.57	73.21	0.7327	0.9992	0.9448	1.0006
FeK	2.04	1.38	0.0170	0.9108	0.9151	1.0000
Total	100.00	100.00				

Figure 5.23 EDAX of the Elemental Analysis of Massive Deposits that Shown in Figure 5.22

SEM investigations at 100 days revealed clusters of ettringite needles filling cavities within the microstructure of the specimen as shown in Figure 5.24. The clusters became more distinct and can be predominantly identified from the SEM micrograph and

EDAX elemental composition analysis. The clusters of the ettringite needles (>100 μm) filled the cavities; the EDAX analysis of the ettringite layer showed a chemical composition of Al = 5.74% wt., Si = 3.57% wt., S = 13.75% wt., and Ca = 72.95% wt. Also in figure 5.24, the EDAX analysis shows 2 peaks for Ca that is due to the intensity of the x-rays and originated from the different electronic shell transitions.

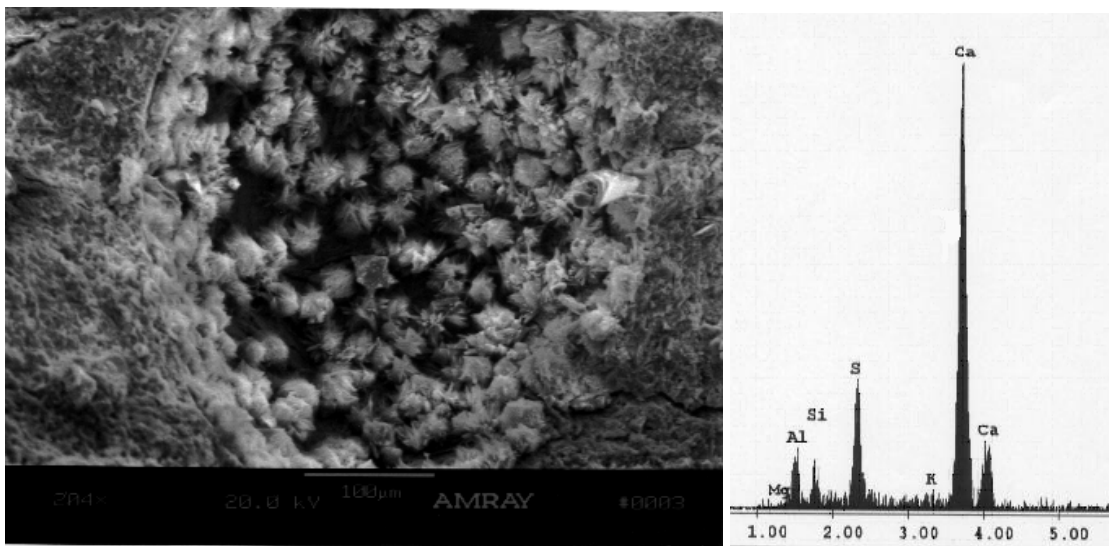


Figure 5.24 SEM and EDAX Analysis of Mortar Specimens in Exposure Condition 1 at Age of 100 days, Showing Clusters of Ettringite Needles Filling Cavities

5.6.2 Mortar Samples in Exposure Condition 2

Mortar samples were prepared and stored in water for 40 days before SEM examination. SEM and EDAX were used to determine or detect the chemical composition of deposits in the cracks and air voids within the microstructure of the specimen. Ettringite spherical balls were found filling the air voids and cavities of the specimens. A crack rim found around the sand aggregate was observed and was partially

filled with DEF as shown in Figures 5.25 and 5.26. The EDAX results indicate that the crack rim has a chemical composition of Al = 5.50% wt., Si = 7.30% wt., S = 9.57% wt., and Ca = 72.79% wt., which is characteristic of DEF.

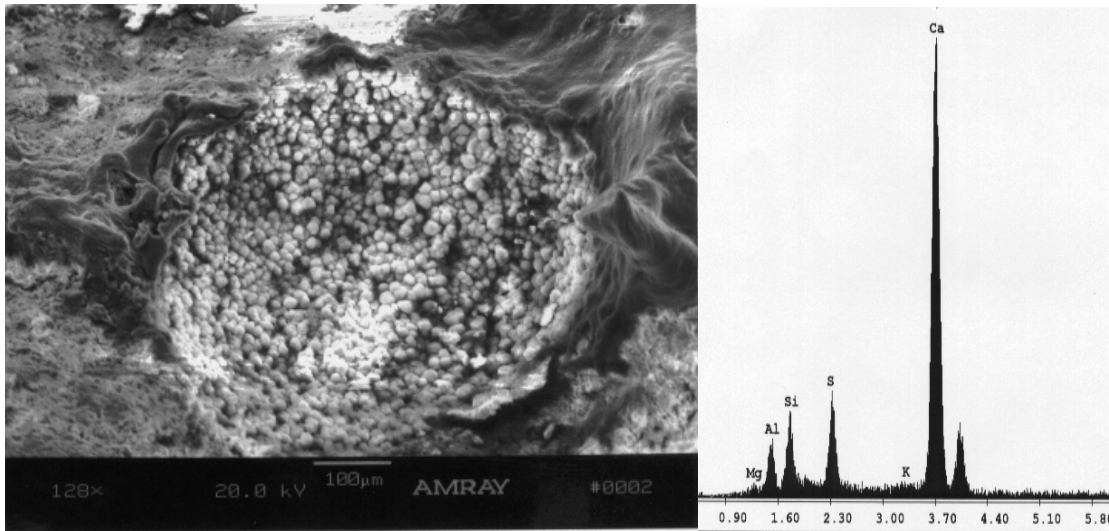


Figure 5.25 SEM and EDAX Analysis of Mortar Specimens in Exposure Condition 2 at Age of 40 days, Showing Ettringite Balls Filling the Cavity

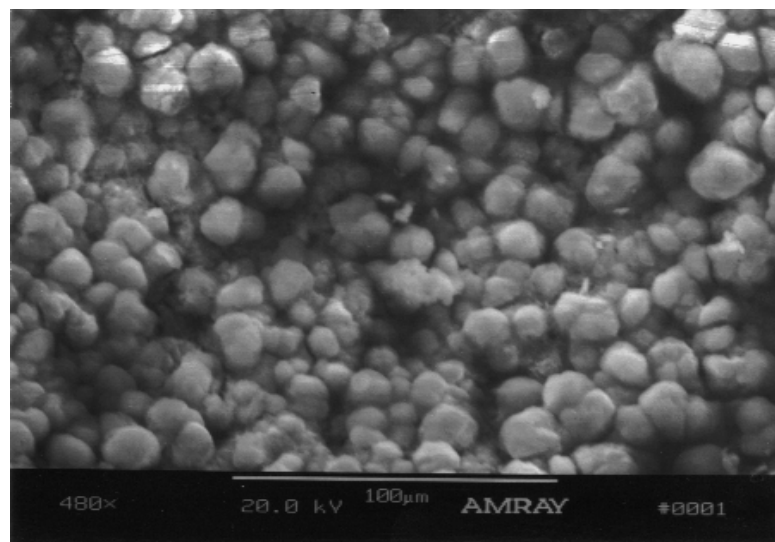


Figure 5.26 SEM of Mortar Specimens in Exposure Condition 2 at a Higher Magnification

SEM results at 100 days show ettringite balls in various locations in the examined mortar specimens. Figure 5.27, shows ettringite balls filling an aggregate pullout. The EDAX elemental mapping of these balls matched with ettringite having a chemical composition of Al = 4.95% wt., Si = 3.82% wt., S = 10.69% wt., and Ca = 76.41% wt.

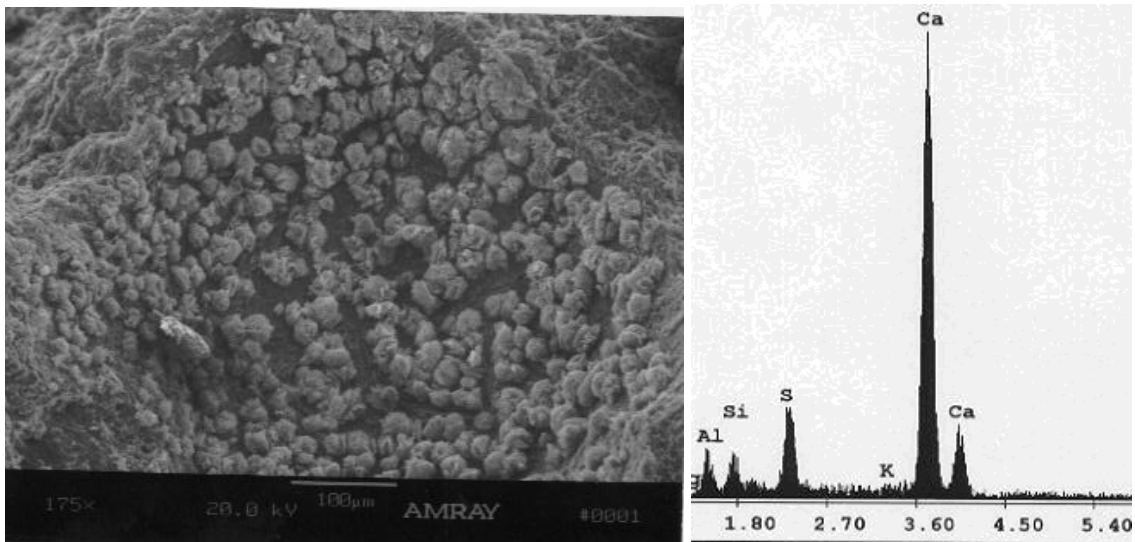


Figure 5.27 SEM and EDAX Analysis of Mortar Specimens in Exposure Condition 2 at Age of 100 days, Showing Ettringite Balls Filling an Aggregate Pull-Out

5.6.3 Mortar Samples in Exposure Condition 3

At 40 days, SEM and EDAX analysis of the specimens in exposure condition 3 show lots of ettringite needles in the air voids and cavities. The EDAX analysis indicates that the ettringite within the cavity of microstructure of the specimen has a chemical composition of Al = 1.51% wt., Si = 6.64% wt., S = 2.68% wt., and Ca = 86.76% wt. Also some calcium hydroxide (CH) crystals are found as shown in Figure 5.28.

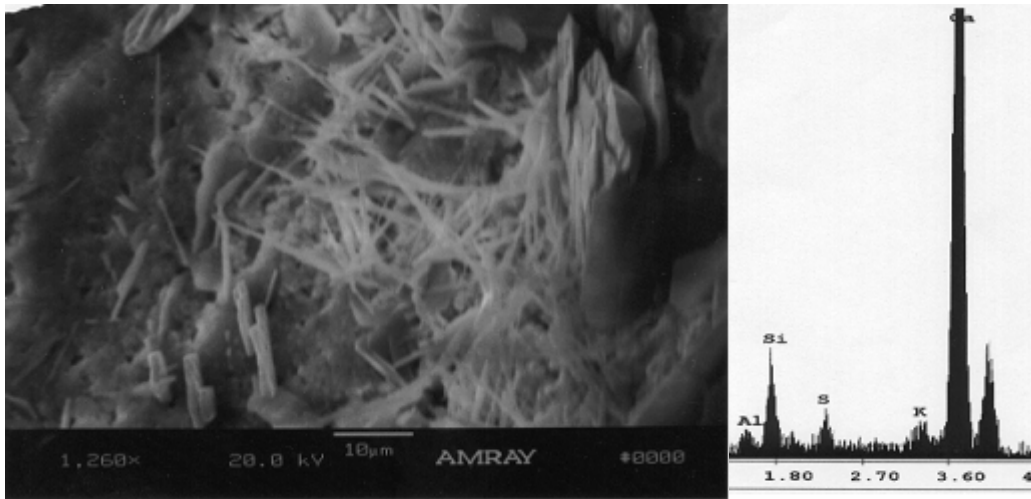


Figure 5.28 SEM and EDAX Analysis of Mortar Specimens in Exposure Condition 3 at Age of 40 days, Showing Ettringite Needles and CH Crystals Filling a Cavity

Results of the specimen examinations at 100 days reveal no ettringite found from the SEM micrograph or any detected by EDAX. Only cement paste, C-S-H gel and calcium hydroxide (CH) were determined by the EDAX elemental composition analysis within the specimen's microstructure.

5.6.4 Mortar Samples in Exposure Condition 4A

Based on the chemical composition and morphology of the material deposits between aggregate and cement, ettringite needles were observed using SEM equipped with EDAX. At 40 days, SEM and EDAX results revealed ettringite needles presence with reduced spectrum peaks. The reduced peaks were due to the presence of lots of calcium hydroxide crystal in the specimen. Figure 5.29 shows ettringite needles coupled with CH crystals for mortar specimens under field conditions. Figure 5.30 shows the EDAX analysis A is for the whole area and the EDAX analysis of B is for the spot (CH

crystal). Analysis of the whole figure reveals ettringite with a chemical composition of Al = 7.69% wt., Si = 1.93% wt., S = 16.02% wt., and Ca = 71.12% wt.

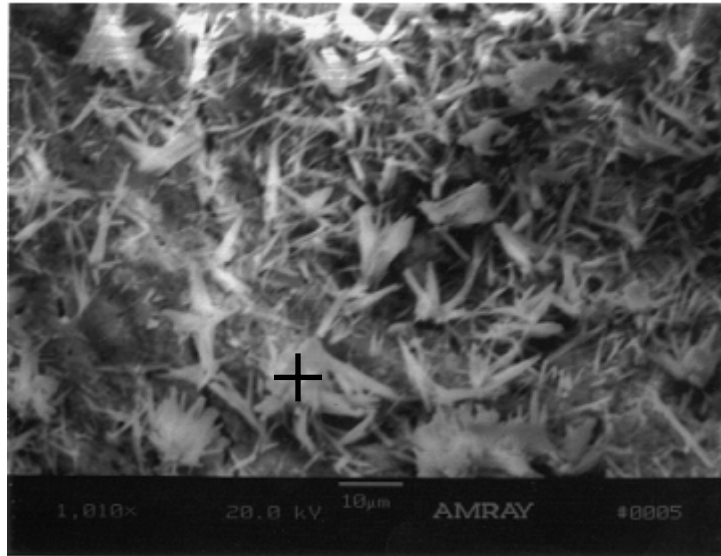


Figure 5.29 SEM Micrograph of Mortar Specimens Under Field Condition 4A at Age of 40 days, Showing Ettringite Needles and CH Crystals Between Aggregate and Cement Paste

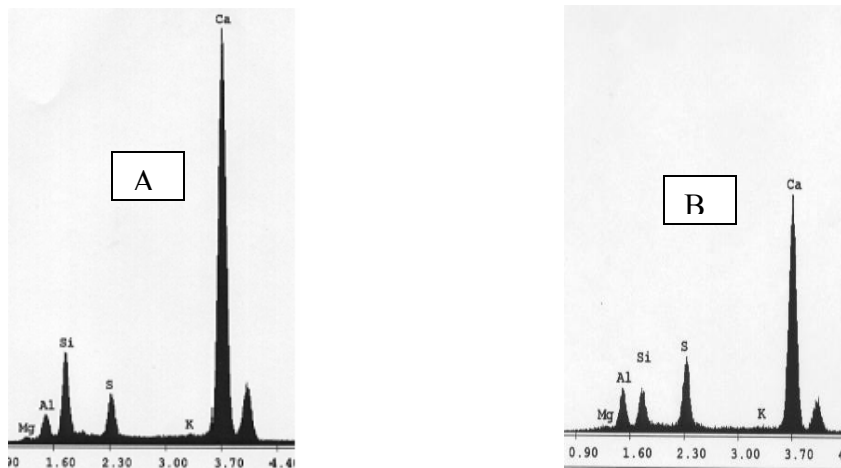


Figure 5.30 EDAX Analysis of whole area (A) and spot B (CH crystals)

At 100 days, concentrations of ettringite needles and clusters of CH crystals were found in the specimen. These massive ettringite crystals can be seen at low magnifications. Figure 5.31 shows the SEM and EDAX analysis of the specimens. The EDAX analysis reveals ettringite with a chemical composition of Al = 3.71% wt., Si = 4.51% wt., S = 7.60% wt., and Ca = 79.71% wt.

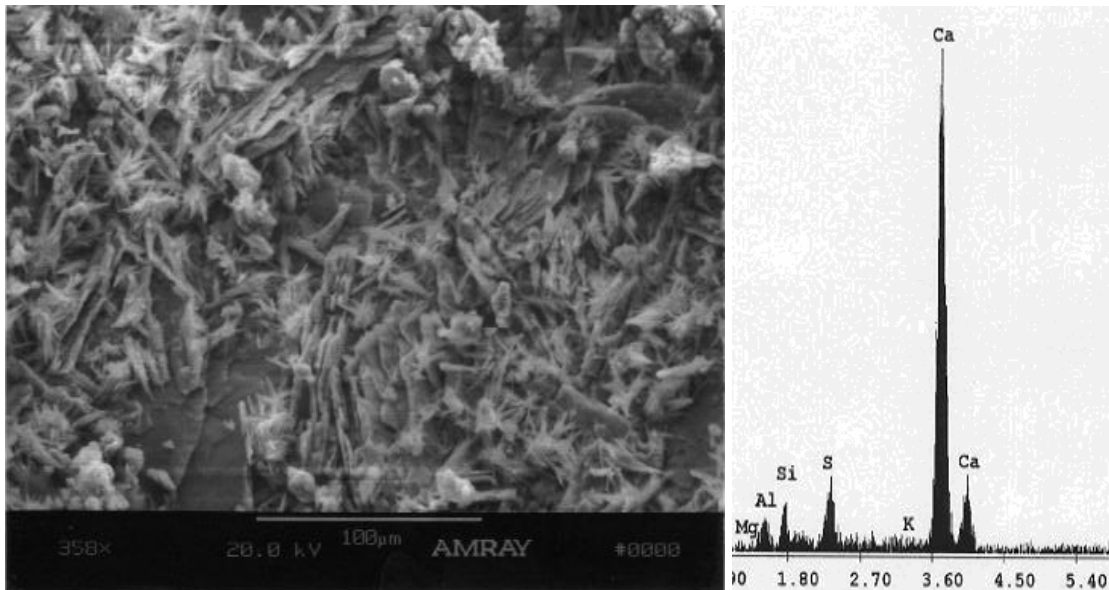


Figure 5.31 SEM and EDAX Analysis of Mortar Specimens Under Field Conditions 4A at Age of 100 days, Showing Ettringite Needles and CH Crystals on the Surface of An Aggregate

5.6.5 Mortar Samples in Exposure Condition 4B

Although the mortar samples were not steam cured at high temperature before being subjected to field conditions, ettringite needles and CH crystals were found from the SEM micrograph results just after 40 days of exposure. The ettringite needles were found around and within the air voids. The occurrences of needles were tentatively identified as ettringite but no EDAX analysis could be obtained. No EDAX spectrum

peaks were obtained because the conditions for maximum X-ray signal were not met due to very low counts. Figure 5.32 shows a SEM micrograph of the ettringite and CH crystals.



Figure 5.32 SEM Micrograph of Mortar Specimens Under Field Conditions 4B at Age 40 days, Showing Ettringite Needles and CH Crystals within Air Voids

At 100 days, no ettringite was found within the voids of the microstructure of the mortar sample. Most of the air voids were either concentrated with calcium hydroxide (CH) crystals or empty. Figure 5.33 shows the SEM and EDAX results of an air void filled with CH crystals. The EDAX confirms that the crystals within the air voids were CH and the chemical composition as Al = 0.00% wt., Si = 0.46% wt., S = 0.15% wt., and Ca = 97.81% wt. This clearly shows that CH crystals predominantly occupied the entire analysis void. Figure 5.34 shows the same air void at a higher magnification.

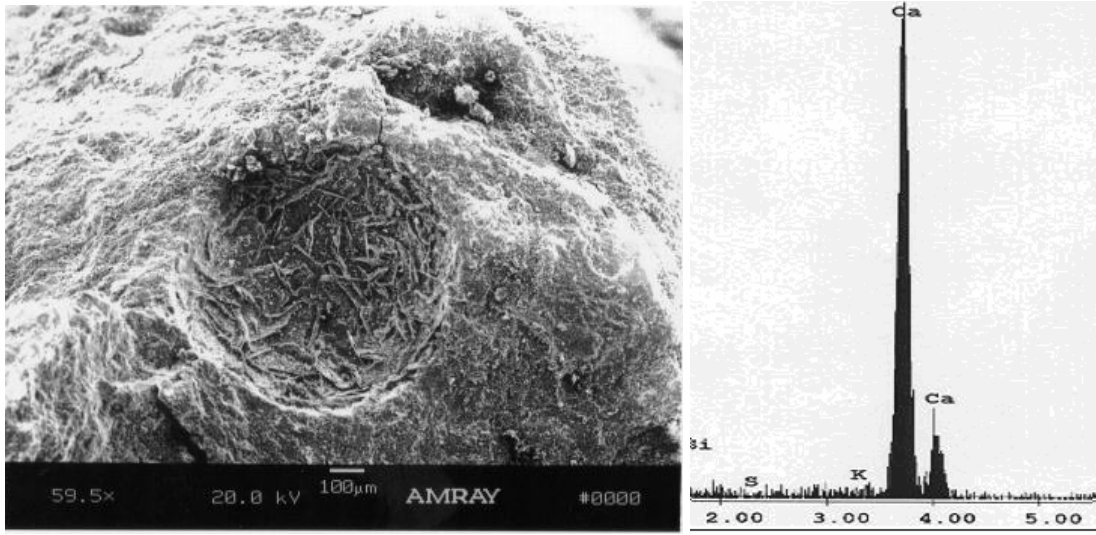


Figure 5.33 SEM Micrograph and EDAX Analysis of Mortar Specimens Under Field Conditions 4B at Age 100 days, Showing CH Crystals within Air Voids

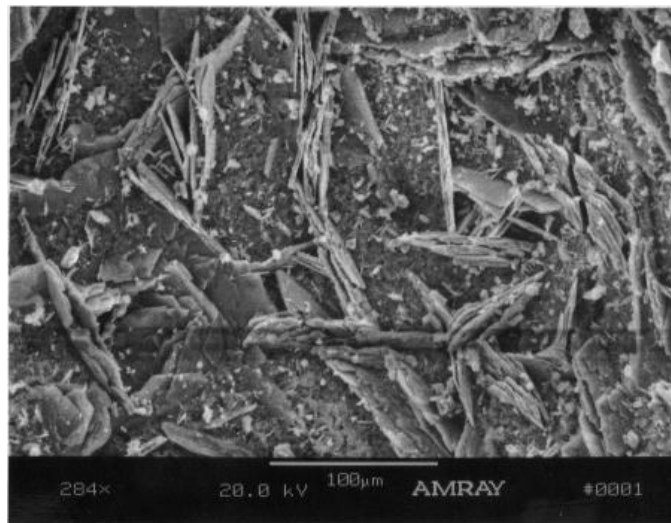


Figure 5.34 SEM Micrograph of Mortar Specimens Under Field Conditions 4B at Age 100 days, Showing CH Crystals within Air Voids at a Higher Magnification

5.7 X-ray Computed Tomography (X-ray CT) Analysis

X-ray computed tomography (X-ray CT) was used to reveal any interior cracks within the microstructure of the mortar specimens. Figures 5.35 and 5.36 show computed tomography images of the mortar specimens after 40 days of storage in the different exposure conditions. The 2” mortar cubes were steam-cured and then subjected to the Duggan heat cycle prior to storage. This method did not reveal any interior cracks in the paste or around the aggregate particles of the specimen’s microstructure. The X-ray computed tomography is a non-destructive test and helps in monitoring the crack initiation and propagation over a period of time.

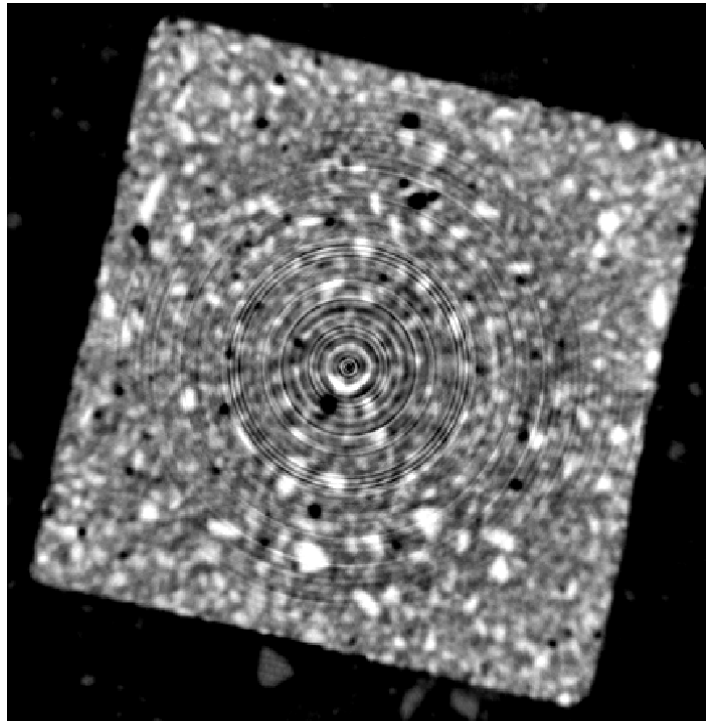


Figure 5.35 X-ray Computed Tomography Image of a Section Through a Control Mortar Cube Stored for 40 days in Exposure Condition 1

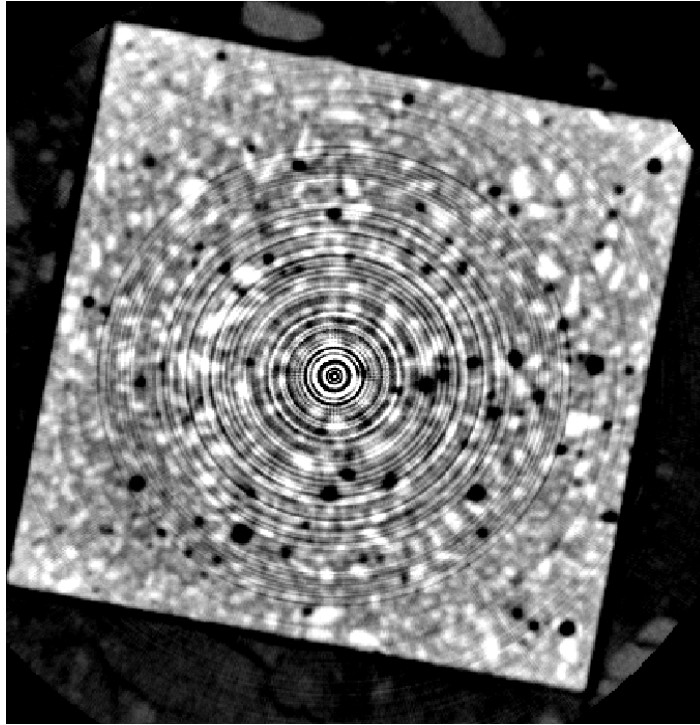


Figure 5.36 X-ray Computed Tomography Image of a Section Through a Control Mortar Cube Stored for 40 days in Exposure Condition 3

5.8 Summaries and Discussion of Control Samples

The Portland cement type III used in this research study exceeds all the threshold values suggested by researchers. In 1994, Taylor outlined threshold values at 0.83% for equivalent Na_2O , 0.22% for Na_2O , 3.6% for SO_3 and $1.6 \pm 0.2\%$ for MgO . These criteria and subjection of the specimens to the Duggan heat cycle influenced the initiation of expansion and premature deterioration due to delayed ettringite formation.

Expansion tests revealed that mortar samples stored in exposure condition 1 (pH maintained at 12.5) exhibit the highest expansion. Expansion values were highest in the storage solution with high calcium content. All mortar samples subjected to the Duggan heat cycle showed significant expansion for the period of storage, and the expansion

continued. Also all mortar samples subjected to the Duggan heat cycle exceeded 0.05% expansion value after 40 days of storage. Expansions of mortar bars subjected to the Duggan heat cycle can be fitted using the Kolmogrov-Avrami-Johnson-Mehl equations (KAJM) (Kruger, 1993). During this research study regression analysis was carried out using linear and polynomial functions to best fit the experimental data.

Shrinkage was observed in the mortar samples exposed to field conditions. Specimens in exposure condition 4A show less shrinkage but similar shrinkage patterns as specimens in exposure condition 4B.

Since the formation of ettringite requires the uptake of water, which results in weight gain of the specimen, mortar bars in exposures 1 and 2 showed significant increase in weight just after a few days of storage. Weight changes in exposure condition 3 (relative humidity of 97%) also revealed changes especially between 37 and 41 days of storage. SEM examination was performed at the 40th day to determine the chemical composition within the microstructure of the specimen. The SEM results revealed ettringite and it is assumed the sudden weight change were solely due to the formation of delayed ettringite. Weight changes of the mortar bars under field conditions were irregular and showed little or no correlation with age.

For 100 days of storage after the Duggan heat cycle, the length and weight changes of the mortar bars were monitored and the results analyzed. Expansion against weight change of mortars in exposure conditions 1 and 2 showed high positive linear correlation. It is assumed that expansion of the mortar bars is primarily due to the growth and formation of ettringite. Grattan-Bellew et al obtained similar results; they concluded

that there was a linear correlation between mass and expansion for mortar bars stored at 23°C in limewater over a period of 17 to 59 days (1998).

Form the early compressive strength testing results, the mortar specimens exposed to field conditions exhibited higher strength than the specimens subjected to the Duggan heat cycle. These test results suggest that the Duggan heat cycle adversely affects the compressive strength of the mortar samples. Further testing will be required to postulate and correlate the compressive strength of the mortar samples with Duggan heat cycle. Several researchers indicated a strength reduction associated with high curing temperatures (Ramadan 2000, Ronne and Sellevold 1994, Taylor 1994).

The presence of alkalis greatly suppressed the dissolution of calcium hydroxide but enhanced the formation of ettringite. The alkali ions accelerate the formation of ettringite (Daerr et al 1977, Wang et al 1986 and Way et al 1989). The hydroxide ions from the hydration of Portland cement result in a pore solution having a pH value of about 12.5 (Diamond 1983). The concentration of alkali hydroxide in the storage solutions was slightly higher in exposure condition 1 than 2. This might be the reason why exposure condition 1 exhibits higher expansions. The high concentration of Ca^{2+} ions in exposure condition 1 can also contribute to the formation of ettringite. This can be confirmed by examinations of the mortar samples with the SEM equipped with EDAX. Researchers believed that formation of reaction gel taking place in concrete and mortar bars depends on the amount and availability of the Ca^{2+} (Struble 1987 and Kilgour 1988).

The microstructural analysis of the control mortar samples subjected to the Duggan heat cycle revealed lots of ettringite formation. The SEM results show the

morphology and crystal size of the ettringite varying for the different exposure condition with time. At 40 days of storage, mortar samples in exposure condition 1 showed ettringite needles ($> 10 \mu\text{m}$) and patches of calcium hydroxide filling air voids and cracks. Mortar samples in exposure condition 2 featured ettringite balls ($> 100 \mu\text{m}$) deposited in cavities. For the mortar samples in exposure condition 3 (relative humidity of 97%), ettringite needles and CH crystals were found filling the cavities after 40 days.

SEM studies of the mortar samples exposed to field conditions reveal presences of ettringite. The steam-cured mortar samples with no Duggan heat cycle show abundant ettringite needles and CH crystals between aggregate and cement paste. For the room temperature-cured mortar samples, ettringite needles were found after 40 days. The ettringite needles were not well developed. The X-ray signal output from the EDAX could not be obtained to further verify the chemical composition of the deposits. The occurrences of the gel deposits were tentatively identified as ettringite due to the shape and size revealed by the SEM micrograph.

X-ray CT image sections of the 2" mortar cubes did not reveal any interior cracks. Specimens that were under field conditions did not show any interior cracks regardless of the changing environmental conditions. Cracks were found by SEM to be filled only with ettringite crystals.

ASR was not found accounted for in any of the examined mortar samples. The absence of ASR suggests that the test parameters used in this research study were not conducive to ASR deleterious mechanism.

CHAPTER 6: MORTAR SAMPLES WITH 1.5% POTASSIUM CONTENT

6.1 Introduction

The research study reported in this chapter focuses on the effects of an increase in potassium content expressed as K_2O in the mortar mixes. Again, five (5) sets of mortar specimens were prepared according to the modified sample preparation method. As described earlier, only potassium carbonate is added to the batch mixes to increase the alkalinity. Some of the samples were steam-cured and others cured at room temperature in the laboratory as before. After steam curing the samples were stored in water for 6 days. Then they were subjected to the Duggan heat cycle, which took 7 days to complete prior to storage of specimens in their respective exposure conditions.

Again, 2” mortar cubes were tested for compressive strength after 28 days of storage. Scanning electron microscopy (SEM) and X-ray computed tomography (X-ray CT) testing were also performed to determine the cause of expansions, cracks and chemical composition of the deposits within each specimen’s microstructure.

The objectives were to study the effect of additional potassium on the expansion of mortar samples and analyze its influence on the expansion rate, weight change and DEF. SEM testing was conducted to identify the deterioration mechanism causing expansion and weight change. X-ray CT was used to analyze the internal microstructure for crack detection. All the test results are discussed and analyzed in this chapter.

6.2 Influence of Potassium Content and Exposure Conditions

The specimens were all prepared with increased potassium content in order to study its influence in the expansions, weight changes, and microstructure of the specimens. Again, expansion and weight change were periodically monitored. As suggested by Duggan, the expansion values at 21 days were compared to the threshold value of 0.05% as pass/fail criteria. SEM equipped with EDAX and X-ray CT testings were conducted at different times to investigate the mechanism responsible for the expansion.

6.3 Mortar Samples Subjected to Duggan Heat Cycles Test Results

For Phase 2, to accelerate the expansion, three mortar batch mixes were subjected to the Duggan heat cycle after one week of casting. All the mixes had an overall potassium content expressed as K_2O of 1.5% by weight of cement added to the mixing water during batching. The experimental results and test performed are discussed and analyzed for the different exposure conditions in the following sections.

6.3.1 Expansion Results

Five (5) mortar bars were used from each of the respective exposure conditions for length change measurements. The mortar specimens made with 1.5% potassium content show higher expansion than the control specimens. Just after 5 days, mortar specimens in exposure conditions 1 and 2 exceeded the Duggan threshold value of 0.05% expansion. Figure 6.1 shows the expansion against time (days of storage after the Duggan heat cycle). Expansion values at 21 days of mortar specimens in exposure

conditions 1, 2, and 3 were 0.117%, 0.200% and 0.055% respectively, which all exceeded the Duggan threshold value. These results also confirmed that an increase in alkali content of the mortar specimens increases the potential for the mortar to expand.

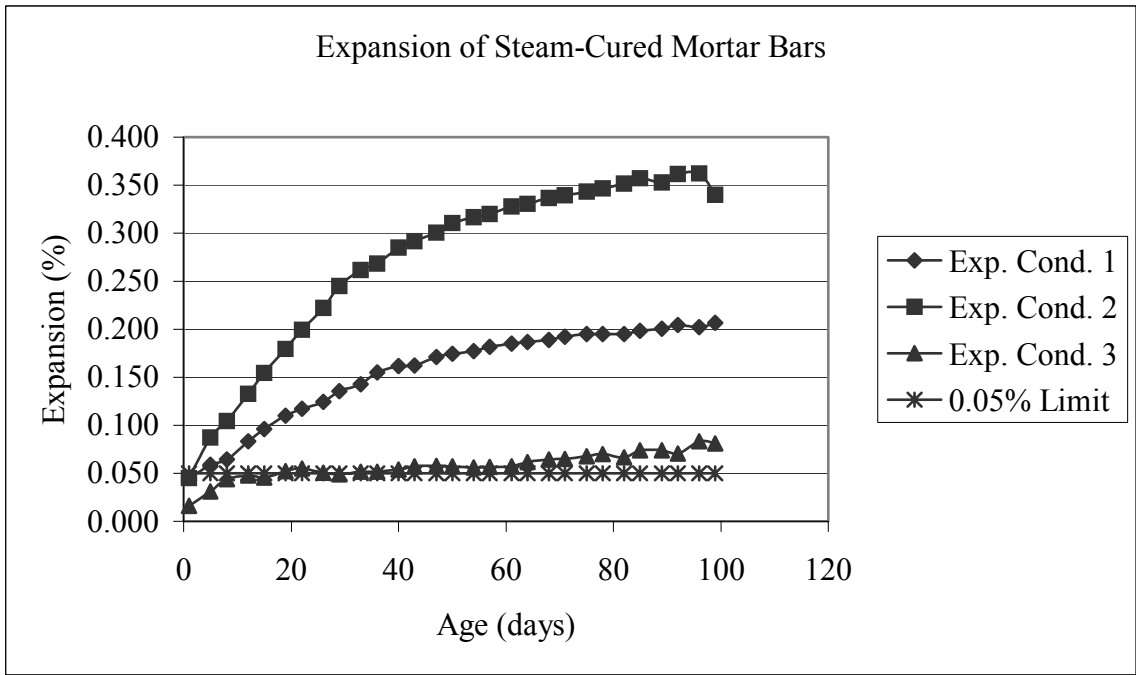


Figure 6.1 Expansion of Mortar Samples Subjected to Duggan Heat Cycle and Stored Under Different Exposure Conditions

Figures 6.2, 6.3, and 6.4 show the linear and polynomial regression analysis of the experimental data. Mortar bars stored in exposure condition 2 (plain water at room temperature) show higher linear and polynomial correlation of expansion against age than the other exposure conditions. Table 6.1 provides a summary of the regression equations used for analysis.

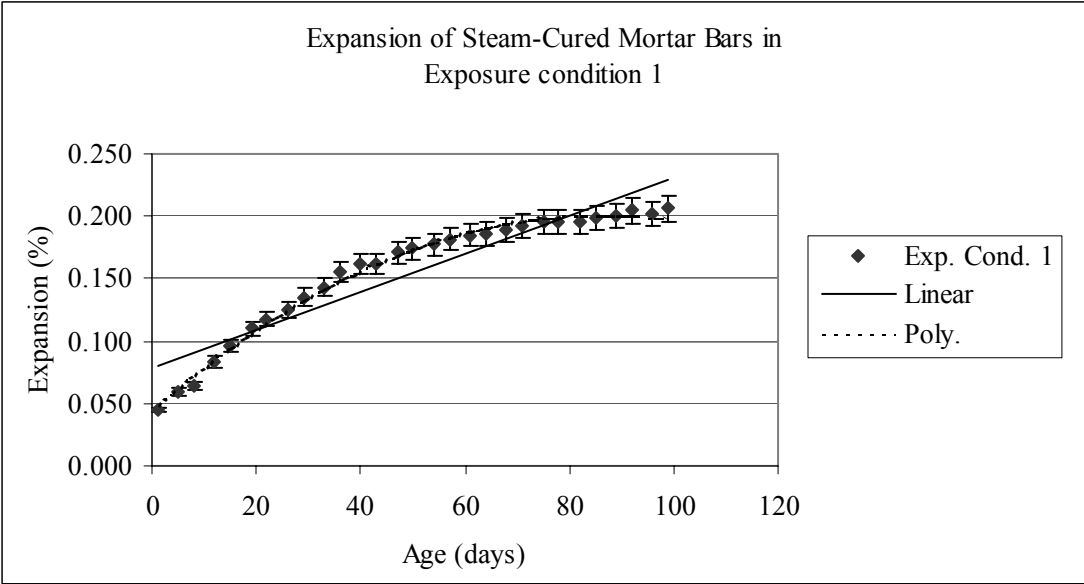


Figure 6.2 Expansion of Mortar Samples Subjected to Duggan Heat Cycle and Stored in Isothermal Water Bath, pH maintained at 12.5 (Regression Curves)

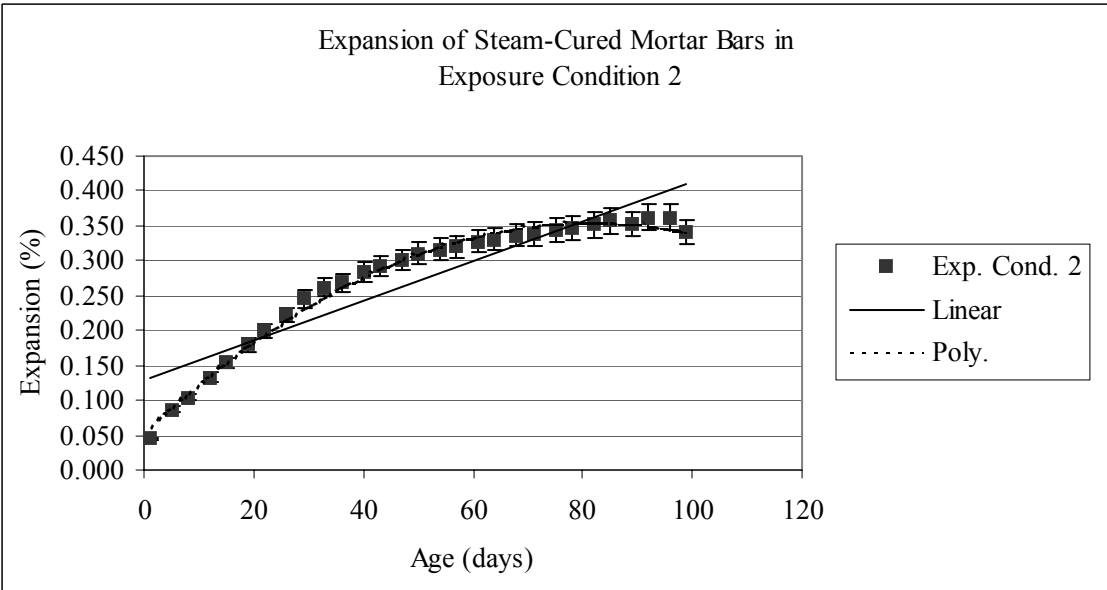


Figure 6.3 Expansion of Mortar Samples Subjected to Duggan Heat Cycle and Stored in Plain Water at Room Temperature (Regression Curves)

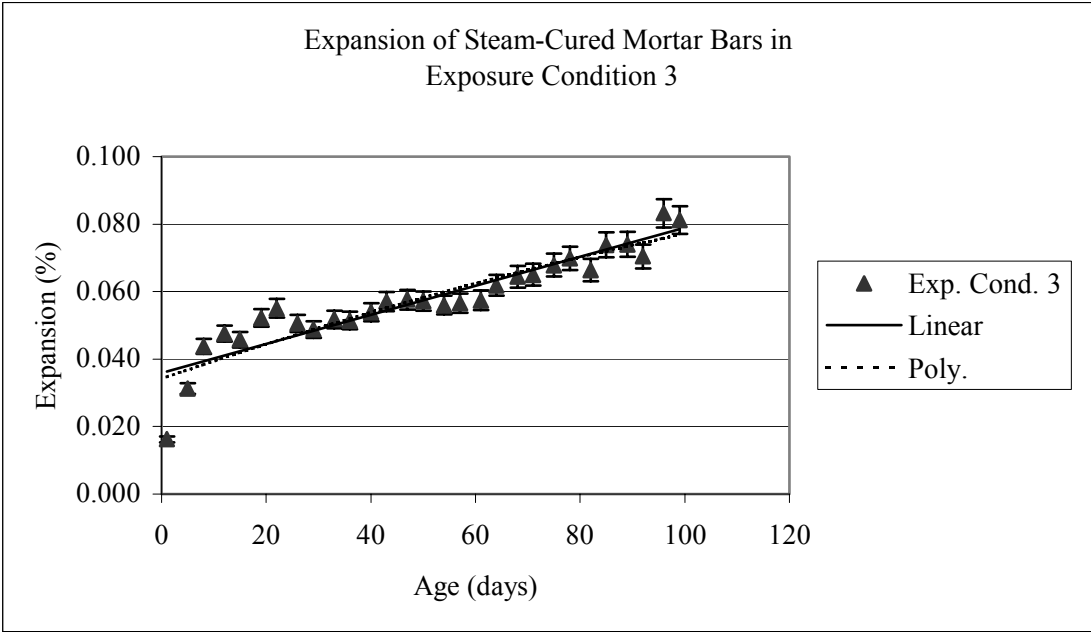


Figure 6.4 Expansion of Mortar Samples Subjected to Duggan Heat Cycle and Stored in Moist Air Chamber, R.H maintained at 97% (Regression Curves)

Table 6.1 Linear and Polynomial Equations for Expansion vs. Age of Steam-Cured Mortar Samples Stored Under Different Exposure Conditions

Exposure Condition 1 (Isothermal water bath, pH 12.5)	Exposure Condition 2 (Plain water at room temp.)	Exposure Condition 3 (Moist air chamber, R.H at 97%)
Linear $y = 0.0015x + 0.0791$ $R^2 = 0.8789$	Linear $y = 0.0028x + 0.1285$ $R^2 = 0.845$	Linear $y = 0.0004x + 0.0359$ $R^2 = 0.8429$
Polynomial $y = -2E-05x^2 + 0.0036x + 0.0442$ $R^2 = 0.993$	Polynomial $y = -5E-05x^2 + 0.0074x + 0.0531$ $R^2 = 0.9916$	Polynomial $y = -1E-06x^2 + 0.0005x + 0.0342$ $R^2 = 0.8462$

6.3.2 Weight Change Results

Weight change of the mortar bars under different exposure conditions is shown in Figure 6.5. It has been shown that for most specimens, significant weight changes take place in the first 100 days of storage. Just after 1 day of storage, a significant weight changes of about 10% were observed in exposure conditions 1 and 2. Up to 100 days of storage, mortar specimens in exposure conditions 1 and 2 posed similar weight change patterns. Weight changes of specimens in exposure condition 3 were the lowest but increased at a steady rate during the time of storage.

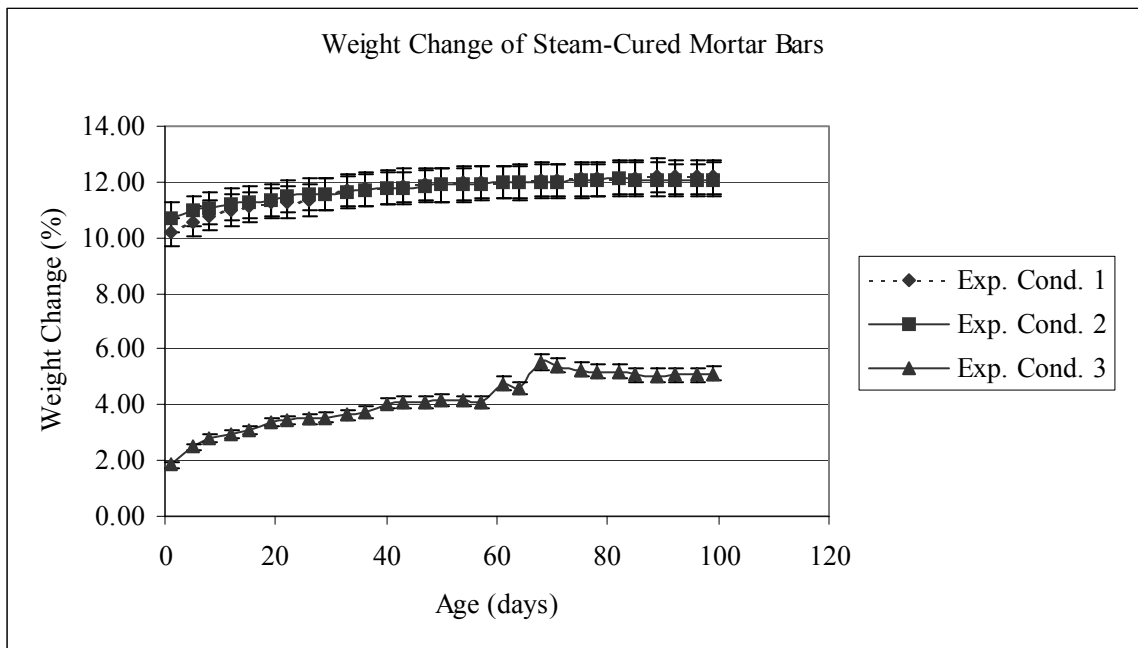


Figure 6.5 Weight Change of Mortar Samples Subjected to Duggan Heat Cycle and Stored Under Different Exposure Conditions

The best correlation coefficient for the weight change against age for the experiment data was obtained using linear and polynomial regression curves. Figure 6.6

through 6.8 show linear and polynomial regression curves fitted to the data. Table 6.2 gives the regression equations of the experimental data.

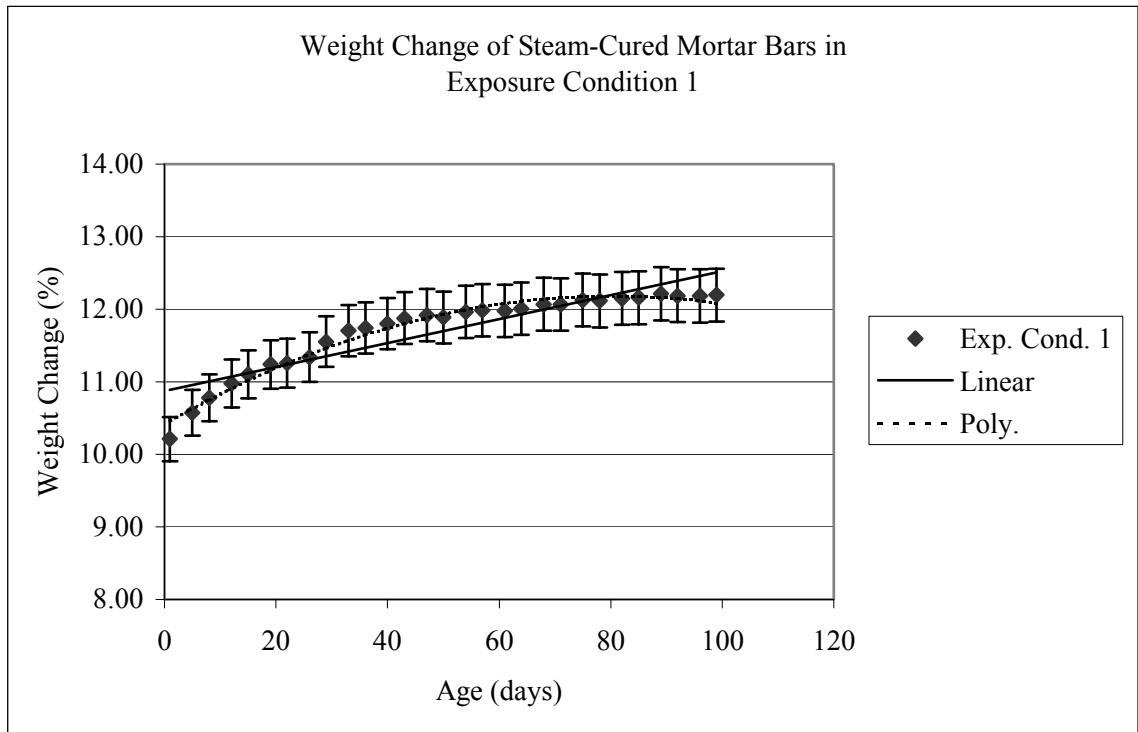


Figure 6.6 Weight Change of Mortar Samples Subjected to Duggan Heat Cycle and Stored in Isothermal Water Bath, pH maintained at 12.5 (Regression Curves)

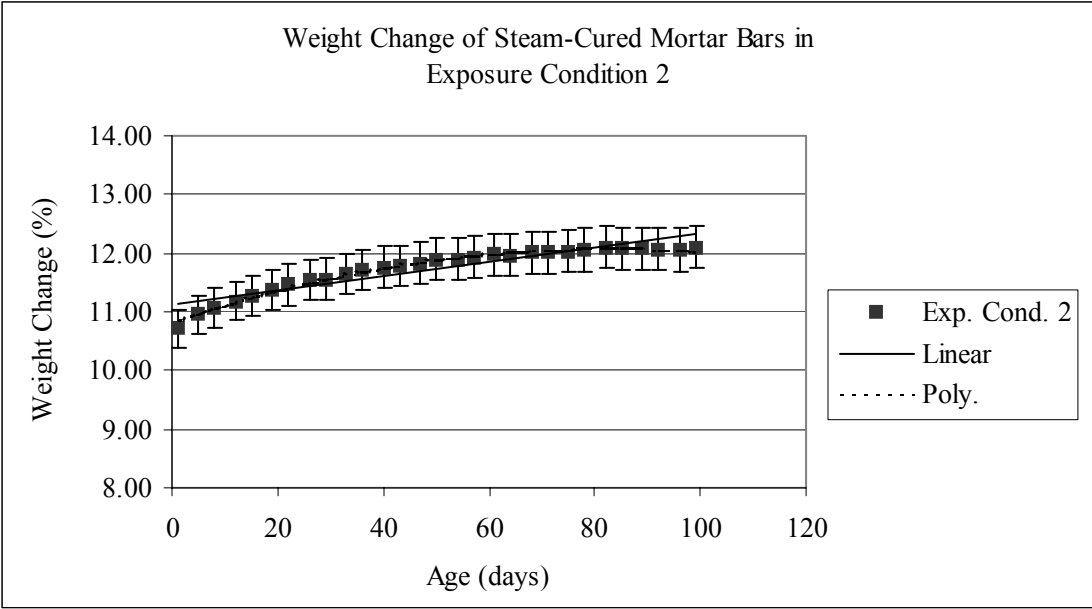


Figure 6.7 Weight Change of Mortar Samples Subjected to Duggan Heat Cycle and Stored in Plain Water at Room Temperature (Regression Curves)

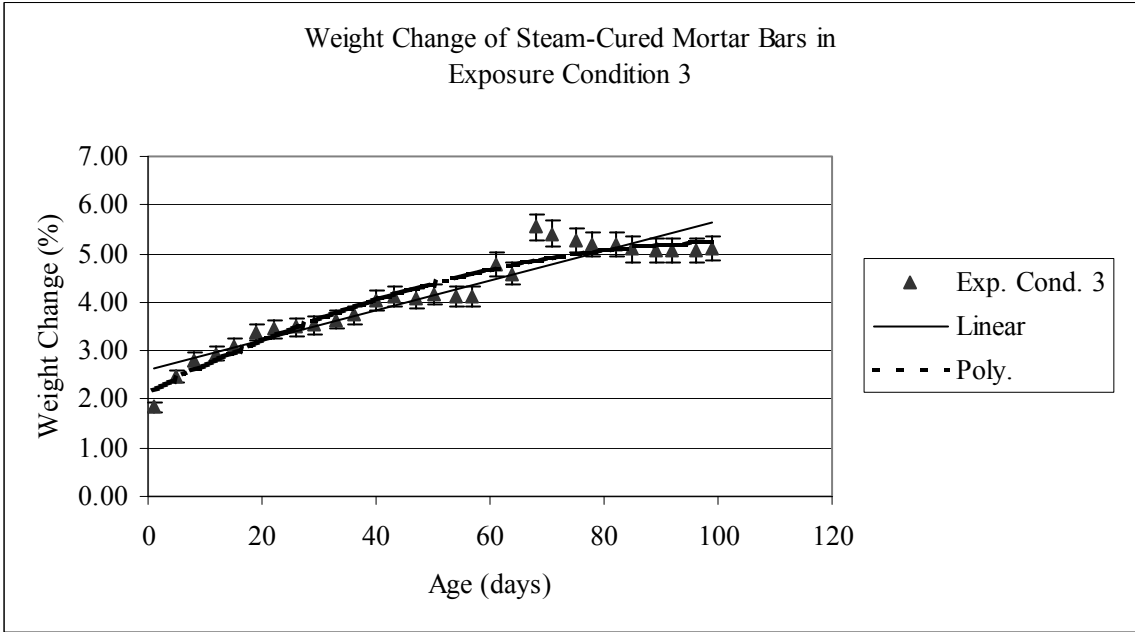


Figure 6.8 Weight Change of Mortar Samples Subjected to Duggan Heat Cycle and Stored in Moist Air Chamber, R.H maintained at 97% (Regression Curves)

Table 6.2 Linear and Polynomial Equations for Weight Change vs. Age of Steam-Cured Mortar Samples Stored Under Different Exposure Conditions

Phase 1 (Mortar Control Samples - subjected to Duggan Heat Cycle)		
Exposure Condition 1 (Isothermal water bath, pHat 12.5)	Exposure Condition 2 (Plain water at roomtemp.)	Exposure Condition 3 (Mbsit Air Chamber, RHat 97%)
Linear $y=0.0165x+10.871$ $R^2=0.8201$	Linear $y=0.012x+11.129$ $R^2=0.8531$	Linear $y=0.0308x+2.6021$ $R^2=0.8856$
Polynomial $y=-0.0003x^2+0.044x+10.418$ $R^2=0.9752$	Polynomial $y=-0.0002x^2+0.0304x+10.824$ $R^2=0.9899$	Polynomial $y=-0.0003x^2+0.0587x+2.1407$ $R^2=0.9346$

6.3.3 Expansion against Weight-Change of Specimens

Mortar mixes with high alkali content show the expansion and weight change experimental data to be linearly correlated. The mortar bars mixed during this phase study have 1.5% K₂O content and were stored under different exposure conditions after the Duggan heat cycle. Figure 6.9 shows the expansion against weight change data results.

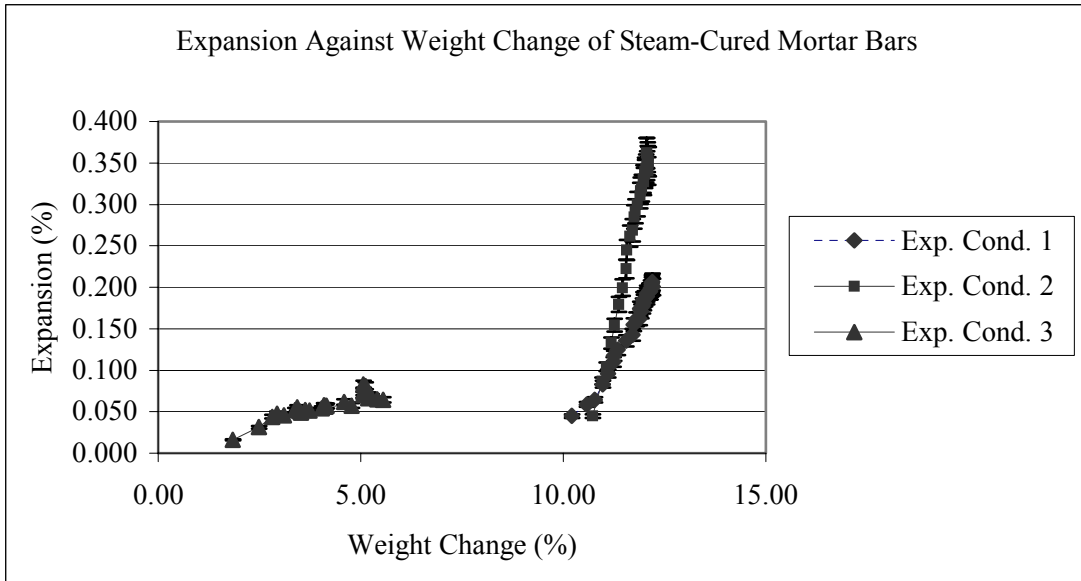


Figure 6.9 Expansion Against Weight Change of Mortar Samples Subjected to Duggan Heat Cycle and Stored Under Different Conditions

The best correlation coefficient for the expansion against weight change of the mortar bars was obtained using linear and polynomial regression analysis. Figures 6.10 through 6.12 show the linear and polynomial regression curves of the mortar bars for the different exposure conditions. The results revealed that a high positive linear and polynomial correlation exists between expansion and weight change of the mortar bars in exposure conditions 1 and 2. Table 6.3 provides the regression equation and coefficient for the different exposure conditions.

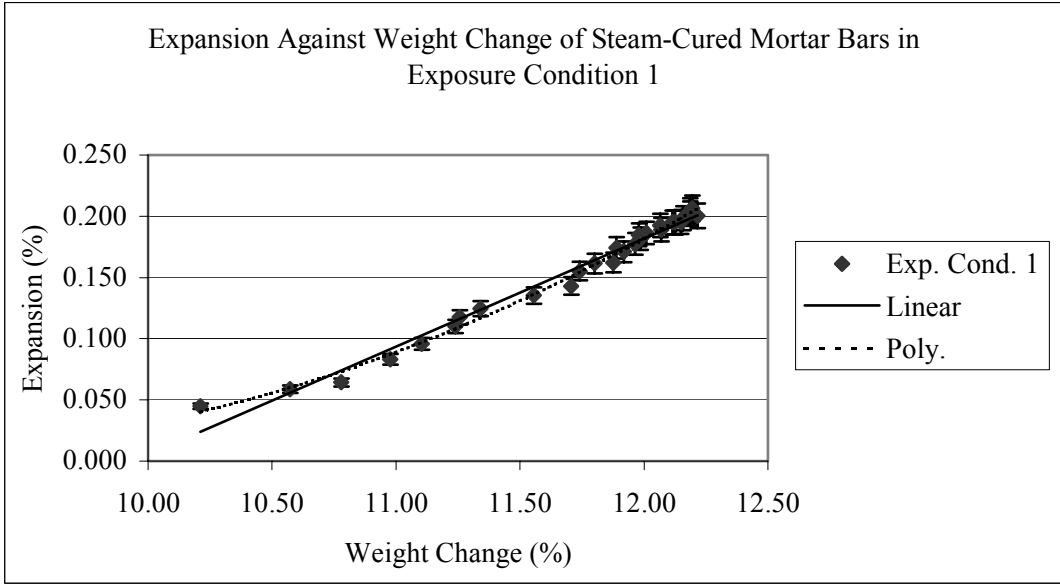


Figure 6.10 Expansion Against Weight Change of Mortar Samples Subjected to Duggan Heat Cycle and Stored in Isothermal Water Bath, pH maintained at 12.5 (Regression Curves)

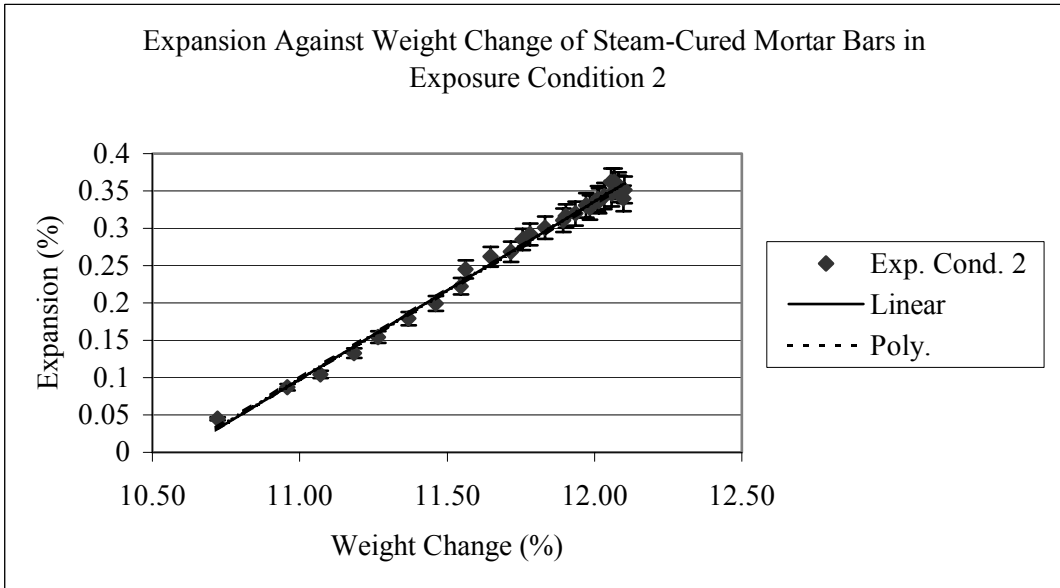


Figure 6.11 Expansion Against Weight Change of Mortar Samples Subjected to Duggan Heat Cycle and Stored in Plain Water at Room Temperature (Regression Curves)

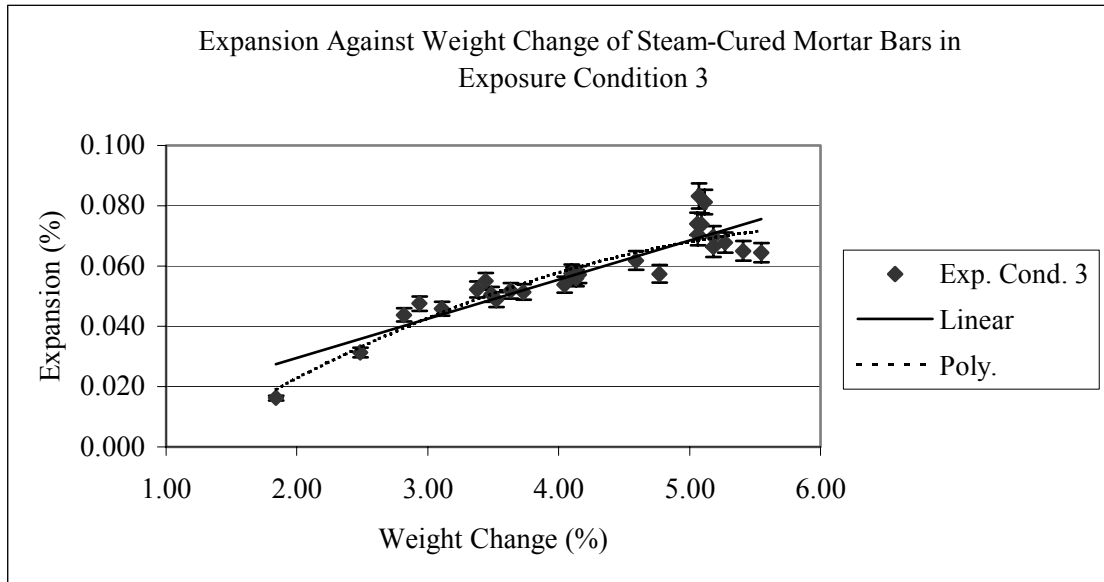


Figure 6.12 Expansion Against Weight Change of Mortar Samples Subjected to Duggan Heat Cycle and Stored in Moist Air Chamber, R.H maintained at 97% (Regression Curves)

Table 6.3 Linear and Polynomial Equations for Expansion Against Weight Change of Mortar Samples Subjected to Duggan Heat cycle and Stored Under Different Exposure Conditions

Phase 1 (Mortar Control Samples - subjected to Duggan Heat Cycle)		
Exposure Condition 1 (Isothermal water,, pH at 12.5)	Exposure Condition 2 (Plain Water at room temp.)	Exposure Condition 3 (Moist air chamber, R.H at 97%)
Linear $y = 0.0883x + 0.8777$ $R^2 = 0.9815$	Linear $y = 0.2381x - 2.5214$ $R^2 = 0.9928$	Linear $y = 0.013x + 0.0036$ $R^2 = 0.8264$
Polynomial $y = 0.0173x^2 - 0.3049x + 1.3522$ $R^2 = 0.9926$	Polynomial $y = 0.0028x^2 + 0.173x - 2.1467$ $R^2 = 0.9928$	Polynomial $y = -0.0024x^2 + 0.032x + 0.0315$ $R^2 = 0.8571$

6.3.4 Compressive Strength Results

The compressive strength testing results after 28 days revealed that the mortar specimens stored under relative humidity of 97% (Exp. Cond. 3) exhibited the highest average strength of 6675 psi. Further compressive strength tests will be needed to postulate the effect of the Duggan regime to the compressive strength of the mortar specimens. The result of the 28 days compressive strength are shown in Table 6.4.

Table 6.4 Compressive Strength of Mortar Specimens Subjected to Duggan Heat Cycle and Stored Under Different Exposure Conditions

28 Days - Comp. Strength (psi)			
Exp. Cond.	1	2	3
	4888	4875	6500
	4420	4750	6900
	4463	4675	6675
Average	4590	4767	6692
Std	258.5	101.0	200.5

6.4 Field Samples (No Duggan Heat Cycle)

Two (2) batches of mortar with 1.5% K₂O content were mixed and subjected to atmospheric conditions outside the laboratory. The first batch was steam cured, then subsequently stored in water for 6 days and stored outside the laboratory. The second batch was cured in the laboratory at room temperature for 24 hours, and then stored under water for 6 days prior to exposure to field conditions. In both mortar batches, no Duggan heat cycle was employed in the sample preparation. Only the potassium content was increased and all other parameters kept constant.

6.4.1 Expansion Results

At 100 days, the maximum shrinkage recorded for exposure conditions 4A and 4B were about -0.0926% and -0.0566% respectively. The shrinkage of the mortar bars made with $1.5\% \text{K}_2\text{O}$ show similar patterns regardless of the pre-curing process. Exposure condition 4B shows less shrinkage than exposure condition 4A. Figure 6.13 shows the length change of the mortar samples made with $1.5\% \text{K}_2\text{O}$ and stored under field conditions.

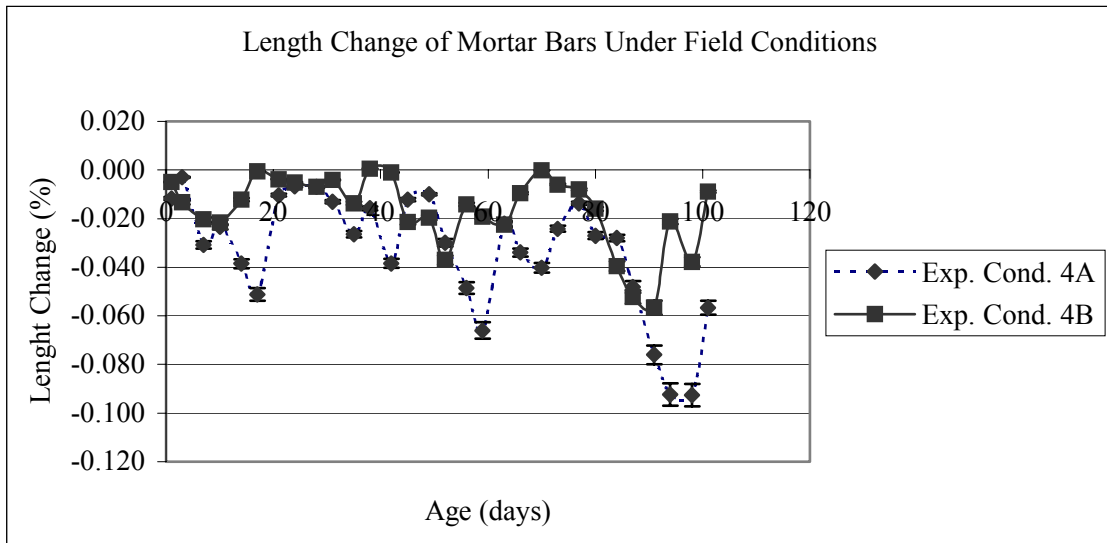


Figure 6.13 Length Change of Mortar Samples Exposed to Field Conditions

Figures 6.14 and 6.15 show the regression analysis curves of the field-exposed mortar samples. Table 6.5 provides the linear and polynomial equations for the best fit to the experimental data. The regression curves show little or no correlation of data.

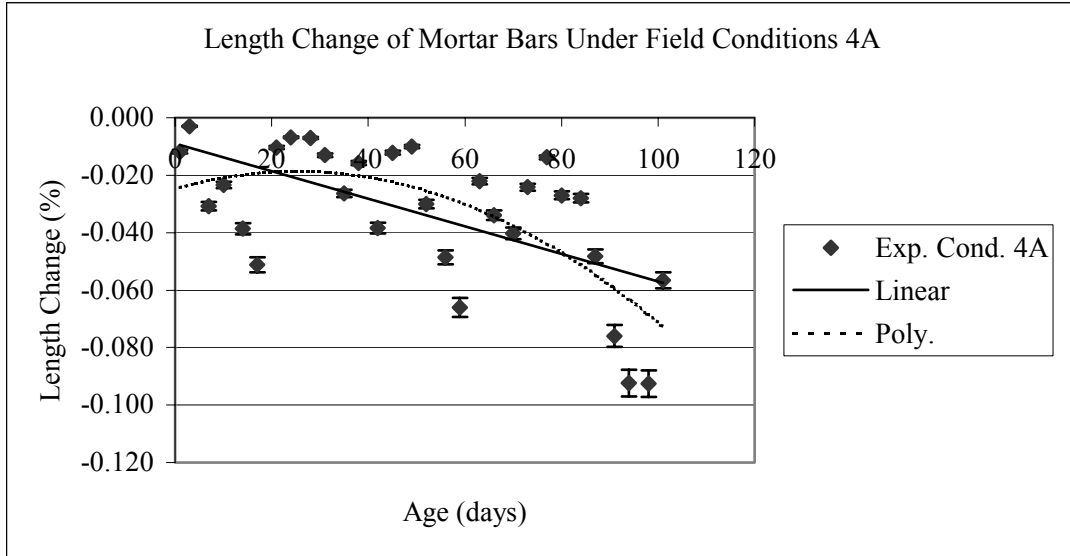


Figure 6.14 Length Change vs. Age of Steam-Cured Mortar Samples and Stored Under Field Conditions 4A (Regression Curves)

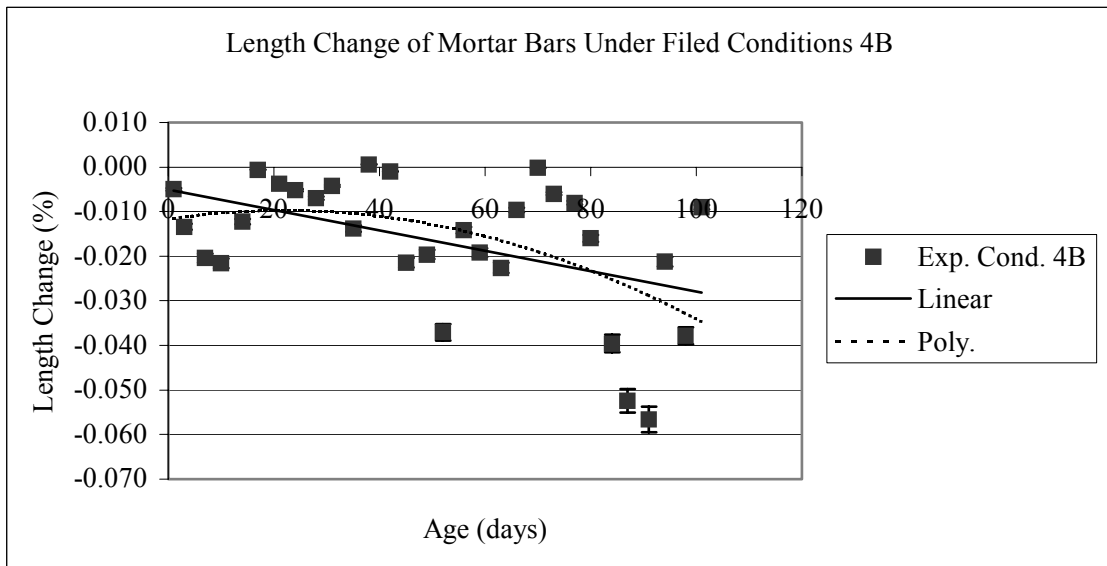


Figure 6.15 Length Change vs. Age of Steam-Cured Mortar Samples and Stored Under Field Conditions 4B (Regression Curves)

Table 6.5 Linear and Polynomial Equations for Length vs. Age of Mortar Samples Stored Under Field Conditions

Phase 1 (Mortar Control Samples - Field Conditions)	
Exposure Condition 4A	Exposure Condition 4B
Linear $y = -0.0005x - 0.0091$ $R^2 = 0.3669$	Linear $y = -0.0002x - 0.005$ $R^2 = 0.2215$
Polynomial $y = -9E-06x^2 + 0.0005x - 0.0247$ $R^2 = 0.4706$	Polynomial $y = -4E-06x^2 + 0.0002x - 0.0116$ $R^2 = 0.2701$

6.4.2 Weight-Change Results

Weight change measurements of the mortar samples made with 1.5% K₂O content show a 5 to 6% decrease in mass for both sets of the field specimens. Figure 6.16 shows the weight change against age results of the field exposed mortar samples. Figures 6.17 and 6.18 provide the regression analysis curves of the data. At 100 days, no correlation or little was found between weight changes against time. Table 6.6 gives the regression equations used for the analysis.

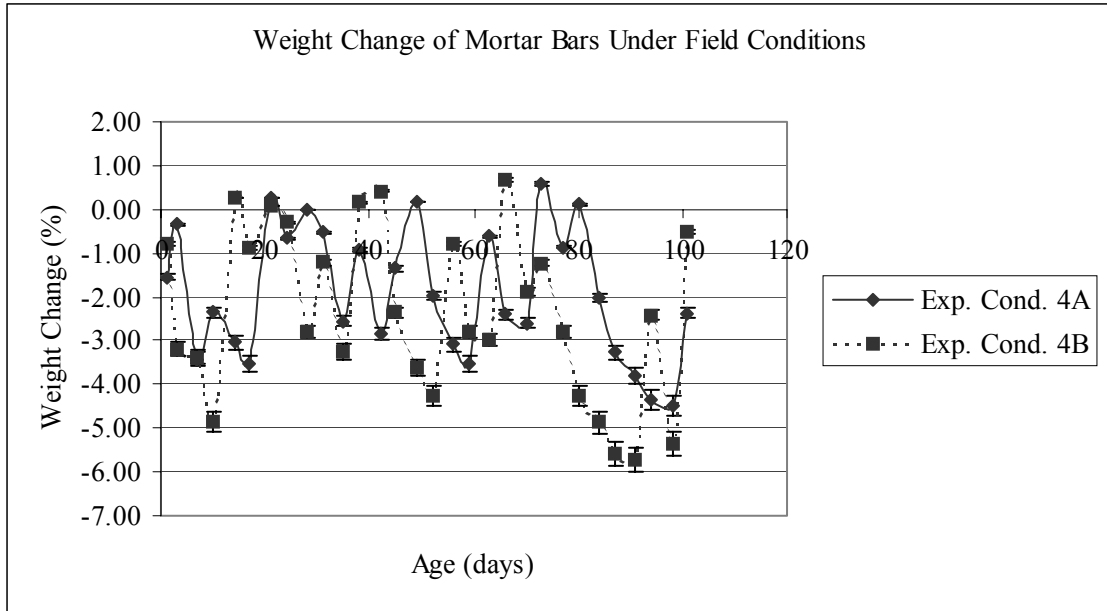


Figure 6.16 Weight Change of Mortar Samples Exposed to Field Conditions

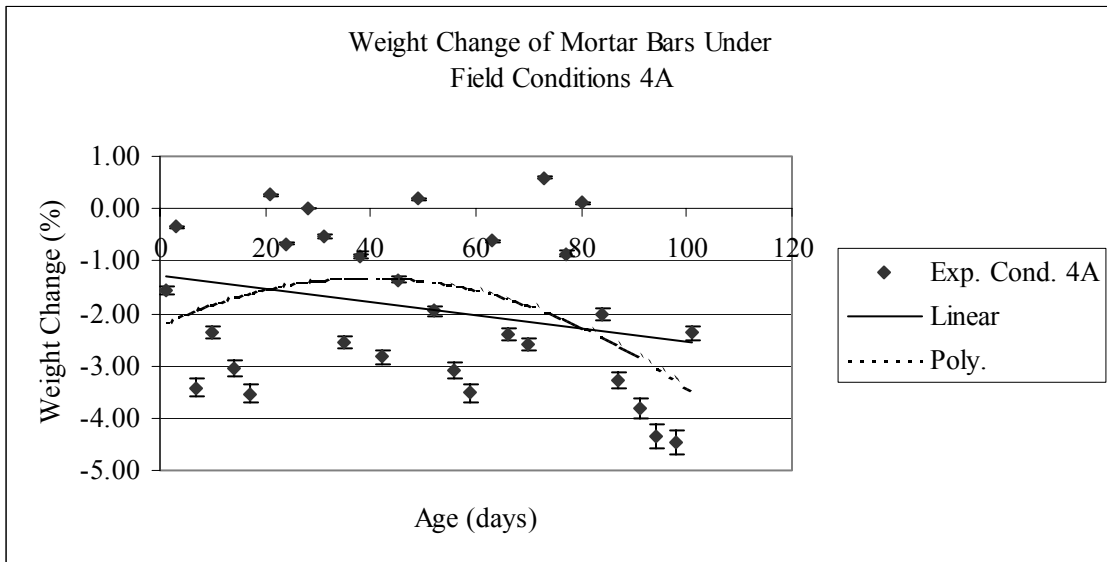


Figure 6.17 Weight Change vs. Age of Steam-Cured Mortar Samples and Stored Under Field Condition 4A (Regression Curves)

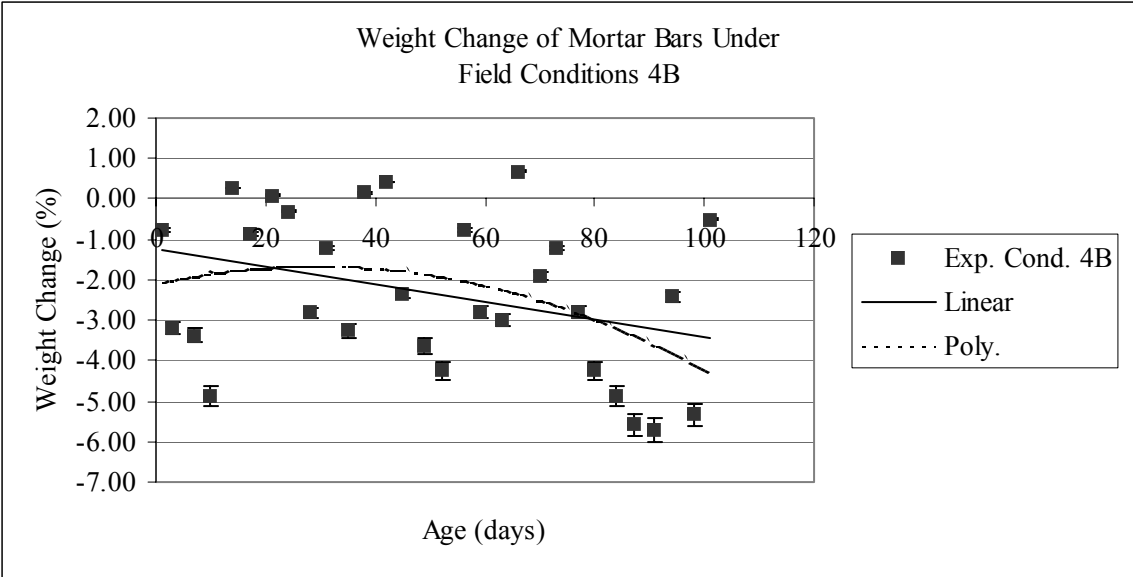


Figure 6.18 Weight Change vs. Age of Mortar Samples and Stored Under Field Condition 4B (Regression Curves)

Table 6.6 Linear and Polynomial Equations for Weight Change vs. Age of Mortar Samples Stored Under Exposed Conditions

Phase 1 (Mortar Control Samples - Field Conditions)	
Exposure Condition 4A	Exposure Condition 4B
Linear $y = -0.0126x - 1.2744$ $R^2 = 0.0678$	Linear $y = -0.0218x - 1.2473$ $R^2 = 0.1192$
Polynomial $y = -0.0006x^2 + 0.0462x - 2.2313$ $R^2 = 0.172$	Polynomial $y = -0.0005x^2 + 0.0304x - 2.0966$ $R^2 = 0.1672$

6.4.4 Compressive Strength Results

After 28 days of storage, the compressive strength testing of the room-cured mortar cubes (Exp. Cond. 4B) exhibited an average of 6996 psi and the steam-cured specimens (Exp. Cond. 4A) exhibited an average of 5043 psi. Table 6.2 shows the compressive strength results of the mortar specimens exposed to field conditions.

Table 6.7 Compressive Strength of Mortar Specimens Exposed to Field Conditions

28 Days - Comp. Strength (psi)		
Exp. Cond.	4A	4B
	4825	6025
	5125	5675
	5180	5475
Average	5043	5725
Std	191.1	278.4

6.5 Water Analysis Results of Storage Solution

The mortar samples made with 1.5% potassium (K_2O) content were stored in similar conditions as the controls and the ion concentrations of their respective storage solutions were monitored. The pH value, Potassium (K^+), Sodium (Na^+) and Calcium (Ca^{2+}) ion concentrations were monitored.

6.5.1 Water Analysis of Exposure Condition 1

After 14 weeks of storage, the amount of alkali leached still increased with time. The highest recorded alkali concentration was 106.4 mmol/l. Figure 6.19 provides a plot

of the results of the total amount of alkali leached against age (from the end of the Duggan heat cycle).

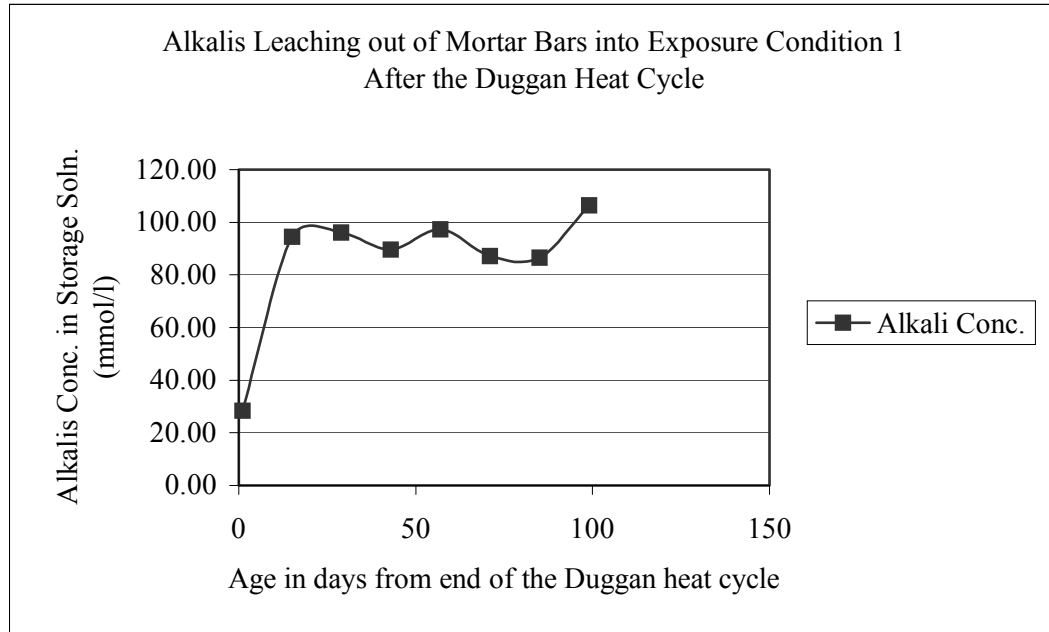


Figure 6.19 Alkalis Leaching from Mortar Samples Stored in Isothermal Water Bath, pH maintained at 12.5

6.5.2 Water Analysis of Exposure Condition 2

Again, the mortar samples stored in exposure condition 2 (water at room temperature) were monitored for pH value, Na^+ , K^+ and Ca^{2+} ion concentrations.

6.5.2.1 Amount of Alkalis

An increase in the amount of potassium (K_2O) contents in the mortar mixes increases the amount of alkali being leached to the surrounding storage solution. After 14 weeks of storage, the amount of alkali leached still increases with time as shown in

Figure 6.20. At 14 weeks from the time of storage, the recorded alkali concentration was 139.4 mmol/l.

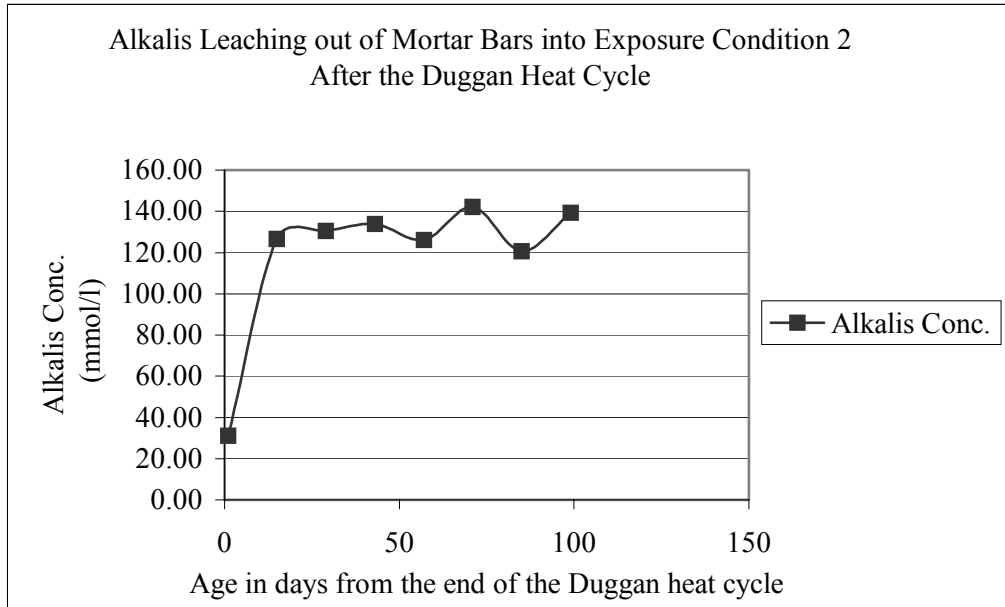


Figure 6.20 Alkali Leaching from Mortar Samples Stored in Plain Water at Room Temperature

6.5.2.3 pH Value

The pH value does change significantly with an increase in the potassium (K_2O) content of the mortar samples. Again, the pH values range from 11.10 to 12.23.

6.5.2.4 Calcium Concentration

For the storage period, the measured calcium concentration in exposure condition 2 decreases with time. The amount of calcium ions leached to the surrounding storage solution seems to be suppressed by the high alkali content of the mortar samples. Figure

6.21 shows the calcium concentration of the storage solution for exposure condition 2.

The highest amount of calcium leached was 122 mmol/l recorded at 1 day after storage of the mortar samples.

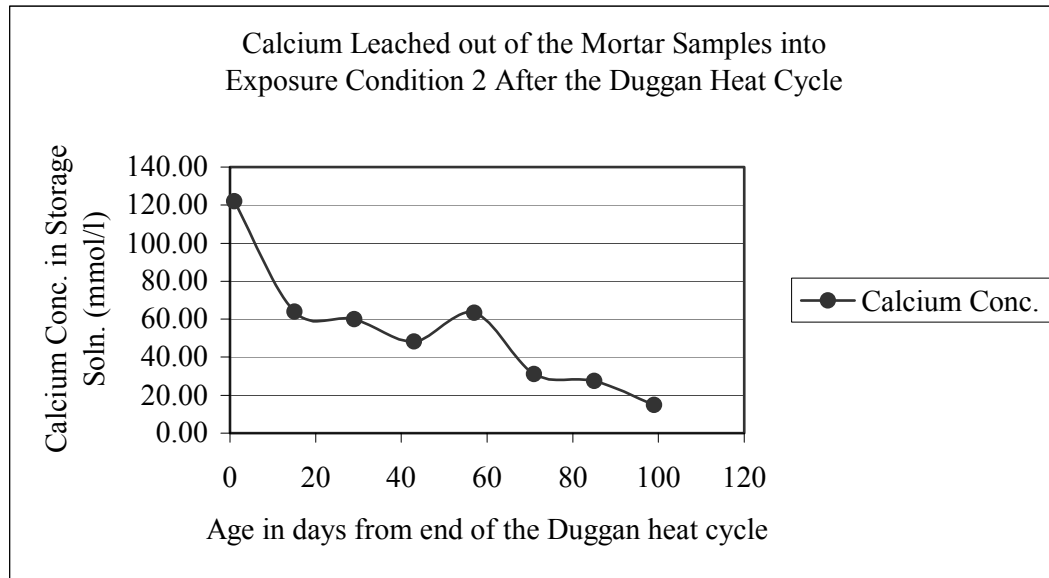


Figure 6.21 Calcium Leached from Mortar Samples Stored in Plain Water at Room Temperature

6.6 Microstructure Analysis Using SEM and EDAX

For each SEM study, three sets of specimens from the samples were collected at different locations for testing. Prior to SEM examinations, specimens were carbon coated for accurate analysis. SEM equipped with EDAX was conducted for elemental analysis of the chemical composition of the gel within the microstructure of the specimens. The specimens were prepared as fractured surface samples for SEM examinations to show DEF in cracks, cavities, and the interface between the cement paste and aggregates. High magnifications by SEM and EDAX elemental analysis were used to identify the

deterioration mechanism and differentiate between different morphologies of ettringite (DEF), alkali-aggregate reaction (AAR), and alkali-silica reaction (ASR) gel.

6.6.1 Mortar Samples in Exposure Condition 1

After 40 days of storage in water with pH maintained at 12.5 (Exp. Cond. 1), a fractured sample was collected for SEM study on the expanded mortar bars. Figure 6.22 shows well-developed spherical balls of ettringite gel identified with the SEM micrograph and EDAX chemical analysis. The EDAX results indicate ettringite having a chemical composition of Al = 5.02% wt., Si = 3.91% wt., S = 6.60% wt., and Ca = 82.79% wt. Also, calcium hydroxide crystals (CH) can be identified within the cavities and cement paste and aggregates of the specimens.

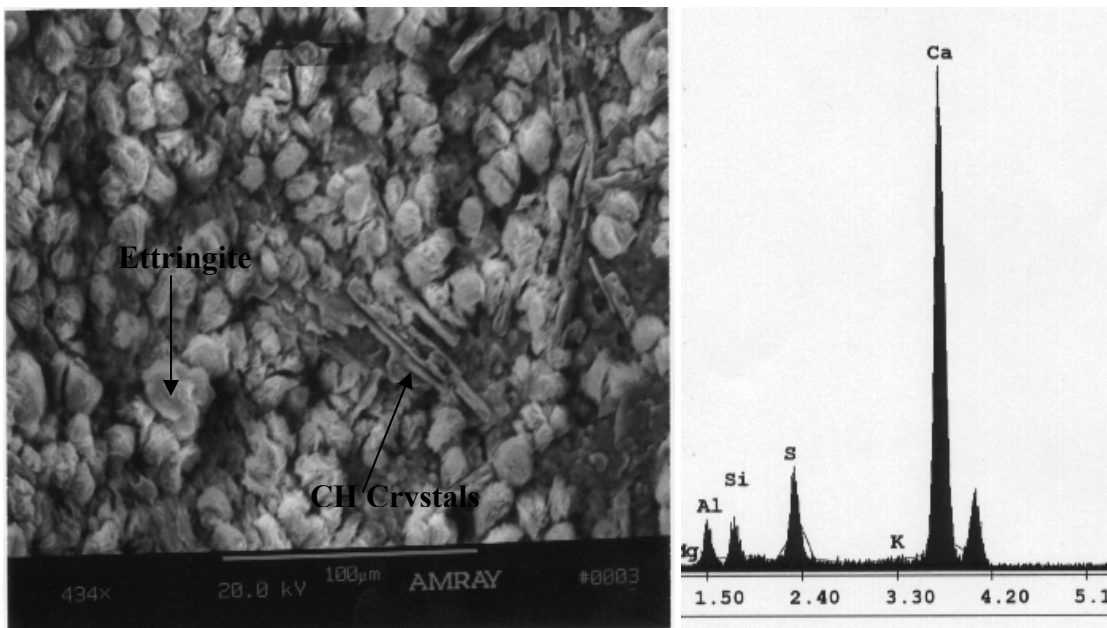


Figure 6.22 SEM and EDAX Analysis of Mortar Specimens in Exposure Condition 1 at Age of 40 days, Showing Ettringite Balls and CH Crystals Filling the Cavity

6.6.2 Mortar Samples in Exposure Condition 2

Well-developed ettringite gels could be identified all over the specimens at only 40 days of storage in plain water at room temperature (Exp. Cond. 1). Little clusters of CH and lots of spherical balls and needles loaded with ettringite were found in the air voids and cavities. Figure 6.23 provides the SEM and EDAX elemental analysis of the layer with ettringite deposits.

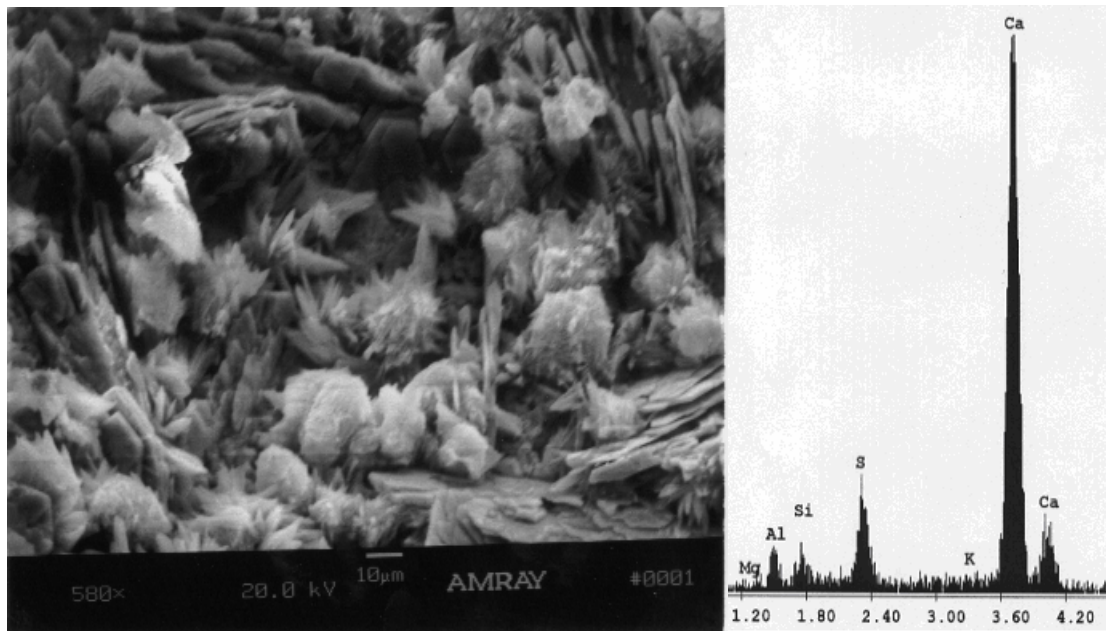


Figure 6.23 SEM and EDAX Analysis of Mortar Specimens in Exposure Condition 2 at Age of 40 days, Showing Ettringite Needles, Ettringite Spherical Balls and CH Clusters Filling the Air Voids and Cavities

6.6.3 Mortar Samples in Exposure Condition 3

At 40 days of storage under relative humidity of 97% (Exp. Cond. 3), no ettringite could be found within the specimen. The EDAX revealed a high peak of potassium (K),

which might be due to the high potassium content in the mortar mix. Figure 6.24 shows the EDAX results.

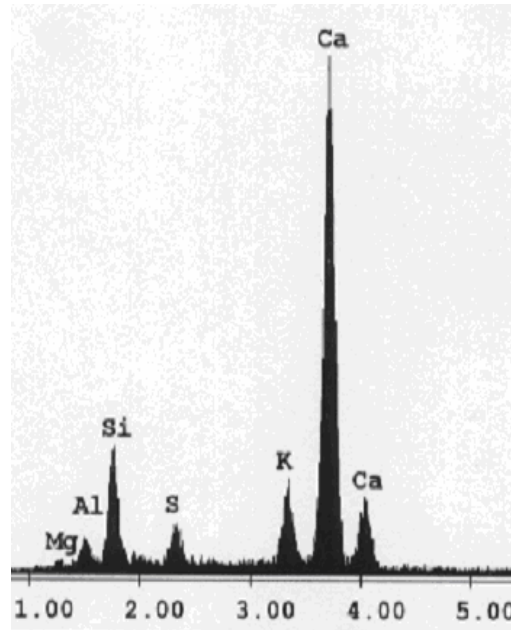


Figure 6.24 EDAX Analysis of Mortar Specimens in Exposure Condition 3 at Age of 40 days

6.6.4 Mortar Samples in Exposure Condition 4A

The mortar samples were steam cured and stored in water at room temperature prior to storing in the field. The SEM and EDAX analysis shows neither ettringite nor its elemental composition peaks at 40 days. A prominently high potassium spectrum peak was observed, due to the high potassium content in the mix (1.5% K_2O by weight of cement). Figure 6.25 shows the EDAX results.

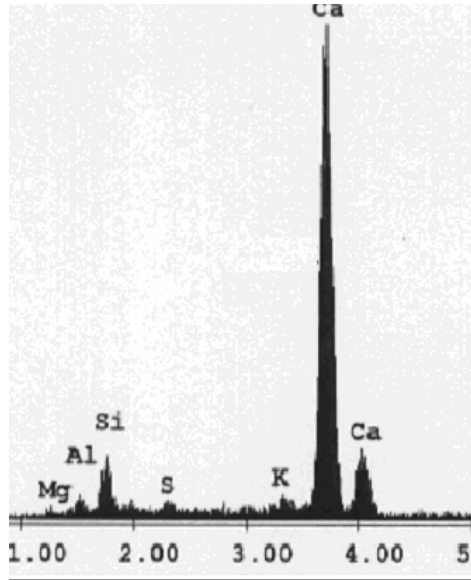


Figure 6.25 EDAX Analysis of Mortar Specimens Under Field Conditions (Exp. Cond. 4A) at Age of 40 days

6.6.5 Mortar Samples in Exposure Condition 4B

At 40 days, SEM results revealed lots of ettringite around the voids and cavities of the specimen. The morphology is characteristic of ettringite deposits but could not be confirmed by EDAX due to low X-ray signals encountered during examination of specimens. Figures 6.26 and 6.27 provide SEM micrographs showing ettringite needles found at several locations.

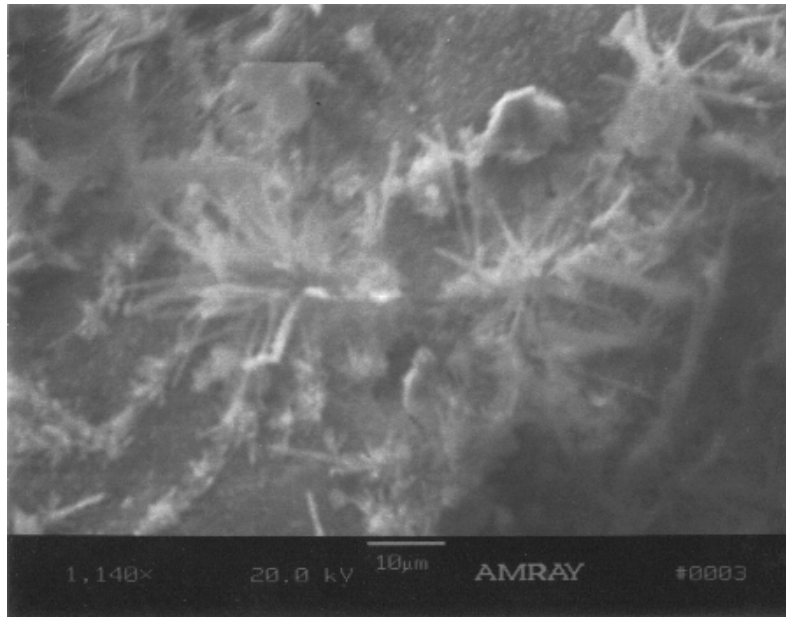


Figure 6.26 SEM Micrograph of Mortar Specimens Under Field Conditions (Exp. Cond. 4B) at Age of 40 days

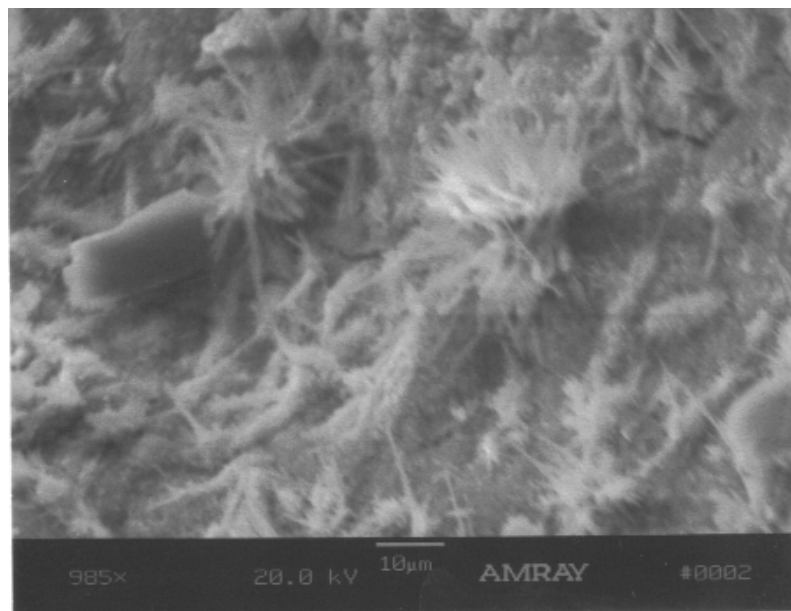


Figure 6.27 SEM Micrograph of Mortar Specimens Under Field Conditions (Exp. Cond. 4B) at Age of 40 days

6.7 X-ray Computed Tomography (X-ray CT) Analysis

The X-ray computed tomography (X-ray CT) method is another technique that was used to reveal the interior cracks within the microstructure of the mortar specimens. The X-ray CT is a nondestructive method and the sample preparation method does not influence the results.

Figures 6.28 through 6.30 show computed tomography cross sectional images of the mortar specimens made with 1.5% K_2O content after 40 days storage in the different exposure conditions. All the mortar specimens that were examined exhibited no visible interior cracks in the X-ray CT images.

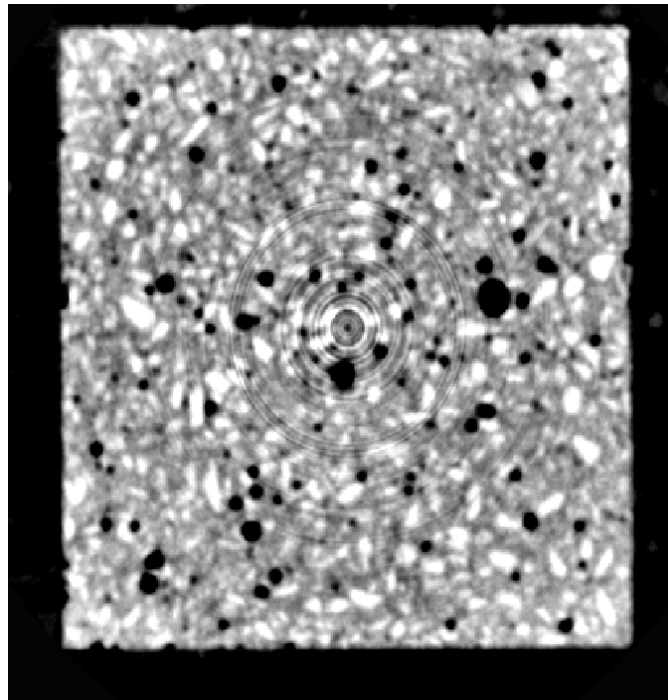


Figure 6.28 X-ray Computed Tomography Image of a Section Through a Mortar Cube Made with 1.5% K_2O Stored for 40 days in Exposure Condition 2

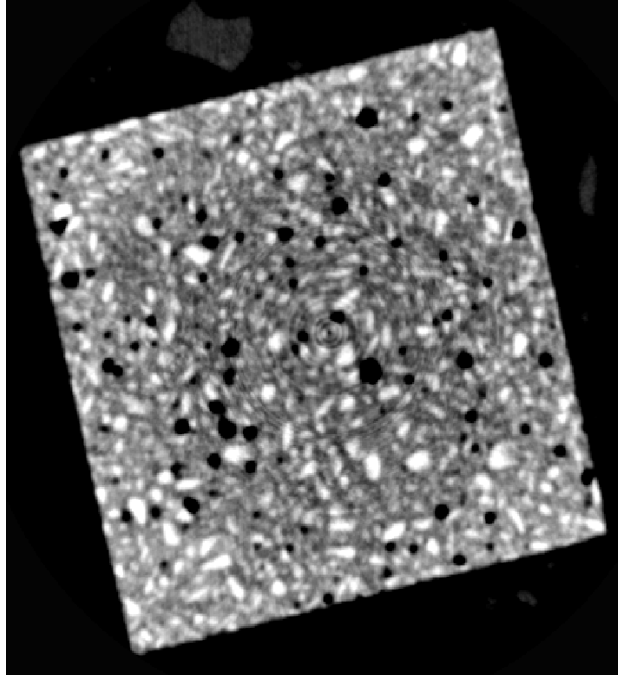


Figure 6.29 X-ray Computed Tomography Image of a Section Through a Mortar Cube Made with 1.5% K_2O Stored for 40 days in Exposure Condition 3

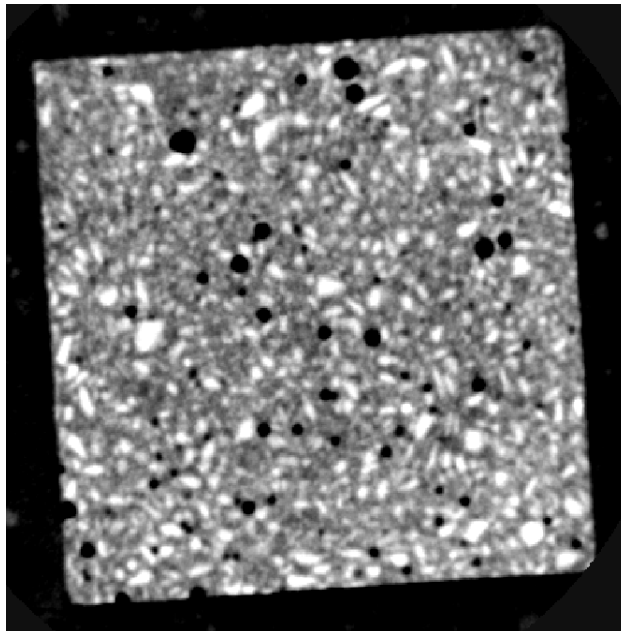


Figure 6.30 X-ray Computed Tomography Image of a Section Through a Mortar Cube Made with 1.5% K_2O Stored for 40 days in Exposure Condition 4B

6.8 Summary and Discussion of Results

The mortar samples were prepared with high potassium (K_2O) content which increased the cement alkalis of the mortar batches. The Duggan heat regime was employed to provide or initiate microcracks within a short period of time in the laboratory-prepared mortar specimens.

Mortar bars stored in exposure condition 2 (water at room temperature) exhibited the highest expansions among specimens subjected to the Duggan heat cycle. All specimens subjected to the Duggan heat cycle showed expansion after 3 days of storage. The mortar bars stored in the various exposure conditions exceeded the 21-day threshold expansion value of 0.05% suggested by Duggan. The expansion results clearly indicated that expansion is accelerated by the increase in the K_2O content. The mortar bars exposed to field conditions that were not subjected to the Duggan heat regime, showed shrinkage for the entire duration of the research study.

Weight change of the mortar specimens was significant for exposure conditions 1 and 2. An increase in weight change up to 10% was revealed just after 1 day of storage in exposure conditions 1 and 2. Weight change of the mortar specimens subjected to the Duggan heat show a steady increase with time. The weight change of the mortar field specimens was found to fluctuate and decreased with time.

Expansion against weight change of mortar bars in exposure conditions 1 and 2 exhibited high positive linear correlations similar to the control mortar specimens. These results were similar to those obtained by Grattan-Bellew et al (1998).

Analysis of the 28-day compressive strength results suggest that an increase in potassium (K_2O) content in the mortar mix significantly reduced strength. The mortar

specimens subjected to the Duggan heat cycle and then exposed to a relative humidity of 97% exhibited the highest average strength. The exposure condition enhanced and influenced the compressive strength of the mortar specimens.

Mortar samples made with higher potassium (K_2O) content showed higher alkali leaching and accelerated formation of ettringite. The alkali concentration was higher in the storage solution of exposure conditions 2 than 1. Also expansion values of mortar specimens in exposure 2 were higher than 1. However, since the cement and all other parameters were the same for both mortar sets, the expansion values may be attributed to the higher concentrations of potassium.

Microstructural observation of the mortar specimens at different stages revealed significant amounts of ettringite balls or crystal filling the cracks and air voids. Calcium hydroxide crystals (CH) were also found within the cavities and cement paste of the mortar specimens. Under exposure condition 3 (relative humidity of 97%), SEM results showed high peaks of potassium (K) but no ettringite was found. Ettringite deposits were discovered under the field exposure conditions but, due to the low x-ray signals encountered, no EDAX could be obtained.

The X-ray computed tomography (X-ray CT) imaging of the mortar cross sections showed no interior cracks within the microstructure. Cracks again were revealed only with SEM examinations and were found filled with ettringite. ASR was not found during the petrographic analysis of the specimens.

CHAPTER 7: SUMMARY AND CONCLUSIONS

7.1 Introduction

Delayed ettringite formation (DEF) is mainly attributed to hardened mortar or concrete cured at elevated temperatures. Generally, researchers paid little or no attention to investigating the influence of exposure conditions and their contributions to potential expansion and DEF of mortar and concrete samples. Researchers often measured dimensional changes mainly for expansion and performed scanning electron microscope (SEM) to analyze the elemental chemical compositions of the deposits within the cracks, voids, cement paste, and aggregate interface without any effective monitoring of the exposure conditions of the samples during storage. It very important to monitor the exposure conditions since the C-S-H gel responsible for DEF changes over time, and differently for different storage conditions (Famy 2001). Monitoring the storage conditions with advanced material testing methods can provide guidelines to mitigate or prevent delayed ettringite formation and its associated expansion, which causes the deterioration of concrete.

7.2 Summary

In this research study, laboratory prepared specimens were tested to investigate the mechanisms of delayed ettringite formations and their associated expansions leading to the premature deterioration of mortar samples. UMD/FHWA modified preparation method was used to enhance the length change measurements of bars according to ASTM C490. The Duggan heat cycle was employed after 7 days of casting to predict the

potential expansion and deterioration of the mortar samples due to DEF. The objectives of this study were: (1) to use applied advanced material testing methods on the complex processes of expansive cracking associated with DEF; (2) to investigate the effects of storage conditions and their influence in DEF pertaining to weight change, expansion/contraction, and damage variables; (3) to study by water analysis the potential of DEF in mortar specimens as a function of the alkali being leached into the storage solution; (4) to study the influence of potassium (K_2O) content on mortar expansion and its potential association with DEF; (5) to investigate and explore the complexity of DEF at several stages.

Portland cement type III was used throughout the entire study. Also the study was conducted in two phases. Phase one was the control with no additional potassium (K_2O) while phase two was made with added potassium carbonate to the batches to bring them to a total of 1.5% potassium (K_2O). From the literature review, two essential factors for delayed ettringite formation are revealed by the presence of sulfates and moisture. Increasing the potassium content (K_2O) by adding it to the mixing water during batching increases the alkali concentration of the samples. Another important factor, steam curing at elevated temperatures has been shown by many researchers to produce damages associated with DEF. The mortar samples were either steam-cured prior to being subjected to the Duggan heat regime or cured at room temperature in the laboratory. The Duggan heat cycle was used to generate initial cracks. At 21 days, the expansion results were compared to the threshold limit of 0.05% expansion as suggested by Duggan as a pass-fail criterion for concrete.

7.3 Conclusions

The following conclusions were reached based on this laboratory study:

1. The rate of expansion of the mortar bars increases with an increase in potassium (K_2O) content of the specimens.
2. High temperature curing regimes were found to enhance DEF but were not the critical factors required for DEF. DEF was found even in mortar specimens that were not subjected to heat cycle.
3. Microstructural observations, which included the use of scanning electron microscopy (SEM) equipped with energy dispersive analysis X-ray (EDAX), and X-ray computed tomography (X-ray CT) of the expanded mortar specimens at several stages revealed the delayed ettringite formation without detecting any sign of ASR.
4. Curing at elevated temperatures followed by severe thermal drying and wetting processes such as the Duggan heat cycle promotes mortar deterioration due to DEF.
5. During the 100 days of storage, the expansions of the mortar bars showed linear correlations with weight change for the submerged specimens.. Even with an increase in alkali content, the expansion against weight change measurements still showed a linear correlation. The expansion vs. weight change relationship for the 97% specimens showed a more complex pattern but it was still significant.
6. Therefore, expansion-related damage can also be monitored by weight change of specimens instead of length change measurements.

7. The Duggan heat cycle and an increase in the potassium (K_2O) content of the mortar samples had a dramatic effect on the early compressive strength. A reduction in compressive strength of about 15 – 20% was recorded in both the mortar specimens subjected to the Duggan heat cycle and field specimens.
8. Steam and room temperature-cured mortar specimens stored under field conditions showed a shrinkage rate of about -0.0144% per day for the duration of the study. The length changes showed little or no trend with time, which suggests that these changes were associated with fluctuations in ambient temperature and humidity conditions.

REFERENCES

- ASTM, 2001 Annual Book of Standards. Volume 04.02 Concrete and Aggregate. American Society for Testing and Materials, Philadelphia.
- ASTM, 2001 Annual Book of Standards. Volume 04.01 Cement; Lime; Gypsum. American Society for Testing and Materials, Philadelphia.
- ASTM, 2002 Annual Book of Standards. Volume 11.03 Atmospheric Analysis; Occupational Health and Safety; Protective Clothing. American Society for Testing and Materials, Philadelphia.
- Atkins, N. H., 1997, "Highway Materials, Soils and Concrete." 3rd Edition, Ed Francis, Ed., pp. 280 – 289.
- Azzam, A., 2002, "Delayed Ettringite Formation, the influence of aggregate types, curing conditions, exposure conditions, alkali content, fly ash and mix water conditioner (MWC)," Ph.D Thesis, University of Maryland, College Park, USA.
- Abo-El-Enein, S. A., Hanafi, S., Hekal, E. E., 1988, "Thermal and Physiochemical Studies on Ettringite II: dehydration and thermal stability, Cemento, Vol. 85, No. 2, pp. 121-132.
- Abo-El-Enein, S. A., Abo-Nuaimi, K. Kh., Marusin, S. L., and El-Hemaly, S. A.S., 1984, "Hydration Kinetics and Microstructure of Ettringite," Proc. 6th Conf. on Cement Microscopy, Int. Cement Microscopy Assoc., Duncanville, TX, pp. 219-231.
- Attigobe, E. K., Wells, J. A., and Rizkalla, S. H., Sept. 1990, "Evaluation of Duggan Concrete Core Expansion Test," Research Report, Sponsored by Canadian National Railway and Transport Institute, University of Manitoba, Winnipeg, Canada.
- BioImaging research Inc. (BIR), 1998, "ACTIS 600/420 Real-Time Radiography/Digital Radiography/Tomography," Report, Bio-Imaging Research, Inc. (BIR), Lincolnshire, IL, 1998.
- Bentur, A. and Berger, R. L., 1979, "Chemical Composition of C-S-H Gel Formed in the Hydration of Calcium Silicate Pastes," Journal of The American Ceramic Society, Vol. 62, pp. 117-120
- Candlot, E. 1890, "Properties des ciments et des liants hydrauliques," Bull. Soc. Encour. Ind. Natn., pp. 682-685.
- Chamberline, W. H., Brewer, H. W., and Shiderler, J. J., August 1952, "Compressive Strength of Steam-Cured Concrete," Report C-621, Bureau of Reclamation, U.S. Dept. of the Interior, Denver.

- Chandra, S., Berntsson, L., Nov-Dec, 1988, "Deterioration of Concrete in Swimming Pool in the South of Sweden," ACI Materials Journal, American Concr. Inst., Vol.85, N6, pp. 489-494.
- Chatterji, S., Thaulow, N., Jensen, A. D., and Christiansen, P., 1987, "Mechanisms of Accelerating Effects of NaCl and Ca(OH)₂ on Alkali-Silica Reaction," Proceedings 7th International Conference on Alkali-Aggregate Reaction, Ottawa, pp. 115-124.
- Cohen, M. D., 1983, "Modeling of Expansive Cement," Cement and Concrete Research, Vol. 13, pp. 519-528.
- Cohen, M. D. 1982, "Microstructural Analysis of Ettringite Formation: Scanning Electron Microscopy Assoc. Duncanville, TX, pp. 204-224.
- Cohen, M. D. and Richards, C. W., 1982, "Effects of the Particle Sizes of Expansive Clinker on Strength – Expansion Characteristics of Type K Expansive Cements," Cement and Concrete Research, Vol. 12, No. 6 pp.717-725.
- Cohen, M. D., Campbell, E. and Fowle, W., 1985, "Kinetics and Morphology of Ettringite Formation," Proc. 7th Int. Conf. Cem. Microsc., Ed. James Bayles, pp. 360-381.
- Colleparidi, M., January 1999, "Damage by Delayed Ettringite Formation – A Holistic Approach and New Hypothesis," Concrete International, Vol. 21, No. 1, pp. 69-74.
- Colleparidi, M., Baladini, G., Pauri, M., and Corradi, M., 1987, "Tricalcium Aluminate Hydration in the Presence of Lime, Gypsum or Sodium Sulfate," Cement and Concrete Research, Vol. 8, No. 5, pp.571-580.
- Dana, E. S., 1932, "A Textbook of Mineralogy," Wiley and Sons, New York.
- Day, R. L., 1992, "The Effect of Secondary Ettringite Formation on the Durability of Concrete:" A Literature Analysis of Portland Cement Association. Skokie, IL.
- Daerr, G. M., Punzet, M., Ludwig, U., 1977 "On the Chemical and Thermal Stability of Ettringite on Dehydration I," Cem. Summ. Contrib. Semin., pp. 42-45.
- Dean, J. A., 1999, "Lange's Handbook of Chemistry," 15th Edition, pp. 5.18.
- Deng, M. and Tang, M., 1994, "Formation and Expansion of Ettringite Crystals," Cement and concrete Research, Vol. 24, pp. 119-126.
- Derucher, K. N., Korfiatis, G. P., Ezeldin, A.S., 1998, "Materials For Civil and Highway Engineers," 4th Edition, pp. 81- 90.
- Diamond, S., 1983, "Alkaline Reactions in Concrete Pore Solution Effects," Proceedings 6th International Conference on Alkalis in Concrete, pp.155-166.

- Diamond, S., 1996, "Delayed Ettringite Formation – Processes and Problems," *Cem. Concr. Composites*, Vol. 18, pp.205-215.
- Diamond, S., 1989, "ASR-Another Look At Mechanisms," *Proceedings 8th International Conference on Alkali-Aggregate Reaction*, Kyoto, Japan, pp. 83-94.
- Diamond, S., 1987, "Cement Paste Microstructure in Concrete," *Proc. Of Material Research Society*, Vol. 85, pp.21-31.
- Diamond, S., Olek, J. and Wang, Y., 1998, "The Occurrence of Two-Tone Structures in Room Temperature Cured Cement Pastes," *Cem. Concr. Res.*, Vol. 28, No. 9, pp. 1237-1243.
- Diamond, S., and Ong, S., 1994, " Combined Effects of Alkali Silica Reaction and Secondary Ettringite Deposition in Steam Cured Mortars," *In Cement Technology*, American Ceramic Society, Westerville, Ohio, pp. 79 – 90.
- Duggan, R. and Scott, F., 1989, "New Test for Deleterious Expansion in Concrete," *Alkali-Aggregate Reaction. 8th International Conference*, Elsevier Applied Science, New York, pp. 403-408.
- El-Sayed, H. A., El-Wahed, M. G. Abd, Ali, A. H., July 1987, "Some Aspects of the Corrosion of Reinforcing Steel in Concrete Marine Atmospheres," *Durability of Building Materials*, Vol.5, N1, pp. 13-25.
- Eriksson, B. E. and Tepponen, P., 1985, "Heat Treatment as the Cause of Concrete Failure," *Betonintuote*, Vol. 2.
- Famy, C., Scrivener, K. L., Brough, A.R., Atkinson, A., 2001, "Influence of the Storage Conditions in the Dimensional Changes of Heat-Cured Mortars," *Cem. Concr. Res.* Vol. 31, pp. 795-803.
- Famy, C., 1999, "Expansion of Heat-Cured Mortars," *Ph.D. Thesis*, Purdue University, USA.
- Farsky, R., Basavarajaiah B. S. Jan. 1971 "Some Studies of Steam Curing of Cement Mortar," *Indian Concrete Journal*, Vol. 45, No. 1, pp. 35-41.
- Fu, Y., 1996, "Delayed Ettringite Formation in Portland Cement Products," *Ph.D. Thesis*, University of Ottawa, Ottawa, Canada.
- Fu, Y., and Beaudoin, J. J., 1996, "Mechanism of Delayed Ettringite Formation in Portland Cement Systems," *ACI Materials Journal*, Vol. 93, No. 4, pp. 327-333.
- Fu, Y. and Beaudoin, J. J., 1996, "Microcracking as Precursor to Delayed Ettringite Formation in Cement Systems," *Cem. Concr. Res.*, Vol. 26, No. 10, pp. 1493-1498.

- Fu, Y. and Beaudoin, J. J., 1996, "On the Distinction Between Delayed and Secondary Ettringite Formation in Concrete," *Cem. Concr. Res.*, Vol. 26, No. 6, pp. 979-980.
- Fu, Y. and Beaudoin, J. J., 1996, "Expansion of Portland Cement Mortar due to Internal Sulfate Attack," *Cem. Concr. Res.*, Vol. 27, No. 9, pp. 1299-1306.
- Fu, Y., Xie, P., Gu, P., and Beaudoin, J. J., 1995 "Kinetic Study of Delayed Ettringite Formation in Cement Systems," *Cem. Concr. Res.*, Vol. 25, No. 1, pp. 63-70.
- Fu, Y., Xie, P., Gu, P., and Beaudoin, J. J., 1993, "Preferred Nucleation of Secondary Ettringite in Pre-existing Cracks of Steam-cured Cement Paste," *Cement and Concrete Research*, Vol. 24, No. 6, pp. 1015-1024.
- Fu, Y., Xie, P., Gu, P., and Beaudoin, J. J., 1994, "Significance of Pre-existing Cracks on Nucleation of Secondary Ettringite in Steam Cured Cement Paste," *Journ. Mat Sci. Let.*, Vol. 12, pp. 1864-1865.
- Gartner, E. M., Young, J. F., Damidot, D. A., and Jawed, I., 2002, "Structure and Performance of Cements." 2nd Edition, J. Bensted and P. Barnes, Ed., pp.57-113.
- Gillott, J. E., Grobowski, E., Jones, T. N., Quinn, T., Scott, J. F., and Duggan, C. R., May 1989, "Mechanism of Expansion in Rapid Test Method for Alkali-Aggregate Reaction," Progress Report # 1, Dept. of Civil Engineering, University of Calgary, Calgary, Canada.
- Ghorab, H. Y., Heinz, D., Ludwig, U., Meskendal, T., Wolter, A., 1980, "On the Stability of Calcium Aluminates Sulphate Hydrates in Pure Systems in Cements," 7th Intl. Congr. Chem. Cem., Vol. IV, 496-503.
- Ghorab, H. Y., Kishar, E. A., Jan. 1985, "Studies on the Stability of the Calcium Sulfoaluminate Hydrate: Part I: Effect of Temperature on the Stability of Ettringite in Pure Water, *Cem. Concr. Res.* Vol. 15, No. 1, pp. 93-99.
- Ghorab, H. Y., Kishar, E. A., 1986, "The Stability of Calcium Sulfoaluminate Hydrate in Aqueous Solutions," Proc. 8th International Congress Chem. Cement, Rio de Janeiro, Vol. V., pp. 104-109.
- Ghorab, H. Y. and Abou El Fetouh, S. H., 1985, "New Approach to the Hydration Reaction of the Tricalcium Aluminate with Gypsum at 30°C, Part I: Effect of Lime," *Zement-kalk-Gips*, Vol. 38, No. 5, pp. 267-270.
- Grabowski, E., Czamecki, B., Gillott, J. E., Duggan, C. R. and Scott, J. F., 1992, Rapid Test of Concrete Expansivity due to Internal Sulfate Attack," *ACI Material Journal*, Vol. 85, No. 5, pp.385-469.

- Grattan-Bellew, P. E & Beaudoin, J. J., 1998, "Delayed Ettringite Formation; Effect of Clinker Particle Size and Composition on Expansion of Mortar Bars," Material Science of Concrete – The Sidney Diamond Symposium, Hawaii, pp. 295-307.
- Grattan-Bellew, P. E & Lefebvre, P. V., 1986, "Effect of Confinement on Deterioration of Concrete Made with Alkali-Aggregate Reactions," Ottawa, Canada, pp. 280-285.
- Gress, D., "Early Distress of Concrete Pavements," Federal Highway Administration, Publication No. FHWA-SA-97-045-53.
- Hampson, C. J. and Bailey, J. E. Nov. 1982, "On the Structure of Some Precipitated Calcium Aluminsulphate Hydrates," Journ. Of Materials Science, Vol. 71, No. 11, pp. 3341-3346.
- Hanson, J. A., Jan. 1963, "Optimum Steam Procedures in Precasting Plants," Journal of American Concrete Institute, Vol. 60, pp. 1-25.
- Heinz, D., and Ludwig, U., 1987, "Mechanism of Secondary Ettringite Formation in Mortars and Concretes Subjected to Heat Treatment," Concrete Durability ACI SP 100 Vol. 2 American Concrete Institute. Farmington Hills, MI, pp. 2059-2071.
- Heinz, D., Ludwig, U., and Rudinger, I., 1989, "Delayed Ettringite Formation in Heat – Treated Mortar and Concretes," Concrete Precasting Plant and Technology, Vol.11, pp. 56-61.
- Heinz, D., and Ludwig, U., 1986, "Mechanisms of Subsequent Ettringite Formation in Mortar and Concretes After Heat Treatment," 8th Int. Cong. Chem. Cem. Secretaria General de 8th CIQC, Rio de Janeiro, Vol. V, pp. 189-194.
- Hekal, E. E., Abo El-Enein, S. A. 1986, "Effect of Compression on Microstructure and Thermal Stability of Ettringite," Proc. Intl. Conf. On Cement Microscopy, 8th, Int. Cement Microscopy Assoc. Duncanville, TX. pp. 227-243.
- Hime, W. G., 1996, "Clinker Sulfate: A Cause for Distress and a Need for Specification," Concrete for Environment Enhancement and Protection, Edited by R. K. Dhir and T.D Dyer, Published by E & F.N. Spon, London. UK., pp. 387-395.
- Hime, W., July-August, 1996, "Delayed Ettringite Formation – A Concern for Precast Concrete," PCI Journal, pp. 26-30.
- Hime, W. G., and Marusin. S. L., 1999, Ettringite: "The Sometimes Host of Destruction," SP-177, B. Erlin, (ed.), American Concrete Institute, Farmington Hills, MI.
- Hunter, D., 1989, "The Geochemistry of Lime-induced Heave in Sulfate Bearing Clay Soils," Ph.D. Thesis, University of Nevada, Reno.

- Idorn, G. M., 1968, "The Effect of Hydration Temperature on the Products of Portland Cement," Proceedings of the 5th International Symposium on the Chemistry of Cement, Tokyo, Japan, Vol. III, pp. 411.
- Johansen, V., Thaulow, N., and Skalny, J., 1993, "Simultaneous Presence of Alkali-Silica Gel and Ettringite in Concrete," Advances in Cem. Res., Vol. 5, No. 17, pp. 23-29.
- Jones, F. E., 1939, "The Quaternary System CaO-Al₂O₃-CaSO₄-H₂O at 25°C," Trans. Faraday Soc. Vol. 35, pp.1484
- Kalousek, G. L., 1941, "Sulphoaluminates of Calcium as Stable and Metastable Phases," Ph.D. Thesis, University of Maryland.
- Kalousek, G. L., and Adams, M., Sept. 1951, "Hydration Products Formed in Cement Pastes at 25 to 150°C," ACI Journal. Proceedings, No. 48-7, pp. 77.
- Kasdan, K. S., Sept. 27, 2003 "Sulfate Attack to Concrete – A Technical Perspective," <http://www.kbla.com/articles>.
- Kennerly, R. A., 1965, "Ettringite Formation in Dam Gallery," ACI Journal, pp. 559-576.
- Kilgour, C. L., 1988, "Composition and Properties of Indian Fly Ashes," Ph.D. Thesis, Purdue University.
- Kjellsen, K. O., 1996, "Heat Curing and Post-Heat Curing Regimes of High-Performance Concrete: Influence of Microstructure and C-S-H Composition," Cement and Concrete Research, Vol. 26, No. 2, pp. 295-307.
- Kjellsen, K. O. and Detwiler, R. J., 1992, Cem. Concr. Res., Vol. 22, pp. 112-120.
- Klemm, W. A., and Adams, L. D., 1990, "Investigation of the Formation of Carboaluminates," ASTM Special Tech. Publ., V-STP, No. 1064, pp. 60-72.
- Klieger, P., June 1958 "Effect of Mixing and Curing Temperature on Concrete Strength," Journal of American Concrete Institute, Vol. 54, No. 12.
- Klieger, P., March 1958 "Early High-Strength Concrete for Pretressing," Portland Cement Association, Research Bulletin RX91.
- Kruger, P. 1993, "On the Relation between Non-isothermal and Isothermal Kolmogorov-Avrami-Johnson-Mehl Crystallization Kinetics," Journal of Physical Chemistry of Solids, Vol. 34, No. 11, pp. 1549-1555.
- Kuzel, H. J. and Strohbauch, G., Aug. 1989, "Reactions Associated with the Action of CO₂ on Heat Treated Hardened Cement Pastes," ZKG International, No. 42, pp. 413-418.

Kuzel, H. J., 1996, "Initial Hydration Reactions and Mechanism of Delayed Ettringite Formation in Portland Cement," *Cement and Concrete Composites*, Vol. 18, pp. 195-203.

Kuzel, H. J., Pollmann, H., 1991, "Hydration of C_3A in the Presence of $Ca(OH)_2$, $CaSO_4 \cdot 2H_2O$ and $CaCO_3$," *Cement and Concrete Research*, Vol. 21, pp. 885-895.

Kuzel, H. J. Mayer, H., 1993, "Mechanism of Ettringite and Monosulfate Formation in Cement and Concrete in the Presence of CO_2 ," *Proceedings of the 15th International Conference on Cement Microscopy*, Dallas, 1993, International Cement Microscopy Association, Duncanville, Texas, 1993, pp. 191-203.

Kuzel, H. J., 1993, "Formation of AFm and AFt Phases in Hydrating Portland Cements," *Proceeding of the 15th International Conference on Cement Microscopy*, Richmond, Virginia, 1994, International Cement Microscopy Association, Duncanville, Texas, 1993, pp. 125-136.

Lachaud, R., March 1979, "Thaumasite and Ettringite in Building Materials," *Annales de l'Institut Technique du Batiment et des Travaux Publics*, No. 370, pp. 1-7.

Lawrence, B. L., Myers, J. J., and Carrassquillo, R. L., 1999, Ettringite: "The Sometimes Host of Destruction," SP-177, B. Erlin, (ed.), American Concrete Institute, Farmington Hills, MI, pp. 141-158.

Lawrence, C. D., 1998, "Physiochemical and Mechanical Properties of Portland Cements," *Lea's Chemistry of Cement and Concrete*, 4th Editions, Arnold Publisher, Edited by P.C. Hewlett, pp. 343-419.

Lawrence, C. D., 1995, "Mortar Expansions Due to Delayed Ettringite Formation – Effects of Curing and Temperature," *Cem. Concr. Res.*, Vol. 25, No. 4, pp.903-914.

Lawrence, C. D., 1993, "Laboratory Studies of Concrete Expansion Arising from Delayed Ettringite Formation," *BCA Publications C/16*, 147 pp. British Association. Crowthome, Berks, UK.

Lawrence, C. D., Dalziel, J. A., and Hobbs, D. W., May, 1990, "Sulphate Attack Arising from Delayed Ettringite Formation," *Interim Technical Note*, 12, British Cement Association, Wexham Springs, Slough, U.K

Lerch, W., Ashton, F. W., and Bogue, R. H., 1929, "Sulphoaluminates of Calcium," *Journ. of Res. of the National Bureau of Standards*, Vol. 2, No. 4, pp. 715.

Lerch, W. and Ford, C. L., 1948, "Long-Time Study of Cement Performance in concrete – Chapter 3. Chemical and Physical Testing of Cements," *Journ. Amer. Concr. Inst.*, *Proceedings*, Vol. 44, pp. 743-795.

- Lieber, W., 1963, "Ettringite Formation at Elevated Temperatures," *Cement Kalk-Gips*, Vol. 9, pp. 364-365.
- Lewis, M. C., Scrivener, K. L., and Kelham, S., 1994, "Heat Cured and Delayed Ettringite Formation," *Mat. Res. Soc. Symp. Proc. No. 370*, pp. 67-77.
- Lewis, M. C., 1996, "Heat Curing and Delayed Ettringite Formation in Concretes," Ph.D. Thesis, University of London.
- Lewis, M. C., and Scrivener, K. L., 1997, "A Microstructural and Microanalytical Study of Heat Cured Mortars and Delayed Ettringite Formation," *Proc. Int. Congr. Chem. Cem.*, 10th Gothenburg, Vol. 4, pp. 409-416.
- Ludwig, U., 1991, "Problems of Ettringite Formation in Heat Treated Mortars and Concretes," 11th International Building Materials and Silicate Conference, EMS European Media Service, Witzmannsberg, Germany, pp. 164-177.
- Macleod, G., Hall, A. J. and Hagleitner, K., 1977, "An Applied Mineralogical Investigation of Concrete Degradation in Major Concrete Road Bridge," *Mineral. Mag.*, Vol.55, N377, pp. 637-644.
- Marusin, S. L., 1995, "Deterioration of Railway Ties in the USA," *CANMET/ACI Intl. Workshop on AAR in Concr.*, Nova Scotia, Canada, pp. 243-255.
- Marusin, S. L., March 28 - April 1, 1993, "SEM Studies of DEF in Hardened Concrete," *Proceeding of the Fifteenth International Conference on Cement Microscopy*, Dallas, Texas, pp. 289-299.
- Marusin, S. L., 1993, "SEM Studies of Concrete Failures Caused by Delayed Ettringite Formation," *Proceeding of the 4th Euroseminar on Microscopy Applied to Building Material*, Visby, Sweden.
- Marusin, S. L., 1995, "Sample Preparation – the Key to SEM Studies of Failed Concrete," *Cement Concrete Composites*, Vol. 17, No. 4, pp. 311-318.
- Mather, B., 1984, "Discussion of Paper Theories of Expansion in Sulfoaluminate-Type Expansive Cements: Schools of Thought," by M.D. Cohen, *Cement and Concrete Research*, Vol. 14, No. 4, pp. 603-609.
- Mehta, P. K., 1969, "Morphology of Calcium Sulphoaluminate Hydrates," *Journ. Amer. Ceram. Soc.*, Vol. 52, No. 9, pp.521-522.
- Mehta, P. K., and Moteiro, P. J. M., "Concrete: Structure, Properties, and Materials", Second edition, Prentice Hall, 1993.

- Mehta, P.K., 1973 “Mechanism of Expansion Associated with Ettringite Formation,” *Cement and Concrete Research*, Vol. 3, No. 1, pp. 1-6.
- Mehta, P. K., 1973 “Effect of Lime on Hydration of Pastes Containing Gypsum and Calcium Aluminates or Calcium Sulfoaluminate,” *Journ. Amer. Ceram. Soc.*, Vol. 56, No. 6 pp. 315.
- Mehta, P. K. and Hu. F., 1978, “Further Evidence for Expansion of Ettringite by Water Adsorption,” *Journ. Ameri. Ceramic Soc.*, Vol. 61, pp. 179-181.
- Mielenz, R. C., Maursin, S. L., Hime, W. G., and Jugovic, Z. T., December 1995, “Investigation of Prestressed Concrete Railway Tie Distress,” *Concrete International*, Vol. 17, No.12, pp. 62-68.
- Midley, H. G., and Pettifer, K., 1971, “The Microstructure of Hydrated Supersulfated Cement,” *Cement and Concrete Research*, Vol. 1, No. 1, pp. 101.
- Miller, F. M., and Tang, F. J., 1996, “The Distribution of Sulfur in Present-Day Clinkers of Variable Sulfur Content,” *Cement and Concrete Research*, Vol. 26, pp. 1821-1829.
- Mouret, M., Bascoul, A and Escadeillas, G., 1999, “Microstructural Features of Concrete in Relation to Initial Temperature – SEM and ESEM Characterization,” *Cement and Concrete Research*, Vol. 29, pp. 369-375.
- Oberholster, R. E., Maree, N., and Brand, J. H. D., 1992, “Cracked Prestressed Concrete Railway sleepers: Alkali-Silicate Reaction or Delayed Ettringite Formation,” pp. 739-749, 9th Int. Conf. Alkali-Aggregate Reaction, Vol. II, The Concrete Society, London.
- Odler, I., 1980, “Interactions Between Gypsum and the C-S-H Phase Formed in C₃S Hydration,” 7th Int. Cong. Chem. Cem, Vol. IV, Editions Septima, Paris, pp. 493-495.
- Odler, I., Abdul-Manula, and Zhongya, L., 1987, “Effect of Hydration Temperature on Cement Paste Microstructure,” in *Microstructural Development During Hydration of Cements*, L. J. Strudl and P. W. Brown, Eds., *Mat. Res. Soc. Symp. Proc*, Vol. 85, pp. 139-144.
- Odler, I., and Chen, Yaixin, 1996, “On the Delayed Expansion of Heat Cured Portland Cement Pastes and Concretes,” *Cem. Concr. Composites*, Vol. 18, pp. 181-185.
- Ogawa, K. and Roy, D. M., 1982, “C₄A₃S Hydration, Ettringite Formation, and Its Expansion Mechanism: II. Microstructure Observation of Expansion,” *Cement and Concrete Research*, Vol. 12, No. 4, pp.577-585.
- Ozol, M, A., Strand, Walter III, June 2002, “Delayed Ettringite Formation at Brewer Stadium, Boone, North Carolina,” *Cement, Concrete Aggregates, CCAGDP*, Vol. 22, No. 1, pp. 24-34.
- Oztek, E., 1984, *Cimento Bull*, Vol. 21, pp. 3-13.

Pauri, M. and Collepari, M., 1989, "Thermo-Hygro-metrical Stability of Thaumasite and Ettringite," *II cement*, No.86, pp. 177-184.

Pettifer, K., and Nixon, P. J., 1980, "Alkali Metal Sulfate-A factor Common to Both Alkali Aggregate Reaction and Sulfate Attack on Concrete," *Cement and Concrete Research*, Vol. 10, pp. 173-181.

Possetti, V. A., Chiocchil, G. and Paolini, A. E., 1982, "Expansive Properties of the Mixture $C_4AH_{12}.2Cl$. An Hypothesis on the Expansion Mechanism," *Cement and Concrete Research*, Vol. 12, No. 4, pp. 577-585.

Powers, T. C., Copeland, L. E., Hayes, J. C. and Mann, H. M. 1954, "Permeability of Portland Cement Paste," *ACI Journal Proceedings*, Vol. 51, No. 3, pp. 267-285.

Ramadan, E., 2000, "Experimental and Theoretical Study of Delayed Ettringite Damage in Concrete," Ph.D. Thesis, University of Maryland, College Park, USA.

Ronne, M., and Hammer, T. A., 1999, "Delayed Ettringite Formation (DEF) in Structural Lightweight Aggregate Concrete: Effect of Curing Temperature, Moisture, and Silica Fume Content," *Cem. Concrete, and Aggregates*, CCAGDP, Vol. 21, No. 2, pp. 202-211.

Rome, M., and Sellevold, E. J., 1994, "LIGTCON.DP2 Material Properties. Report 2.3 Effect of Hydration Generated Temperature-Literature Survey," SINTEF report STF70 A978424. Trondheim. Norway, (in Norwegian).

Sagrera, J. L., May 1972, "Study on the Durability of Sulphate Application of Le Chatelier-Anstett Method to an Ordinary Portland Cement," *Cement and Concrete Research*, Vol. 2, No. 3, pp. 253-260.

Satava, V. and Veprek, O., 1975, "Thermal Decomposition of Ettringite under Hydrothermal Conditions," *Journ. American Cerem. Soc.*, Vol. 58, No. 7-8, pp. 357-359.

Saul, A. G. A., March 1951, "Principals Underlying the Steam Curing of Concrete at Atmospheric Pressure," *Magazine of Concrete Research*, Vol. 2, No.6, pp. 127-140.

Schlörholtz, S., and Bergeson, K. L., 1993, "Evaluation of the Chemical Stability Durability of Iowa Fly Ash Concrete," final report, Iowa Department of Transportation project HR-327, ERI project 3295, ISU-ERI Ames 93-411.

Schlörholtz, S., and Amenson, J., 1995, "Evaluation of Microcracking and Chemical Deterioration in Concrete Pavements," final report, Iowa Department of Transportation project HR-358, Engineering Research Institute, Iowa State University.

Schwiete, H. E., Lucwing, V., and Jager, P., 1966, "Investigations in the Systems $3CaO.Al_2O_3-CaSO_4-CaO-H_2O$," Symposium on Structure of Portland Cement Paste and Concrete," Highway Research Board, Special Report 90, pp. 353.

Scrivener, K. L., 1984, "The Development of Microstructure During the Hydration of Portland Cement," Ph.D. Dissertation, University of London.

Scrivener, K. L., and Damidot, D., and Famy, C., 1999, "Possible Mechanisms of Expansion of Concrete Exposed to Elevated Temperatures During Curing (Also Known as DEF) and Implications for Avoidance of Field Problems," Cement, Concrete, and Aggregates, CCAGDP, Vol. 21, No. 1, pp. 93-101.

Scrivener, K. L., and Pratt, P. L., 1984, "Microstructural Studies of the Hydration of C_3A and C_4AF Independently and in Cement Paste," Br. Ceram. Proc., Vol. 35, pp. 207.

Scrivener, K. L., 1992, "The Effect of Heat Treatment on Inner Product C.S.H.," Cement and Concrete Research, Vol. 22, pp. 1224-1226.

Scrivener, K. L., and Taylor, H. F. W., 1993, "Delayed Ettringite Formation: A Microstructural And Microanalytical Study," Adv. Cem. Res., Vol. 5, p.139.

Seligmann, P. and Greening, N. R., 1964, "Studies of Early Hydration Reactions of Portland Cement by X-Ray Diffraction," Highway Research Record, No. 62.

Shayan, A. and Quick, G. W., 1992, "Microscopic Features of Cracked and Uncracked Concrete Railway Sleepers," ACI Material Journal, Vol. 89, pp. 348-361.

Shayan, A. and Ivanusec, I. 1996, "An Experimental Clarification of the Association of Delayed Ettringite Formation with Alkali Aggregate Reaction," Cem. Concr. Comp., Vol. 18, pp. 161-170.

Shayan, A. and Quick, G., 1989, "Microstructure and Composition of AAR Products in Conventional Standard and New Accelerated Testing," In Proc. Of the 8th Int. Conf. on Alkali-Aggregate Reaction, Kyoto, Japan, pp. 475-482.

Shayan, A., 1995, "Behavior of Precast Prestressed Concrete Railway Sleepers Affected by AAR," Real World Concrete, N. R. Swamy Symposium, pp. 35-56.

Siedel, H., Hempel, S. and Hempel, R., 1993, "Secondary Ettringite Formation in Heat Treated Portland Cement Concrete: Influence of Different W/C Ratios and Heat Treatment Temperatures," Cem. Concr. Res. Vol. 23, No. 2, pp. 453-461.

Skolinskaya, N. N., Krasil'nikov, K. G., Nikitina, L. V., Varlamov, V. P., 1975, "Changes in Crystal Structure of Ettringite on Dehydration II," Cement and Concrete Research, Vol. 5, No. 5, pp. 419-31.

Skolinskaya, N. N., Krasil'nikov, K. G., 1975, "Changes in Crystal Structure of Ettringite on Dehydration I," Cement Concrete Research, Vol. 5, No. 4, pp. 381-393.

- Stark, J. and Bollmann, K. 1999, Ettringite: "The Sometimes Host of Destruction," SP-177, B. Erlin, (ed.), American Concrete Institute, Farmington Hills, MI, pp. 183-198.
- Struble, L. J., 1987, "The Influence of Cement Pore Solution on Alkali Silica Reaction," Ph.D. Thesis, Purdue University, U.S.A.
- Sylla, H. M., 1988, "Reactionen im Zementstein durch Warmbebehandlung," Beton, Vol. 38, pp. 449-454.
- Taylor, H. F. W., 1994, "Delayed Ettringite Formation, Advances in Cement and Concrete," Proceedings, Engineering Foundation Conference, Durham, New Hampshire.
- Taylor, H. F. W., 1997, "Cement Chemistry." 2nd Edition, Thomas Telford, Ed.
- Tepponen, P. and Eriksson, B. E., 1987, "Damages in Concrete Railroad Sleepers in Finland," "Nordic Concr. Res., No. 6, pp. 199-209.
- Thaulow, N., Johansen, V. and Hjorth Jacobsen, V., 1996, "What caused Delayed Ettringite Formation?," Ramboll Bulletin No. 60, pp. 8.
- Thermo Orion, 2001, "Ion Selective Electrode – Instruction Manual, Ka^+ , Na^+ and Ca^{2+} ," pp. 3-13.
- Verbeck, G. J. and Foster, C. W., 1950, Proceedings American Soc. Test. Mat., Vol. 50, pp. 1235.
- Verbeck, G. J. and Helmuth, R.H., 1968, Proceedings 5th Intl. Conf. Chem. Cem., Tokyo, pp. 1-32.
- Vitousova, L., April 1991, "Concrete Sleepers in CSD Tracks," International Symposium on Precast Concrete Sleeper, Madrid pp. 253-264.
- Volkwein, A. and Springenschmid, R., Sept. 5, 1981, "Corrosion of Reinforcement in Concrete Bridges at Different Ages due to Carbonation and Chloride Penetration, 2nd Intl. conf. on durability of Building Materials and Components," 14 – 16, Publ. By NBS, Washington D.C., pp. 119-209.
- Wang, S., Ji, S., Lui, and Hu, K., 1986, "Effect of Alkali on Expansion of Sulphoaluminate Cement," J. Chinese Cera. Soc., Vol. 14, No. 3, pp. 285-292.
- Way, S., J., Shayan, A., Sept. 1989, "Early Hydration of Portland Cement in Water and Sodium Hydroxide solutions, Compositions of Solutions and Nature of Solid Pastes," Cement and Concrete Research, Vol. 19, No. 5, pp. 759-769.
- Wells, J. A., Attiogbe, E. K., and Rizkalla, S. H., 1990, "Deleterious Expansion of Cement Paste Subjected to Wet Dry Cycle," Reprint.

Xie, P. and Beaudoin, J. J., 1992, "Mechanism of Sulfate Expansion II. Validation of Thermodynamic Theory," *Cement and Concrete Research*, Vol. 25, pp. 845-854.

Yang, R., and Lawrence, C. D., 1995 "Mortar Expansions due to Delayed Ettringite Formation. Effects of Curing Period and Temperature," *Cement and Concrete Research*, Vol. 25, pp. 903-910.

Yang, R., Lawrence, C. D., and Sharp, J. H., 1996, "Delayed Ettringite Formation in 4-Year Old Cement Pastes," *Cem. Concr. Res.*, Vol. 26, No. 11, pp. 1649-1659.

Zhang, F., Zhou, Z and Lou, Z., 1980, "Solubility Product and Stability of Ettringite," 7th Intl. Congress Chem. Cem. Vol. 2, Paris, II/88-II/93.